Università degli studi di Padova

Dipartimento di Ingegneria Industriale

Corso di Laurea Magistrale in Ingegneria dell'Energia Elettrica

Electric Bus Demand Management through Unidirectional Smart Charging

Relatore
Roberto Turri
Università degli studi di Padova

Correlatore
Keith Sunderland
Technological Univerisity Dublin

Laureando
Nicolae Darii

Matricola
2018908

Anno accademico
2022-2023

"Mess around and find out"
— The scientific method

Abstract

The difficulty of controlling the charging of electric buses (EBs) and their effects on network demand are discussed in this study. The solutions suggest a call for worldwide, complex infrastructures that manage EVs and EBs equally. Additionally, the Distribution Network (DN) must be prepared for an increased prevalence of reverse power flow caused by widespread distributed renewable generation. This paper focuses exclusively on EBs since they have higher capacity and predictable charging patterns, which makes them more significant for the DN in the context of a transition to complete vehicle electrification and technologies that are mature enough to be hosted. The proposed algorithm employs the Day-Ahead Energy Market (DAEM) in the Smart Charging (SC) to forecast the network operating circumstances. Additionally, the technique makes it possible to facilitate distributed photovoltaic (PV) generation, allowing network demand to be referenced depending on net demand. It also identifies an appropriate individual charger current per vehicle and per-time-step with load-levelling or peak-shaving as its primary goal. The final real demand demonstrates that a coarse correction of the demand is possible. According to the analysis of the DN voltage profile and associated line losses, the ideal node position location of the CS is dependent on PV penetration.

In questa tesi vengono discusse le difficoltà di controllo della ricarica degli autobus elettrici (EB) e i loro effetti sulla domanda elettrica. La letteratura suggerisce l'utilitzzo di infrastrutture complesse, capaci di gestire la carica di ciasun veicolo elettrico, in genere non facendo distinzione tra veicoli privati e pubblici. Inoltre, la rete di distribuzione (DN) deve essere predisposta per una maggiore prevalenza di flussi di potenza inversi, causati dalla diffusione di sistemi generazione rinnovabile distribuita. L'elaborato si concentra esclusivamente sugli EB, poiché hanno una capacità maggiore e pattern di ricarica prevedibili, il che li rende più significativi per la rete di distribuzione nel contesto di una transizione verso l'elettrificazione completa dei veicoli e nuove tecnologie sufficientemente sviluppate. L'algoritmo proposto utilizza il mercato dell'energia del giorno prima (DAEM) come riferimento per la ricarica Smart (SC) per prevedere le nuove condizioni operative della rete. Inoltre, la tecnica consente di facilitare l'incremento di generazione fotovoltaica distribuita (PV), permettendo di fare riferimento alla domanda di rete, al netto del contributo derivante sai sistemi fotovoltaici e storage. Inoltre, identifica un'appropriata corrente di ricarica individuale per veicolo e per fascia oraria, con l'obiettivo primario di livellare la domanda o di ridurre i picchi. La domanda reale finale dimostra che è possibile una correzione grossolana della domanda. In base all'analisi del profilo di tensione DN e delle perdite di linea associate, la posizione ideale del nodo CS dipende dalla penetrazione del fotovoltaico.

Contents

Abstract v

List of figures ix

List of tables xi

Listing of acronyms xiii

1 Introduction 1

2 Review of the electric vehicles' storage, charging systems and context 5
- 2.1 Literature review . . . 5
- 2.2 Battery . . . 7
  - 2.2.1 Battery types . . . 7
  - 2.2.2 Battery models . . . 8
  - 2.2.3 High currents and safety limits . . . 12
- 2.3 The significance of the Battery Charger . . . 15
  - 2.3.1 Fast Charging . . . 15
  - 2.3.2 Charger's configuration . . . 17
  - 2.3.3 Standards and safety . . . 20
  - 2.3.4 Charger Model . . . 23
- 2.4 Load management . . . 24
  - 2.4.1 Necessity . . . 24
  - 2.4.2 Peak Shaving and Load Levelling . . . 27

3 Methodology 31
- 3.1 Extrapolation of Battery and Charger's information . . . 31
  - 3.1.1 Battery's usage limits . . . 31
  - 3.1.2 Current controlled DC/DC Buck behaviour . . . 33
- 3.2 Algorithm . . . 40
- 3.3 Colour Maps . . . 48

4 Scenarios 51
- 4.1 Ideal Scenarios . . . 51
  - 4.1.1 Scenario without PV and storage . . . 53
  - 4.1.2 Scenario with PV . . . 57
  - 4.1.3 Scenario with PV and Storage . . . 60
- 4.2 Optimisation of the charging station . . . 62
- 4.3 Real-world fleet consideration . . . 65

5 Effects on the Distribution Network 69

5.1 Power Flow 69
5.2 Discussion 74
5.3 Conclusion 77

References **79**

Listing of figures

2.1 SoC-Voltage Curve. . . . 12
2.2 SoC-Voltage-Temperature Curve. . . . 13
2.3 Charge/Discharge cycles effect Curve. . . . 13
2.4 Relation between current and core's temperature patterns. . . . 15
2.5 Fast Charging with relaxation. . . . 15
2.6 CC-CV charging pattern. . . . 16
2.7 Extended CC pattern. . . . 17
2.8 Schematic EV DC-Bus. . . . 18
2.9 DC-DC Half-Bridge. . . . 19
2.10 Efficiency DC-DC converters. . . . 19
2.11 DC-DC Buck. . . . 19
2.12 ACD Charging methods. . . . 20
2.13 Volvo's OppCharger and EB. . . . 22
2.14 Current, Voltage an SoC with the average model. . . . 23
2.15 Current. . . . 24
2.16 Voltage. . . . 24
2.17 SoC. . . . 24
2.18 Synchronous Generators stability range. . . . 25
2.19 Duck curve during different seasons. . . . 25
2.20 Peak mitigation. . . . 26
2.21 Valley mitigation. . . . 26
2.22 Aggregator operation. . . . 28
2.23 EV share forecast NZS Scenario. . . . 28

3.1 SoC-Voltage and Extracted parameters. . . . 32
3.2 Limited Polarisation effect between 20% and 80% SoC. . . . 33
3.3 Charger *Simulink*^{TM} Model. . . . 35
3.4 Current step-response with PID. . . . 37
3.5 Buck's Power 38
3.6 Buck's Energy 39
3.7 DAEM Load curve. . . . 40
3.8 EBs SoC at time step t and t+1. . . . 42
3.9 Internal power matching and discretization. . . . 42
3.10 Ideal and real connection patterns. . . . 44
3.11 Connection with initial $SoC = 20\%$ for all EBs 44
3.12 Connection with uniformly distributed SoC 45
3.13 Final demand with load levelling. . . . 46
3.14 Algorithm flowchart. . . . 47
3.15 Colour map $\mathbf{SoC}_{\%}$. . . . 48
3.16 I_e representation. . . . 49

4.1 Demand with no PV 53

4.2 New Demand with no PV . . . 53
4.3 Current with no PV . . . 54
4.4 $SoC_{\%}$ with no PV . . . 55
4.5 Connection with no PV. . . . 56
4.6 Demand with PV . . . 57
4.7 New Demand with PV . . . 57
4.8 Current with PV . . . 58
4.9 $SoC_{\%}$ with PV . . . 59
4.10 Connection with PV. . . . 59
4.11 Demand with PV+Storage . . . 60
4.12 New Demand with PV+Storage . . . 60
4.13 Current with PV+Storage . . . 61
4.14 $SoC_{\%}$ with PV+Storage . . . 61
4.15 Connection with PV+Storage. . . . 62
4.16 Real connection with PV+Storage. . . . 65
4.17 New real Demand with PV+Storage. . . . 66
4.18 Real Current with PV+Storage . . . 66
4.19 Real $SoC_{\%}$ with PV+Storage . . . 67
4.20 Comparison between forecasted and real demand . . . 68

5.1 Eleven-Node Feeder. . . . 70
5.2 Load coefficients. . . . 72
5.3 Voltage profile at sensible nodes. . . . 73
5.4 Power line losses. . . . 73
5.5 Active and reactive power at feeder node. . . . 74

Listing of tables

2.1 Battery modelling approaches and applications. 10
2.2 Parameters Tremblay's Equation. 10
2.3 Tremblay's model assumptions and limitations. 11
2.4 Standard Charging and Fast Charging. 16
2.5 Chargers Standards. 21
2.6 IEC levels. 21
2.7 Volvo Charger and EB. 22
2.8 Reasons to implement Peak Shaving or Load Levelling. 27

3.1 Buck's input and output parameters. 36
3.2 PID parameters. 37

4.1 Scenarios' parameters. 52
4.2 Scenarios results. 62
4.3 Numerical allocation of the load levelling graphical error. 63
4.4 CS input parameters test. 64
4.5 Results with real world fleet. 65

5.1 PV and loads data. 70
5.2 Data lines. 71
5.3 Data transformers. 71
5.4 Load coefficients legend. 71
5.5 Summary of the performances by changing CS's node. 72

Listing of acronyms

CS ..... Charging Station

$\mathbf{P}_{r(CS)}$ ..... CS Power vector with I_r

$\mathbf{P}_{s(CS)}$ ..... CS Power vector with I_s

DAEM ..... Day Ahead Energy Market

$\mathbf{Cnn}_{real}$ ..... EB's real connection schedule vector

Cnn ..... EB's connection schedule vector

EB ..... Electric Bus

EV ..... Electric Vehicle

ΔE_{CS} ..... Element of $\mathbf{E}_{load}$ vector

$\mathbf{E}_{load}$ ..... Energy difference vector

$E(Wh)$ ..... Energy in [Wh]

$E_{j(r)}$ ..... Energy of EB j charged with I_r

$E_{j(s)}$ ..... Energy of EB j charged with I_s

$\mathbf{P}_{newload}$ ..... Final New DN's demand after smart-charging

$\mathbf{P}_{load}$ ..... Initial Demand power vector

Is ..... I_s Matrix

m ..... Number of EBs in the CS

z ..... Number of fully charged EBs

z' ..... Number of connected EBs in the real case

$\mathbf{P}_{objective}$ ..... Objective Demand power vector

PV ..... Photovoltaic

C_r ..... Rated Capacity

I_r ..... Rated current

V_r ..... Rated Voltage

RDG ..... Renewable Distributed Generation

F_{ideal} ..... Size of the ideal EB's fleet

F_{real} ..... Size of the real EB's fleet

SC ..... Smart Charging

I_e ..... Smart current for almost-charged vehicles

I_s ..... Smart current

SoC ..... *SoC* Matrix

SoC ..... State-of-Charge

i ..... Time-step index

Δt ..... Time-step

j ..... Vehicle index

1 Introduction

The aim of this thesis is to provide an algorithmic approach for managing EBs charge. The created method may be utilised in two ways: as a scenario builder with a specified CS or to construct a CS using the DSO's defined load and generation curves. The thesis is complementary with two articles: the first was presented at 57th International Universities Power Engineering Conference (Istanbul) and published as a conference paper on IEEE Xplore [1], while the second was expanded and published as a journal paper on MDPI Electronics [2]. The reason for the topic selection was the need to find a transitional solution to the electrification of the automotive sector, which must be considered because the electrical grid is not currently capable of hosting this new type of load, which, from a DSO/TSO perspective, is a load that can also function as storage. The thesis focuses on EBs, a subset of the EV legacy with the distinct feature of having a predictable connecting pattern and a significant energy capacity. On the other hand, an electrical load such as a CS might provide a significant difficulty for the electrical service if the charging process is not properly controlled. The thesis justification emerged from a hackathon project at Tsinghua Global Summer School 2021, where the project was offered in order to create an alternative monetary resource for the public sector in order to boost service availability, in addition to the primary decarbonisation goal. Because the project won the "Most Investable Team" honour, it was determined to do more research.

The thesis is divided into four chapters. The first examines the environmental and technical backdrop in more depth in order to offer a clear justification. The chapter continues with a review of the various storage methods already in use, as well as the structure of the many available chargers, in order to be consistent with the main goal of providing an instantly usable solution. The chapter finishes with the rationale for load management (load-leveling, peak-shaving) and illustrates the benefits of this service as well as how it might be achieved.

The second chapter examines the analytical component of the storage and charging system by modelling the charging process using SIMULINK^{TM}. When the system operates within a specific *SoC* range, the potential of linear process behaviour was proven. This served as the foundation for algorithm development because MATLAB^{TM}'s matrix framework allowed for simple linear computations. As a consequence, the internal workings of the algorithm are described, as well as the outcomes that it is capable of producing, such as the planned current and

connection pattern, and the ultimate effect on the load at the primary HV/MV transformer.

The third chapter discusses the many scenarios that may be found in the present DN and how the CS and network interact with one another. In this chapter, an example of CS and EBs characteristics design and comparison with genuine Volvo EBs is also shown. The final section of the chapter focuses on the usage of stricter limitations to produce more concrete results.

The last chapter examines the DN using power-flow methods to determine the impacts of a CS managed by the proposed algorithm on the other nodes and lines. This is accomplished by connecting the CS in each node and determining the best connection point. It is then completed with the work's overarching considerations.

L'obiettivo di questa tesi è fornire un approccio algoritmico per la gestione della carica degli EB. Il metodo creato può essere utilizzato in due modi: come costruttore di scenari con una CS specifica o per dimensionare una CS utilizzando le curve di carico e generazione definite dal DSO. La tesi è da considerarsi complementare a due articoli: il primo è stato presentato alla 57^{a} *International Universities Power Engineering Conference (Istanbul) e pubblicato come articolo di conferenza su IEEE Xplore [1], mentre il secondo è stato ampliato e pubblicato come articolo di rivista su MDPI Electronics [2]. La scelta dell'argomento è stata motivata dalla necessità di trovare una soluzione transitoria all'elettrificazione del settore automobilistico, che deve essere presa in considerazione perché la rete elettrica non è attualmente in grado di ospitare questo nuovo tipo di carico che, dal punto di vista di un DSO/TSO, è un carico che può funzionare anche come accumulo. La tesi si concentra sugli EB, un sottoinsieme degli EV con la caratteristica distintiva di avere un pattern di connessione prevedibile e una capacità energetica significativa. D'altra parte, un carico elettrico come un CS potrebbe creare notevoli difficoltà al servizio elettrico se il processo di ricarica non è adeguatamente controllato. La motivazione della tesi è emersa da un progetto hackathon alla Tsinghua Global Summer School 2021, dove il progetto è stato proposto per creare una risorsa finanziaria alternativa per il settore pubblico al fine di ampliare la disponibilità del servizio a più utenti, oltre all'obiettivo primario della decarbonizzazione. Poiché il progetto ha vinto il premio "Most Investable Team", si è deciso di approfondire il progetto di ricerca. La tesi è suddivisa in quattro capitoli. Il primo esamina in modo più approfondito il contesto ambientale e tecnico per offrire una chiara giustificazione. Il capitolo prosegue con una rassegna dei vari metodi di stoccaggio già in uso, nonché della struttura dei numerosi caricabatterie disponibili, per essere coerenti con l'obiettivo principale di fornire una soluzione immediatamente utilizzabile. Il capitolo si conclude con la logica della gestione del carico (load-leveling, peak-shaving) e illustra i vantaggi di questo tipo di servizio e le modalità di realizzazione. Il secondo capitolo esamina la componente analitica del sistema di accumulo e di ricarica, modellando il processo di ricarica con SIMULINK^{TM}. Quando il sistema opera entro uno specifico intervallo di SoC, è stato dimostrato il potenziale di un comportamento lineare del processo. Ciò è servito come base per lo sviluppo dell'algoritmo, poiché la struttura matriciale di MATLAB consente di ricondure il problema a semplici calcoli lineari. Di conseguenza, vengono descritti il funzionamento interno dell'algoritmo e i risultati che è in grado di produrre, come la pianificazione della corrente di ricarica e lo schema orario di connessione, nonché l'effetto finale sulla domanda al trasformatore primario AT/MT. Il terzo capitolo illustra i numerosi scenari di carico che si possono comporre nella rete di distribuzione ed il modo in cui il CS e la rete interagiscono tra loro. In questo capitolo viene anche mostrato un esempio di progettazione delle caratteristiche di CS ed EB ed un confronto con le Autobus elettrici Volvo. La sezione finale del capitolo si concentra sull'applicazione di limitazioni più severe per produrre risultati più concreti. L'ultimo capitolo esamina la rete utilizzando studiando i flussi di potenza per determinare l'impatto di una CS gestita dall'algoritmo proposto sugli altri nodi e linee. Ciò avviene collegando le CS in ogni nodo e determinando il miglior punto di connessione. Si*

conclude quindi con le considerazioni generali del lavoro.

2

Review of the electric vehicles' storage, charging systems and context

2.1 Literature review

The introduction of EVs in the vehicles market is an important opportunity towards Net-Zero Emissions. EVs are not just a possibility for the transport sector, it is widely accepted that they have the potential to be one of the key-actors for future Smart-Grid development [3]. Further, the technology has scope to work as a service providing diffused storage for the electrical grid. This opportunity has resulted in the study of several scenarios and techniques to exploit the capabilities of this technology. Consequently, the study of the implementation potential of EV in consideration of its different capabilities has led to the Vehicle-To-Grid (V2G) system's concept. This type of system, in turn, encompasses other subtopics. These include the understanding of how the single parts of the system (batteries, charging systems, EVs availability, etc.) behave in this new environment, which is not just the transport sector, and how the implementation of the V2G could influence the response of the electrical grid and the electricity market. Consequently, many research areas have studied the mutual effects of the EV and the electrical power system. In addition, EVs have introduced the possibility to investigate many scenarios, including the extension of renewable generation (especially in a distributed energy context). These factors serve to justify the intense interest prevalent in literature concerning the feasibility of this new paradigm involving EVs as a central actor in electrical power systems, even if it is a complex challenge [4]. At the core of the V2G paradigm, there is the storage system and more specifically the batteries, which need special attention. Their charging and discharging pattern and operational limits have an important influence over the overall planning of V2G by the variation of electrical or atmospheric parameters (e.g., ambient temperature) and cost. Parameters such as the degradation of the available capacity over time have a significant relevance. If an EV's battery might incur a capacity reduction

by 15,7% in five years [5],then such an implication must be considered in the design. Further, the future basic components of the batteries are uncertain [6]. Moreover, planning the future strategies on prioritised technologies, for example just on Li-Ion batteries, could be a losing strategy. Therefore, as there is a plethora of research on the best combination [7, 8, 9],an approach that forecasts the possibility to change the system as function of the future components is essential. The knowledge of the characteristics of the storage system by itself is not enough to describe how the entire system will react. That is why, even if the EVs (batteries) are connected to the Low-Voltage level (LV), their cumulative effect could result in different effects and consequences on the (voltage) levels above. By considering the LV level it is possible to find research that suggests possibilities in the control of small renewable generation by mitigating their effects during peak-production and influence in compensating any supply deficits [10, 11]. Also, and more in the context of controllable energy harvesting, the islanding effect and the synchronisation issues, studied as storage from the EVs, can introduce these implications.

Another subtopic connected to the control of the power-flow, are the Smart-Charging (SC) and Smart-Metering (SM) Systems. As it is possible to find in [12],for effective SC, a control facility is required. Such a facility can synergise the demand and the production, and thereby stabilise the power absorption while maintaining system network operational parameters (such as voltage, frequency, THD, etc.) within accept able limits. At the same time, and according to Klaina, *et al.* [13], it is necessary to have a SM infrastructure to communicate the data from the new users (the "Prosumer", or a consumer that is also able to produce) to the Aggregators, which will manage the electrical and economical flow. In this regard, even the communication system is one of the focal research areas around EVs. The combination of these approaches could, as Niasse *et al.* [14] states, have an effect even on the High Voltage (HV) level and therefore, even an effect of the Frequency-Control at the Transmission Level. Such consequences are analysed in [14] and the influence of V2G in assisting the containment of low- frequency oscillations induced by hydro power-power plants. On a related point, and in respect to the effect on HV, from the EVs connected at LV, it could be possible, as[15] suggests, to control the congestion and voltage of the Distribution Network at Medium Voltage (MV) level. The studies at MV are particularly interesting because a hypothetical introduction of aggregated Plug-In Electric Vehicles, without adequate control of the charging pattern, could determine an important decrease in the reliability of the Distribution Network, as a consequence of reduced line capacity or the voltage volatility due to the uncontrolled power flow.

A contrary position suggested that with an appropriate control the response of the network, the reliability concerns are not affected [16]. These juxtapositions suggest that there is a need for more conclusive research into the associated issues. Other aspects, such as the positioning of the EVs in the network is crucial for a correct confinement of the power losses as Chukwu tested in [17], or the effective possibility to have the desired amount of EV in the Charging-Station (CS) [15]. The revenue derived from the V2G [18] and the initial cost of the EV and CS [4] are also important challenges due to their unpredictability derived from the EVs market. Even if the introduction of the EVs into the grid is characterised by many important difficulties, they are necessary for their potential as distributed generation in the Distribution Network. That said, since it is characterised by a low level of Short Circuit Power and not designed for bidirectional power-flow, the Distribution Network is sensitive to over-voltage and increase of THD caused from the inevitable increase of distributed generation [19].

In general, and in consideration of an evolving Distribution Network, the literature suggests many important future innovations such as V2G [20], distributed renewable generation [19], Smart-Grids [3] and the use of Internet-Of-Things [21], etc. . However, at the same time several important challenges remain because the network is not designed to support these innovations. The research on the topic is usually characterised by many

proposals, but usually defined by a high level of complexity. For instance, the proposal to study case by case the long-range communication or the wireless system for the V2G proposed by [20]. Even if the results could introduce important progress in the development of the V2G in the Distribution Network, they require pre-existing infrastructure or technologies that are not yet available. In general, the literature on the topic focuses on the proposals of different scenarios, as suggested by Pavan *et al.* [22] where a pre-existing complex communication infrastructure and an already existing Smart Grid is required. Other authors as Thirugnanam *et al.* [23] propose the possibility of using wireless CS, or more generally the studying how V2G could behave with a massive introduction of private EVs, which requires the certainty of the market and user's behaviour. Generally, it is possible to find ideas that offers suggestions rather than easy to deploy solutions. All the topics then converge in the macro-topic of Smart-Grids or Smart-Cities. Uhlig *et al.* [3] state that the Smart-Grids are inevitable to contain the future high costs of the Distributed Network's expansion to host the new technologies. But at the same time, it is a long-term goal.

2.2 Battery

2.2.1 Battery types

Batteries are at the core of the system. This component has a strategic role in the EV field. Therefore, there are plenty of studies on the topic. Some of the technologies employed include: Molten Salt (Na-NiCl2), Nickel Metal Hydride (Ni-MH), Lithium Ion (Li-Ion) and Lithium Sulphur (Li-S). In [24] study it is possible to find a comparison among these technologies on the same vehicle. Firstly, Ni-MH batteries are widely used because of their high energy/power density. They are able to guarantee 300 km of autonomy and have an acceptable "charge to weight " ratio of 70 Wh/Kg. The last terms are crucial in the EV field because of the mutual effect of the charge available, and the energy needed to move a relatively heavy vehicle. Since there is limited space available in the vehicles, it is important to find technologies that allow more energy density in less volume and weight. Ni-MH batteries have the ability to work unaltered until (Depth-Of-Discharge) DoD of 80% and operate in regenerative energy mode. Thanks to their excellent thermal proprieties, that allows them to work effectively in a range of temperatures between -30° and 70°, Ni-MH batteries are classified as relatively safe technology because of the guaranteed safety during the charging and discharging cycles. Systems that have used these batteries are considered easy to control as a whole.

Another type of battery that is used in EVs is the Na-NiCl2, also called the "Zebra" *. Generally, this technology is used for public transport. The main feature of this technology is the stability during the charging/discharging cycle, thanks to the stability of its internal Resistance (R_{int}). This parameter encloses the physical and chemical phenomena that introduce a drop in the voltage at the terminals and heat production in the cells. The robustness of the battery and increased life-cycle make it suitable for EVs that are operational harsh conditions as remote hot or cold locations (e.g. antennas). Since this storage system works by melting the Na-NiCl2, the drawback is the fact that this technology requires an operational temperature between 270° and -350° to keep the salts in this state. This is a benefit for the vehicles placed in extremely cold temperatures, but it requires at least 90Wh of energy to

*Zeolite Battery Research Africa Project, started in South Africa in 1985

avoid the freezing of the electrolyte even during the steady state condition. Otherwise, it would require an average of 12-15h to come back to operative conditions.

The most commonly used commercially is the Li-Ion battery. This technology is characterised by a high charge to weight rate of 250 Wh/Kg and power of 2000 W/Kg. Therefore, the Ni-MH are substituted bi Li-Ion mainly for this reason. This battery has a small "memory effect" that reduces the initial capacity over time. Even though the energy density is higher, the tests in outlined in [24] demonstrated that, for the same conditions, the Li-Ion has less autonomy (battery duration at a specific load level) than Ni-MH. In fact, this is one of the drawbacks of this technology. In addition to this, its operation is extremely dependent on temperature. In fact, Li-Ion requires an auxiliary system called a Battery Management System (BMS) that tracks the temperature and voltage of the battery in order to prevent dangerous working conditions. Thus, a requirement for safety management is another drawback of this technology.

There are studies on the Li-S, that considered an extremely high charge to weight of 2500 Wh/Kg, but in its current state of maturity this typology has a reduced lifespan and an energy retention capacity (the ability to retain the capacity during long operational-circuit condition). Further, at the end of their operational lifespan, there is also a high recycling cost.

In conclusion, the Li-Ion is currently the most convenient battery technology, even with the associated strong drawback related to the autonomy and temperature sensitivity. Further, due to the fact that the 25-50% of the entire cost of an EV concerns the battery, it is important to be conscious of the associated implications. The Li-Ion has a strong competitive price. This is important in the context of an aspirational fast transition to EV. So it is compulsory to implement technologies that are economically competitive in order to incentivise the transition. Consequently, the battery type that will be taken into account in this work is the Li-Ion because it is the one that applies most satisfactorily to the relevant technology transition considerations.

2.2.2 Battery models

In order to understand how batteries behave in the context of EVs, it is necessary to build a model. There are several models that describe the internal and external phenomena associated with battery operation. This device also has the peculiarity of an extremely nonlinear relationship between the key variables. In the cases of extreme charging/discharging patterns or temperatures, the Li-Ion batteries lead also to uncontrollable reactions that cannot (currently) be modelled. For this reason, it is necessary to define correctly the limits of the model. In the thesis, the model is not used directly in the algorithm, but it is necessary to extrapolate important assumptions on the battery state variables (voltage, energy, current and power), in order to justify the choices upon which the algorithm is based. Alternatively, by increasing the computational effort, it is possible to directly introduce an analytical method based on a model to find the state variables in the algorithm.

Generally, the most important functions that define the state of the battery are the Equation (2.1) and Equation (2.2):

$$SoC_{\%} = \frac{1}{(C_{rated} V_{rated})} \int_0^t i(\tau) v(\tau) d\tau \tag{2.1}$$

$$v = f(SoC_{\%}) \tag{2.2}$$

The Li-Ion batteries could be controlled by adjusting the: voltage, current, temperature and the load attached to the battery, as suggested in [25], this makes them suitable for electrical vehicles and grid applications. In addition to these variables, there are some that could be considered as parasitic phenomena, such as: deterioration, diffusion, number of working cycle, etc. These are generally not controllable, even if they have an effect on the battery's operation. The most impactful phenomenon is the Solid Electrolyte Inter-phase (SEI), which deteriorates the electrolyte and could cause also dangerous working conditions, and leads to the general loss of capacity of the battery over time.

In Iclodean *et al.* [25] defined three ways to model the battery depending on the purposes. This is implemented because it is not possible to use a single model to describe the batteries due to their complexity, non-linearity and mutual effects between the numerous variables. The Mechanistic Model is one that describes mathematically the physical and chemical relations. This requires a deep knowledge of the internal processes, the components and the final effects on the performance. This model is useful when it is necessary to describe the battery on a microscopic level, but it is extremely heavy on the computational side, thus it is not practical to use it in EV applications. The Data Driven Model represents batteries from a historical point of view. It requires real-time data and an intensive monitoring in order to diagnose, design, understand and define them. For the purposes of the thesis, this approach is not useful because one of the main aims is to be independent of complex communication infrastructures. The last approach, which is the most commonly used in grid and vehicular field, is the Equivalent Circuit Method (ECM). This approach describes (with some limits) the battery by an appreciation (knowledge, or measurement) of the electrical parameters, current and voltage, which collectively represent the internal phenomena from the electrical point of view. The model is composed of lumped components: resistors, capacitors and ideal (or controlled) voltage generators. The number of lumped components is proportional to the level of accuracy, but generally the components, with similar time constant τ, are generally condensed. This model facilitates a wide range of operation with an acceptable level of accuracy and with a relative light computational overhead.

It is possible to find two types of ECM, one that includes physical and chemical phenomena and the other, which does not. The first one is based on RC circuits where R (resistance) and C (capacitance) have no mutual effects. This allows for fast calculations, but with a low level of accuracy. In order to exploit the lumped components, precise measurements on the battery are necessary. The precision of the model is therefore proportional to the measurement accuracy. Generally, these studies are carried out with small signals, so the behaviour of the battery at high current/voltage inputs could be inaccurate due to the dynamics of the batteries in these conditions. In conclusion, this type of model could fail when it is solicited to high inputs. To simulate more complex phenomena, it is possible to introduce in the controlled voltage generator the dependence of: temperature, ageing, C-rated (rate of the charging cur- rent compared to rated current), SoC, etc. This will lead to a non-linear behaviour, slightly more robust simulations, but more accurate. A synthetic visualisation of the characteristics of the different models are summarised in Table 2.1 [26].

Table 2.1: Battery modelling approaches and applications.

Model approach	Accuracy	Computational Complexity	Configuration Effort	Analytical Insight	Purpose
Physical	Very High	High	Very High	Low	Battery design and model validation
Empirical	Low-Medium	Low	Low-Medium	Low	Battery performance estimation
Abstract	Low-High	Low-Medium	Low-High	Medium	Battery performance estimation
Mixed	High	Medium	Low-Medium	High	Battery performance estimation

One of the most used ECM models is the one suggested by Tremblay in [27]. This model has the peculiarity that requires just three points from the manufacturer's discharge SoC-Voltage curve to obtain the parameters. In addition to this, the *SIMULINK*^{TM} software uses his model in the SimScape library as the battery. This model is characterised by two components: a fixed resistance R_{int} that models the complex physical and chemical reactions that causes voltages drop and heat (modelled as Joule Effect). The latter is an ideal controlled voltage generator, that represents the V_{oc} (Open Circuit Voltage) of the battery. The parameters of the equation proposed by Tremblay does not require an analysis of the impedance Z(ω) of the battery at different frequencies, just data already present in the battery's data sheet. The equation varies depending on the battery type, so in our case it is just shown in Equation (2.3). To built the Equation (2.3) it is necessary to extrapolate the parameters Table 2.2 [27] from the battery's data sheet. The Table 2.2 have to be extrapolated from Voltage-SoC manufacturer's curve, however it is possible to use *SIMULINK*^{TM} that uses Tremblay's model and has implemented automatically the extraction of Table 2.2, starting from the battery's rated capacity and voltage.

Since the discussion in [27] considers an ECM model that has the limitations mentioned in Table 2.1, it is necessary to be aware of the hypothesis used by the model in order to do not overestimate the results of the algorithm. The Equation (2.3) works with these assumptions Table 2.3.

Table 2.2: Parameters Tremblay's Equation.

$E_0[V]$	$R[\Omega]$	$K[\Omega, V/(Ah)]$	$A[V]$	$B[Ah]^{-1}$

$$V_{batt} = E_0 - R \cdot i - K\frac{Q}{Q - it} \cdot it - K\frac{Q}{it - 0.1 \cdot Q} \cdot i + Aexp(-B \cdot it) \tag{2.3}$$

Table 2.3: Tremblay's model assumptions and limitations.

Assumptions		
R_{int} constant	Discharging curve = Charging curve	No Peukert effect
Temperature independency	No self-discharge	No memory effect
Limitations		
No-Load $V_{min} = 0$	No-Load $V_{max} = 2 \cdot E_0$	$Q_{max} = Q_{rated}$

In respect to equation Equation (2.3) there are two components relative to the polarisation. In the electrochemical context, the "polarisation" is referred to each phenomenon that causes the voltage's departure from its ideal value founded according to Nernst[†] equations. Generally the polarisation is correlated with a current flow and causes two types of polarisation: ohmic and the voltage relevant. These are correlated to internal phenomena as: heating, charge transfer, crystallisation, concentration of materials around the electrodes, etc. These effects combined will result as an increase of voltage during the charging phase, and a decrease during the discharging. There is another unwanted effect called Peukert effect which modifies the capacity Q function of the C-Rate during the discharging process. Since the algorithm manages the Unidirectional Smart Charging (so the charging process), the lack of accuracy for what concern this effect Table 2.3 is negligible. Therefore, the resultant voltage at the terminals is correlated with the current that it is absorbed or delivered and its SoC. For the work it is important to consider just how the voltage behaves during the charging pattern because it is focused just on the unidirectional smart charging process. In order to compute the actual energy that is stored in the battery, it is necessary to know the voltage at the terminals as it is possible to see in equation Equation (2.1). Since the SoC is computed (generally) from the integral of the current, the charge would be in terms of [Ah]. Therefore, it is necessary to convert it into [Wh] for it to be suitable for electrical grid computations. This aspect is not trivial, since the voltage is required theoretically every instant in order to compute the integral in Equation (2.1), however since the power computation in the DAEM is done with a time-step of 15 min, the voltage has to be know with the same sample time. It would be possible to consider just the V_{rated} as constant, but to be more accurate it is possible to use the SoC-Voltage manufacturer curve which presents a Equation (2.2) relation. For a first qualitative analysis, so as to reduce the computational time of the algorithm, the two polarisation effects will be neglected that might alter the voltage proportionally to the charging current's magnitude. Instead a poly-fitted extrapolation of the manufacturer-stated Voltage-SoC curve, is considered. This will underestimate the voltage, thus the energy. However, the results may be considered pessimistic in facilitating the algorithms' iterations. The tabulated method is also used in (Battery Energy Storage System) BESS systems to avoid SoC algorithm estimations and SoC-Voltage is used as a reliable reference in most methods as stated in [28]. The error will be more incisive with higher values of the current and when the SoC is closer to 0% or 100% as illustrated in Figure Figure 2.1.

[†] the Nernst equation is a chemical thermodynamical relationship that permits the calculation of the reduction potential of a reaction from the standard electrode potential

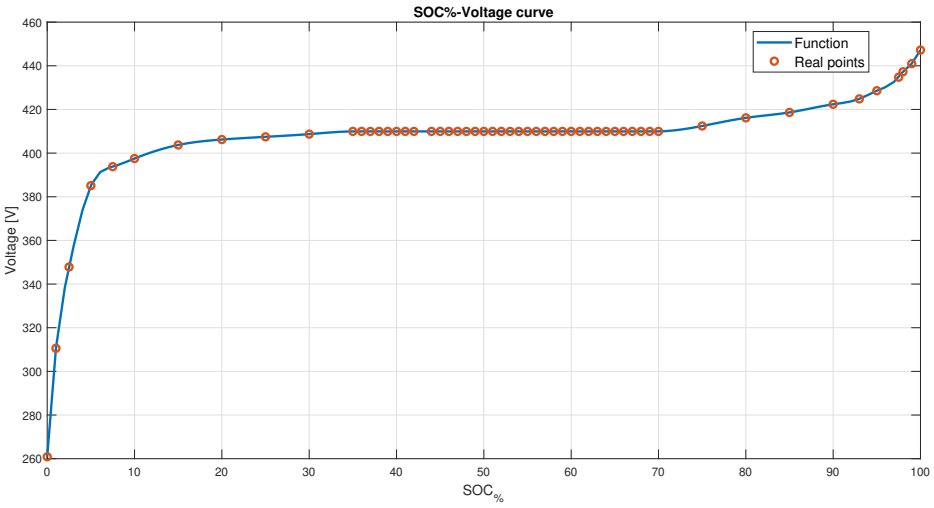

Figure 2.1: SoC-Voltage Curve.

2.2.3 High currents and safety limits

Li-Ion batteries have the peculiarity to be extremely sensitive to temperature, which reveals a correlation between voltage, current and (ambient) temperature Figure 2.2 [29]. In addition to the influence on the output characteristic, there are important internal phenomena that could occur if the battery is used without caution. The most important limit is at 69°C according to Gaehring *et al.*[29], at this temperature the passivation layer (the one that covers the anode for safety reasons) decomposes. When the electrode and the electrolyte come into contact,a reaction occurs that produces flammable hydrocarbon gasses. Then in cascade a phenomenon called "thermal run- away" occurs, where the temperature increases drastically, at the anode H_2 is produced and O_2 at the cathode. The combination of these elements causes the ignition of the battery. Frequent charge/discharge cycles will also decrease the live cycle of the batteries, especially because there are some constructive inequalities between the anode and cathode, which would result in unbalanced working conditions Figure 2.3 [30]. Also, the internal resistance changes over time when the internal structure of the electrodes changes. The effects are more intense when the batteries is operating at high C-rates.

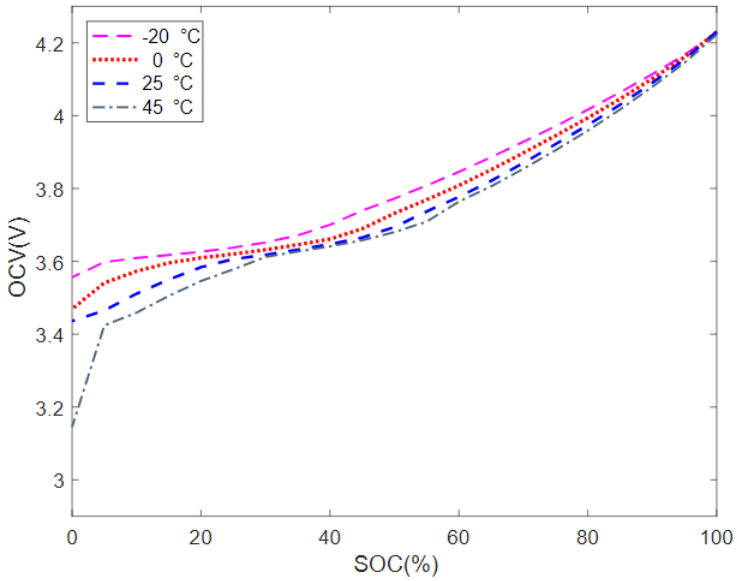

Figure 2.2: SoC-Voltage-Temperature Curve.

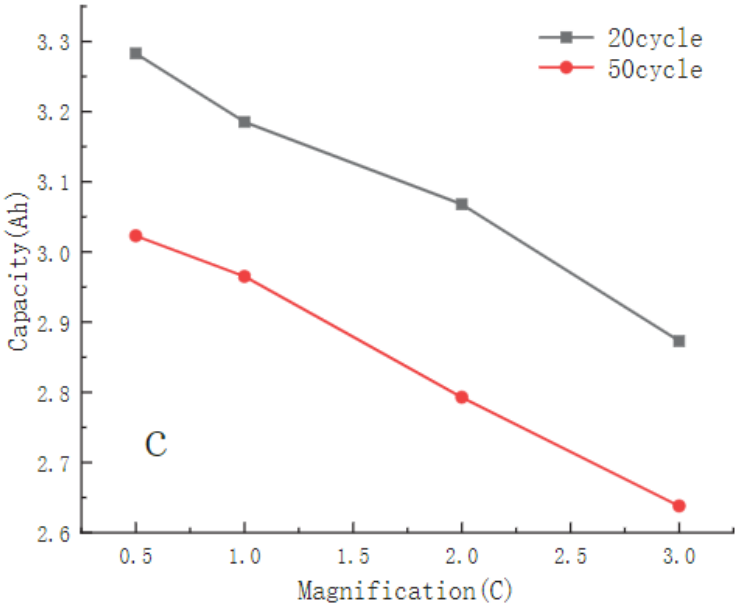

Figure 2.3: Charge/Discharge cycles effect Curve.

With an excessive fast charging lithium could electroplate on the anode. The growth of these solid formations (Lithium Planting) could pierce the separator causing internal short circuits. The phenomenon is directly pro-

portional to the energy density of the cells, which are more sensible to the C-rate [28]. In order to do not incur in the mentioned negative effects caused by the fast charging, it is common to restrict the battery's use just at their nominal C-rate, however Amietszajew *et al.* in [28], proved that it is possible to use the cells in a wider C-rate range. Since the batteries of an EV could be solicited to employ higher currents (for example, an EB), it is necessary to know what is the $SoC_{\%}$ range that could resist to the fast charging. The first safety limit is to impose a lower limit to the SoC, since the voltage has a drastically drop when the SoC is close to the lowest values, for instance, an SoC of 20%. When the battery reaches the highest values of SoC, the internal resistance of the battery tends to grow, therefore increasing the: over voltage, Joule Effect[‡] and degradation of the cathode. Therefore, safety limit is imposed to an SoC of 80% in order to border the temperature, lithium planting and extreme polarisation (which causes a voltage spike when the $SoC \cong 100\%$). This is the same reason that imposes the adoption of a high Constant- Current (CC) charging for SoC of less than 80%, and Constant-Voltage (CV) charging with SoC greater than 80% in fast charging techniques. Even if this is the most common charging protocol, it is also the least time-efficient. That the possibility to charge the batteries at higher rates when 20% < SoC < 80% is suggested in [28]. Amietszajew *et al.* suggestion is the possibility to charge the cells with a maximum of 2C-rate, which is double the current that manufacturers indicate in the data sheets. The main constraint in charging batteries at 2C is that the temperature rises rapidly Figure 2.4. Therefore, the suggestion is to gradually decrease the magnitude of the current after the peak of 2C in order to give the time to the cells to "relax" the internal chemical and physical phenomenons as diffusion, because of different time constants Figure 2.5 (The standard current here is 3A, therefore 2C rate is at 6A). The most relevant temperature is the core one in Figure 2.5 because it represents the most critical and higher values, however it is represented also the "can" temperature which is the one of the external case.

Within the project, the first safety precaution that is taken is to do not overcome the 80% SoC value. In order to do not have dangerous polarisation overvoltagese, it is imposed a cap to the max C-Rate. In order to achieve a safe charging pattern it is not necessary to impose on purpose a gradual reduction of the C-Rate, the current magnitude will follow the Load demand which increases and decreases naturally and gradually. In addition, outside the periods where there is an under load demand (so high currents to compensate it), the charging current is less or equal to the rated one. In addition, since the state variable that increases the hazard is the current, it is possible to choose an high voltage charging system in order to have a low current's magnitude.

[‡]a physical law expressing the relationship between the heat generated and the current flowing through a conductor

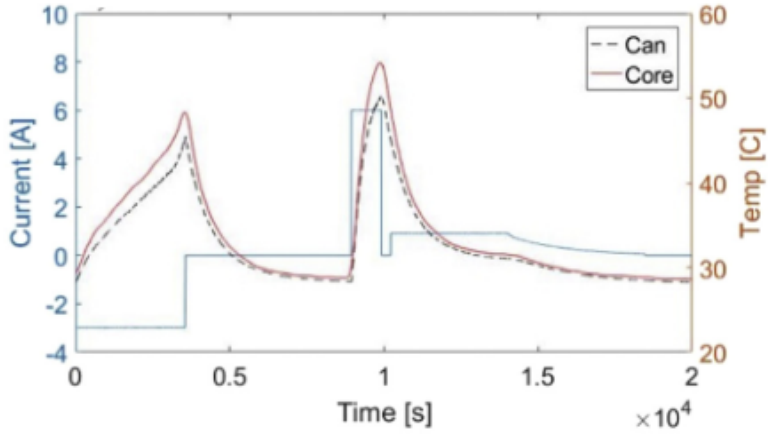

Figure 2.4: Relation between current and core's temperature patterns.

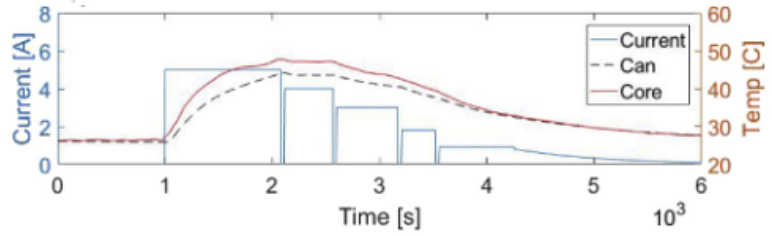

Figure 2.5: Fast Charging with relaxation.

2.3 The significance of the Battery Charger

2.3.1 Fast Charging

In addition to the 80% SoC cap, there is also the 20% SoC minimum threshold. If the battery reaches this level the voltage drops to a critical value for every electrical application, and it is not advisable to use the battery in fast charging modality at that level for safety reasons. The last 80-100% SoC could be capitalised even if suggests that it is a dangerous zone due to the increase of R_{int} with the related problems. When the $80\% \leq SoC \leq 100\%$ the R_{int} tends to increase, therefore a fast charging (high current magnitude) is not recommenced due to the over-voltage and high temperature risk. Thus, the current in this range has to be lower (not anymore a fast charging) and must be inversely proportional to the voltage rise in order to counterbalance the polarisation effect. The capitalisation of that SoC's range is usually facilitate by imposing a Constant-Voltage (CV) charging pattern, the current in that range evolves naturally as in Figure 2.6 by deceasing to zero. In the first range of $0\% \leq SoC \leq 70\%$ (in this case) the controlled parameter is the current, that is why it is called Constant-Current (CC). The voltage is

counted as state variable that evolves naturally by following the curve that is usually seen in the data-sheets (which by definition is defined by charging/discharging the battery at the C-rated). The $SoC_{\%}$ evolves linearly until the voltage reaches the V_{max}, from them on the charger switches the modality and the V_{max} is maintained constant until the $SoC = 100\%$ condition. In this phase the current is the state variable that decreases exponentially.

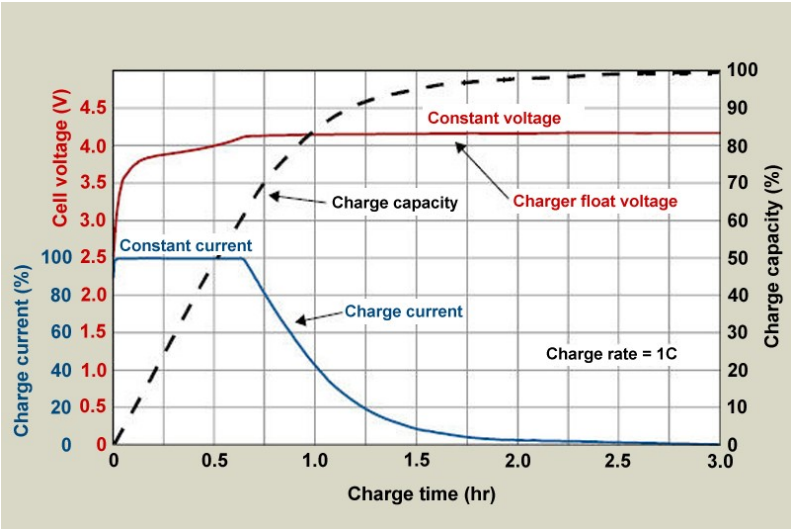

Figure 2.6: CC-CV charging pattern.

The CV part of the process is the most inefficient and difficult to control because the voltage must be fixed to the maximum value and the current is a dependent state variable. Therefore there are no degrees of freedom. In addition, CC mode is the one where most of the fast-charging methods are developed as it is possible to see in the Table 2.4 [28]. The drawback is that the last CV mode is the slowest one and usually it is difficult to reduce its duration. This aspect is crucial in order to further justify why it is not possible to use all the batteries capability.

Table 2.4: Standard Charging and Fast Charging.

Charging mode	0-80% Soc	80%-100% SoC
Standard	2h 39min 49s	3h 55min 30s
Rapid	30min 41s	1h 30min

The are techniques to enhance the fast charging by increasing the CC mode, so by reducing the length of the CV period. A method is proposed by Lin *et al.* in [31], where by measuring and controlling the resistance at the battery's terminals, it is possible to shift the voltage reference in order to increase the capitalised SoC in fast-charging modality. This requires further parameters that the thesis does not take into account, but proves that it is possible to improve the capitalisation of the battery's capacity Figure 2.7. In the specific case the extension of the CC range is associated to the fact that terminal voltage at the cell level V_{BATO} is less than the one measured at

the terminals V_{BAT}. Therefore the proposed method uses as switching moment from CC to CV the instant when the V_{BATO} (the internal) reaches the maximum value, so uses an higher voltage as reference during the CC mode and a lower one during the CV. By doing so it is possible to increase the CC range, which is the one suitable for the fast charging.

Alternatively it is possible to use an over sizing technique Equation (2.4) in order to have the desired max capacity at SoC of 80%, and it is done by imposing (for example) a $SoC_{min} > 40\%$ in order to compensate the two 20% capacity ranges that are not used. This would also increase the lifetime of the battery by not using it in its critical ranges.

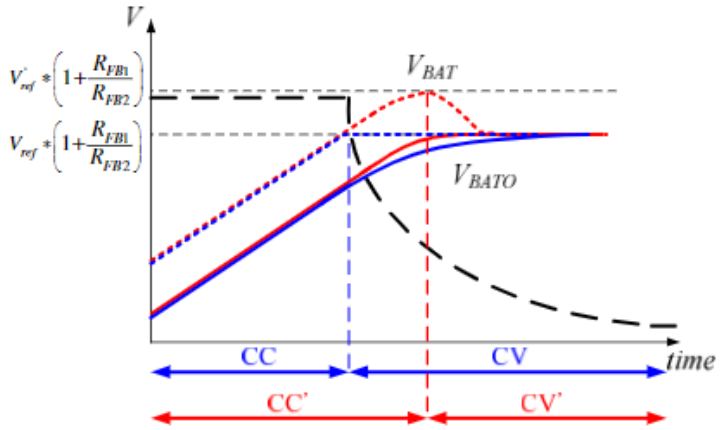

Figure 2.7: Extended CC pattern.

$$C^* = \frac{C}{1 - SoC_{min}} \cdot 100 \tag{2.4}$$

2.3.2 Charger's configuration

The charger choice has an important influence over the way in which the batteries are employed. The first differentiation is the possibility to have an internal charger (converter) in the EBs or one that is accessed externally. The internal charger, an On-Board Charger, is practically a controlled rectifier. This method is mostly used for private EVs that have to be charged in domestic environments by connecting the vehicle directly to a low voltage AC supply via Plug- In devices. Therefore the size of the internal charges are limited to small powers/capacity and it is not possible to have an external control because the vehicle self-modulates the power imposed by its charging protocol. For the purposes of this thesis, there will be an emphasis on external chargers, which are usually connected to a Charging Station. The charger typology could supply more power, and use higher voltages in order to reduce the current magnitude, thus the losses. There are two possibilities: to use a combination of an inverter and a DC-DC converter per vehicle, or to use a DC-DC per vehicle and connect all the converter primaries to a common DC-Busbar and then a single larger inverter connects the vehicles to the grid. The first method is mostly for isolated charging columns and has the peculiarity of a relatively small inverter's size. The first typology is useful

when there is the possibility to combine a small size of renewable distributed generation, with an EV. By controlling the DC-DC and the EV's inverter, it is possible to track the power from the DG (for example a domestic PV generation) and compensate the power in order to absorb a more uniform power from the distribution network [32]. The effectiveness of this method depends on the quality of the power tracking system and the coordination between all the vehicles attached to the specific node. When there is an increased number of vehicles attached to the same CS, the coordination of the DC-DC and inverters is more complex, therefore the second configuration is preferable Figure 2.8 [32]. With the second configuration it is possible to modulate the current absorbed by each EV by controlling the DC-DC converters and then by regulating the single big size inverter to the grid's necessities. The coordination in this case is simpler, but it is necessary to rely on a more expensive inverter, in addition to this, there is no redundancy if the inverter gets damaged.

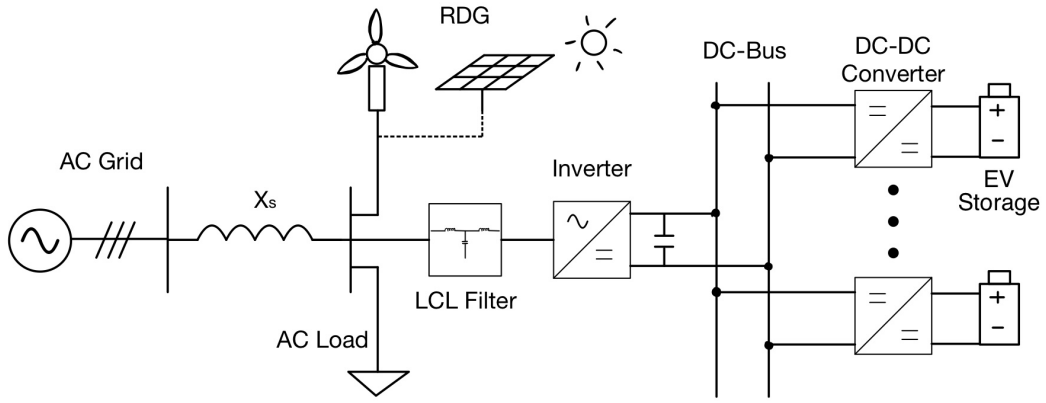

Figure 2.8: Schematic EV DC-Bus.

The application of these two configurations could have a great improvement in the distribution network's performance. As said in [32], it is possible to reduce the overall costs of the use of BESS systems, it is possible to introduce the participation of the energy (ancillary) market, peak-shaving/load-levelling services, etc. The effect of the controlled charging should be more effective as the CS is closer to the DG generation's, so the electrical central node where it is possible to find around the most of the distributed generation. In conclusion, this service could enhance the load factor and reduce the grid congestion.

The utilisation of half-bridge DC-DC converters Figure 2.9 is suggested by Ullah Khan *et al.* in[32], this typology has a bi-directional power flow, therefore the EVs could also provide power to the DN when it is required. This service requires a precise communication infrastructure among EVs, smart chargers and the DSO. This is necessary because the renewable DG has an average predictable pattern, but the instantaneous value can vary significantly. Since the energy that an EV could exchange is limited, in this case the service is more effective as "Power intensive" rather than "Energy Intensive", in order to chase the power fluctuations. The instantaneous value of the power generated by the DG has to be tracked and communicated rapidly in order to have an effective control over the devices. Even if studies like this proved the effectiveness of the method, the technology required is not yet available and the DN is not ready to host proficiently this type of service. Therefore, since the thesis aims to focus on a feasible method, mono-directional power-flow is prioritised. In this regard, the choice of the DC-DC con-

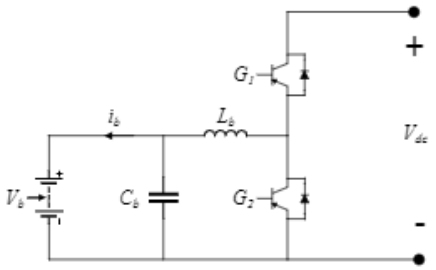

Figure 2.9: DC-DC Half-Bridge.

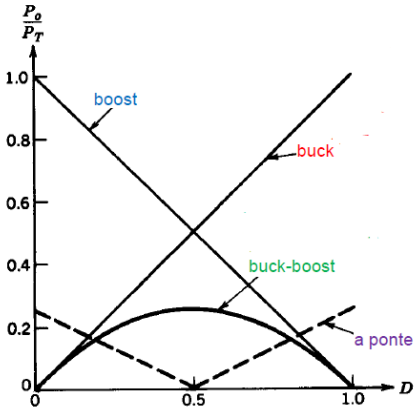

Figure 2.10: Efficiency DC-DC converters.

verter could be further discussed in order to obtain a more efficient and economical service. The bi-directionality of the half-bridge is possible just because of the introduction of more components rather than a DC-DC Buck or Boost [33]. Thereby the efficiency is sacrificed in order to obtain a bi-directional power flow, which would not be used in our case, so a DC-DC Buck converter is preferable Figure 2.10.

However, since the thesis aims to focus on a transitional method, it is assumed that in the future, the DN will be ready to host the bi-directional power flow of EVs. So, an economical advantage of using the Buck converter over the Half-Bridge needs to be investigated. If a CS has only Buck converters, a transition to a bidirectional power flow would require a huge investment in order to change all the CS converters. On the other hand, even if a Half-Bridge is less efficient, a transition to the new configuration could be implemented in a cost-less way. In conclusion, it must be verified that the energy cost with Buck DC-DC Figure 2.11 is more than the cost of renewing the CS. This is strongly dependent of the years that are required to have a full transition, but this is postponed to further studies.

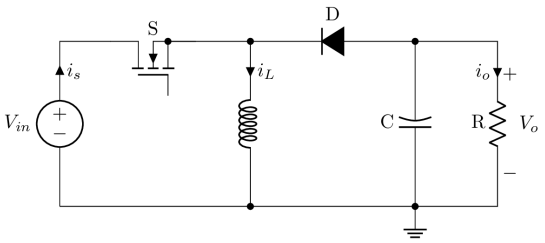

Figure 2.11: DC-DC Buck.

The other problems involving EVs and the CS, include: uncertainty of the EV's parking pattern; plugging problems; different typologies and sizes of the batteries, etc [32]. These aspects add randomness to the EV's charge planning and management. Fortunately, the thesis will focus on the EBs rather than private EV, which have: higher batteries' capacity, same size and typology, scheduled mission that eliminates the randomness.

2.3.3 Standards and safety

Since the thesis focuses on feasible technologies, therefore a standardised approach is required. This is stated also in [34], where it is said that a standard approach is necessary in order to ensure a smooth transition on the EB's utilisation. In 2021 the EB quota was 4% of the global bus fleet. It is forecasted that is necessary to have at least 20% of EB over the total fleet by 2030 in order to achieve the Net Zero Scenario [35]. This shows the necessity to have a common approach in order to incentivise the production of universal components and methods. At the moment in the market there are several charging technologies that can be categorised in this way: conductive charging, wireless charging and battery swapping. The last two technologies do not yet have a market in Europe, therefore for simplicity (economically and constructively) the best choice is to use conductive methods. The conductive chargers could be via Plug-In service or via Automated Connection Devices (ACDs), the first one in more suitable for small private vehicles since they usually have a range of 60-150kW, the second one if preferable for public EVs because they could host a power range between 150-600kW. The ACDs could be catheterised in this way: including infrastructures mounted (Type A), roof-mounted (Type-B) and floor-mounted (Type C) Figure 2.12.

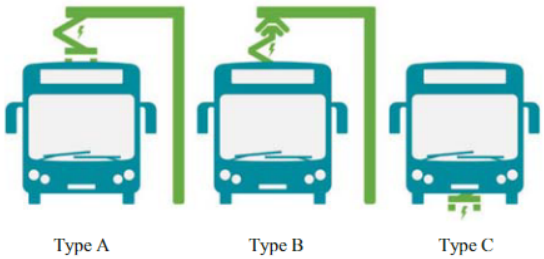

Figure 2.12: ACD Charging methods.

Even if the directive 2014/94/EU of the European Parliament (AFI Directive) provides some direction for charging infrastructures, there is not specific information regarding EBs. This is crucial, especially as EBs are forecasted to be the first real user that will be fully implemented in the electrical grid [36]. Farzam *et al.* have stated that there are projects as ZeEUS (Zero Emission Urban Bus system) that aims to build a standardisation approach to EBs technologies [34], then CEN-CENELEC (European Committee for Electrotechnical Standardization) start to use the ZeEUS's guidelines. Another project is the ASSURED, which aims to have an unified fast charging approach for every public vehicle (EBs, electrical garbage trucks, delivery trucks, etc). This project is the continuation of the ZeEUS one and focuses principally to the already cited ACDs charging methods. In addition to this, there is also the ASSURED 1.0 that aims to develop a interoperability reference and test protocol for the charging infrastructures [37, 38].

The safety topic is also important considering that EBs need more power in comparison to the private EVs, therefore if a public infrastructure will facilitate EBs, it is mandatory to be aware of a preferable method in order ensure safety in operation. It is possible to find some indication on what are some safety measures in addition to the compulsory one that are focused just on the battery [39, 40]. For other devices as the connector, which are a crucial point because in the case of Plug-In services that are in contact with civilians during the charging process, requires a particular caution. For example, the SAE J1772 regulates the connectors use according to the voltage type and magnitude Table 2.5.

Table 2.5: Chargers Standards.

Charging Standards				
Level	Type	Voltage	Current	Power
1	AC	120 V	16 A	/
2	AC	208-240 V	80 A	19.2 kW
1	DC	50-1000 V	80A	/
2	DC	50-1000 V	400 A	/

The thesis instead focuses on an ACD (Type B) because of the enhanced performances. In that case the levels of voltage and currents are higher because of the higher requested power from the EBs. In the IEC 61851 it is possible to find some indications on the relative: power, voltage, and current that an ACD "Opportunity Charger" could host Table 2.6 [41]. More specifically the Volvo's Opp Charger and EBs Table 2.7 and Figure 2.13 will be taken into account in order to base the algorithm on values that have a physical and feasible meaning [42].

Table 2.6: IEC levels.

Output requirements	
Power levels (kW)	150, 300, & 450 kW
DC Voltage (V DC)	450-750 V
Frequency (Hz)	50/60 +- 2
Output Current (A)	0 to 200 A, 750V, 150kW 0 to 400 A, 750V, 300kW 0 to 600 A, 750V, 450kW

Figure 2.13: Volvo's OppCharger and EB.

Table 2.7: Volvo Charger and EB.

Volvo OppCharger	
Maximum charging power level for EB (kW)	450
Output DC voltage (VDC)	500-750
Max output current at 750 VDC (A)	200/400
Ambient temperature (°C)	30
Volvo 7900 Electric Articulated	
Battery type	Li-Ion
Voltage (VDC)	600V
Capacity (kWh)	264-396

2.3.4 Charger Model

In order to study how batteries behave to different current input values and patterns, it is necessary to define a model of the charger. Usually the charge process is implemented using CV and CC patterns by using ideal generators. In the case of the thesis, it is necessary to model a charger that will have different current inputs. Therefore, it is necessary to use a DC-DC converter current controlled. M.Ahmed proposes a simple model that controls an ideal current generator, by using a PID controller [43]. In this case an average model permits a fast simulation of the charger and powerful for high level algorithm estimations. From the battery's side a model of already mentioned. The Tremblay's model is also used by M.Ahmed and the voltage, current and SoC pattern that is possible to appreciate at battery's terminals are Figure 2.14.

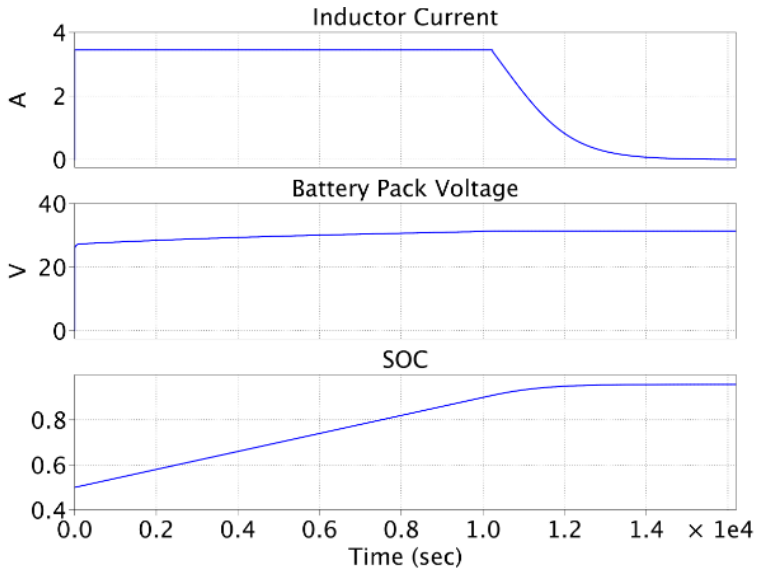

Figure 2.14: Current, Voltage an SoC with the average model.

However, in order to be more accurate and include the converter's switching effect, a controlled DC-DC Buck instead of a current generator is employed. In this way, the output also reveals the contribution of the switching (current and voltage ripples). This could be useful to appreciate if the ripples could have an incisive effect on the final computation of the energy. Therefore, it is possible to appreciate the difference between the Figure 2.14 and Figure 2.15, Figure 2.16 and Figure 2.17. Holistically, the behaviour of the DC-DC Buck controlled respects the average model's pattern, so it could be considered acceptable and more realistic.

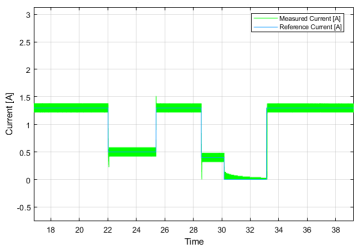

Figure 2.15: Current.

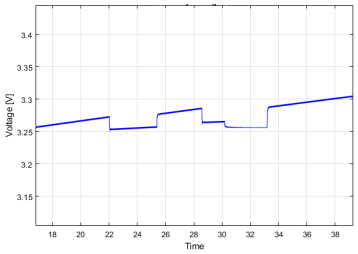

Figure 2.16: Voltage.

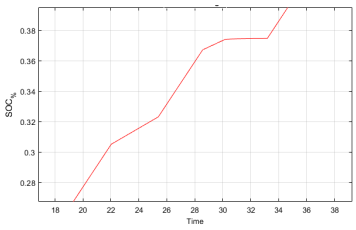

Figure 2.17: SoC.

These considerations are necessary to extrapolate the SoC, Energy and Power patterns when there is not a CC condition. In order to do not weight down the algorithm by introducing inside the mathematical battery and charger's mathematical model, it is possible to simulate a charging pattern via $SIMULINK^{TM}$ in order to verify which are the conditions that keeps the state's variables linear or constant. In this way it is possible to decouple the charger and battery model from the algorithm with the purpose to keep the algorithm light and to ensure its convergence.

2.4 Load management

2.4.1 Necessity

The electrical load is intrinsically linked to the final users' power demand. Therefore it does not follow a reasonable pattern. On the contrary, the load follows rules that are deeply connected with several complex parameters as social, economical, climate, etc. For example the load pattern might vary from the summer to winter due to the increase of HVAC systems. It might follow different patterns also that depend form the type of loads (industrial, residential or commercial) which have different patterns and magnitudes. In the last years there is the introduction of new actors that are able to change drastically the load, the distributed renewable generation and electric vehicles. Both these elements are characterised by high uncertainty. The problem comes because the electrical system must follow as a rule that all the power that is produced must be consumed, and vice versa. If this rule is not respected it might have disastrous consequences. The overproduction, if is not controlled, could cause the acceleration of the Synchronous Generators (SG) rotor Equation (2.5), on the other hand if the demand is too high and in the worst case overcomes the production, the SG would not be able to maintain the stability Figure 2.18. In both cases if the level of unbalance is not excessive, it is possible to act with the Frequency Regulation in order to keep the stability.

$$J\frac{d\Omega}{dt} + b\Omega + C_{em}(P_{out}) = C_m(P_{in}) \tag{2.5}$$

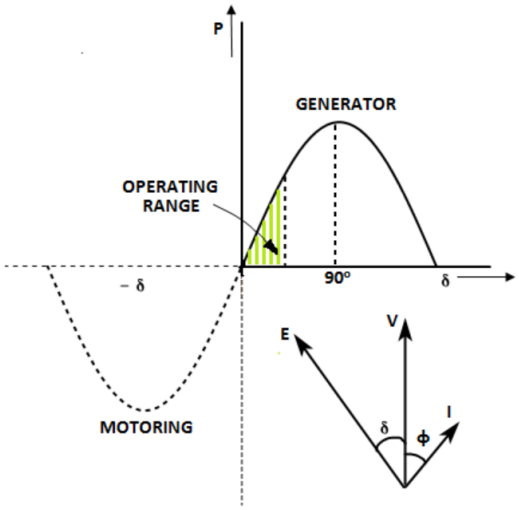

Figure 2.18: Synchronous Generators stability range.

If the stability is maintained, there is another problem with a load that varies continuously and often significantly. The electrical service follows the Electricity Market's (EM) rules, therefore when there is a high power demand the price have the tendency to rise, and vice versa. In addition, since the RES are also in the market, the EM has imposed that their production must have the priority in the merit order [44]. Therefore, the volatility of the RES production is connected to the price of the electricity. A typical sign of the RES production and how changes the daily load is the "Duck Curve" Figure 2.19 [45].

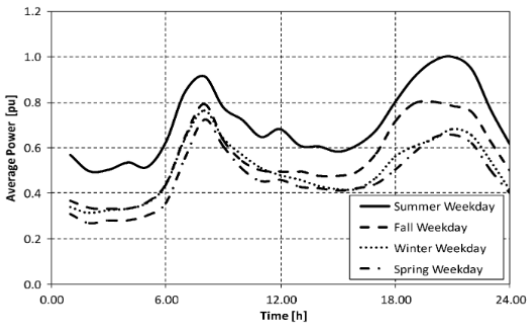

Figure 2.19: Duck curve during different seasons.

This load curve is generally forecasted by the Transmission System Operator (TSO) or the Distribution System Operator (DSO), then it is used in order to build the prices in the Day Ahead Electricity Market (DAEM) in order to assign to each generator their production share. There is also the Ancillary Market, which prepares the quota of production that must be ready to cover a production holes, or to reduce the power of some in case of power mismatching.

Another type of problem that a non-managed load could cause is presented in [46], where the unavoidable increase of the DRG in the DN might cause problems as over voltages, uncontrolled reverse power flow that might congest the lines, protection (since the DN is not equipped with distance protections which are able to track faults in both directions), etc. According to Uddin *et al.* the problem of the small capacity power plants is presented, such as small gas power plants or diesel generators [47]. These are widely used to mitigate the peaks Figure 2.20 or the valleys Figure 2.21 [12].

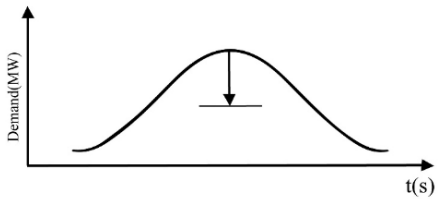

Figure 2.20: Peak mitigation.

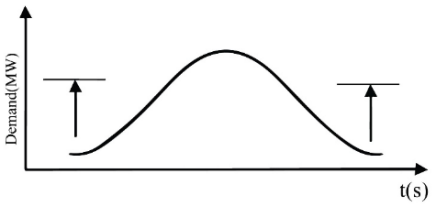

Figure 2.21: Valley mitigation.

The problem of this type of action according to Uddin *et al.* is the economical and environmental cost. Usually these type of plants are not efficient and a broad use can cause a non-trivial amount of emissions (the actual production of CO_2 by the power plants and the indirect one by the transports that are necessary to supply the fuel). In addition to this, the best amortisation of the plants is achieved by using them at the rated power for as long as possible. However, since their aim is to provide an occasional adjustment of the load, they cannot cover the investment, and the operational and maintenance cost. L. A. Wong and V. K. Ramachandaramurthy addresses also the problem of the ramp produced by the RES production, which is difficult to be followed by traditional power plants due to their slow reactivity and latency in the communication process [46]. Another action could be done at the Low Voltage (LV) level as stated in [48], which proposes a solution to harness the unbalance among phases.

It is possible to find a detailed study on the reasons to push on Peak Shaving or Load Levelling (load management) solutions Table 2.8 [47]. Therefore, the improvement of the load with peak shaving or load levelling is becoming an important research area due to its effects of several critical areas ad: network losses, congestion, generator's management, costs, etc.

Table 2.8: Reasons to implement Peak Shaving or Load Levelling.

Grid Operator	
Power Quality	Instability Voltage fluctuation Total blackout
System Efficiency	$P_{loss} = I^2 xR$
RES integration	T & D life extended Stability and Reliability Reduction of fossil fuels
Efficient energy utilisation	High Load Factor $LF(\%) = P_{avg}/P_{peak}$
Cost Reduction	System design for lower capacity Save of fuel and maintenance costs
End User	
Cost	Reduction of the electricity price

2.4.2 Peak Shaving and Load Levelling

The "Peak Shaving" is referred to the practice of cutting the highest and the lowest load peaks. On the other hand, the "Load Levelling" is the practice to modify the shape of the load in order to have a constant demand at a particular node of the network. The latter is a more challenging task because it aims to modify continuously the demand in order to keep it constant. According to Uddin *et al.* there are three macro strategies that are possible at the moment: the recourse of Battery Energy Storage Systems (BESS), Demand/Response (DR) or the management of the Electric Vehicles (EV). The BESS are designed to work just on the load balancing, therefore it is an efficient solution and the most promising. It works with the implementation of batteries with a considerable capacity that are able to provide services as: frequency regulation, maximise the RES output and peak shaving. However, this type of technology is not economically convenient at the moment. The BESS sizing is a crucial aspect because if it is implemented correctly, it might increase the costs since these type of systems have an economical reward just when they are actively working. Although, BESS are by definition an Ancillary Service, and as such, will only be used in critical conditions. If the BESS is oversized, the cost has to be charged on the few working hours. That is why such service could be introduced just with economical incentives. Lastly, if there is an incident, there is an extreme fire risk with large BESS systems, so the storage plant position has to be studied correctly (even more in urbanised areas).

The DR system involves the final user in order to modulate the load. The user is awarded to connect or disconnect loads (or EVs) with a specific schedule, and this process is managed by an aggregator Figure 2.22, which is a figure that governs the final users in order to satisfy the TSO/DSO's requirements. It manages the energy and economical flow with tailored contracts and methods on the user's side [49].

This is considered the most challenging method to manage the load, as it relies on the users behaviour. It requires a solid market system to offer reasonable awards not just based on the electricity price. In addition, it requires complex communication infrastructures which are not available at the moment [13], so the complexity of the entire system is high since it has several actors that have to be managed.

The last type is the management of the EV, which is not possible at the moment since there are not enough vehicle and infrastructures to deliver an effective service. However, the number of the EV sales share in the Net Zero Scenario (NZS) is forecasted to grow exponentially Figure 2.23 [50], therefore there will be an important amount of energy (EV count as load and storage) to manage. The peak shaving and load levelling in this case is done by cleverly charging the vehicles ("Smart Charging" techniques) to achieve the desired load at the grid side, from the other side to have the vehicles charged in time.

This approach has some challenges too, because the EVs are only active on the grid when they are parked. A single vehicle has a weak effect on the load side and the charging synchronisation is a complex task since it relies on the user's random behaviour. Controlled charging infrastructures are not sufficiently available anywhere, and it is more challenging to develop them in urban environment. That is the reason why this project wants to focus mainly to EBs in order to introduce the V1G (or Unidirectional Smart Charging) that might solve the capacity, scheduling and cost problems. Even if the IEA has reported in [51], that globally less than 10% EBs stock in 2020, there is an opposite trend for urban environments. In order to move towards more environmental scenarios some important cities, reported in [52], they started to move to (partially) "car-free" cities and to shift to public transports systems.

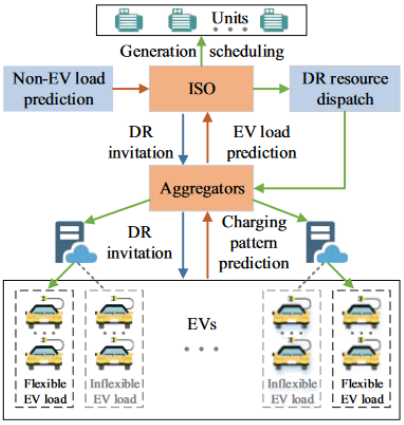

Figure 2.22: Aggregator operation.

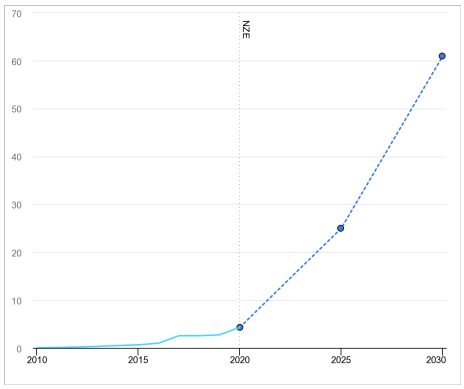

Figure 2.23: EV share forecast NZS Scenario.

As a comparative approach to verifying the algorithm's performance is not viable with the examples described in the literature aiming for different results, a separate criterion must be used. The strategy used in this paper involves several stages. To begin, EB and CS data that make physical sense are employed, but this approach will not always achieve optimal results. The first goal is to determine which scenario fits with a relative random EB

and CS and to confirm that it fits with the tendency of the future DN's composition (moving towards DNs with prevalence of RDG and storage). The second stage prioritises the 'best' scenario to determine the most suitable configuration or the EB/CS (charging voltage, number of charging slots, fleet size, etc) and compare it to currently existing CS regulations in Table 2.6 and EBs in Table 2.7.

3 Methodology

3.1 Extrapolation of Battery and Charger's information

Software as *SIMULINK*^{TM} permits the link through different processes in order to simulate complex models that does not have a linear solution. In order to do so, are used methods to solve ODE (Ordinary differential equations) by using variable-step/variable-order solver based on the numerical differentiation formulas. Even though it is an effective method, from a computational point of view it requires too much time in order to solve even relative simple systems as a battery connected to a charger. If it is assumed to simulate a fleet of vehicles, this method becomes totally impossible. It is possible to model a current controlled DC/DC Buck as an ideal controlled current generator in order to lighten the process, however by doing this inevitably some of the dynamics of the original device is lost.

Since the aim of the project is to built an algorithm that is simple, in terms of the required inputs, and robust in terms of the computational effort and convergence, it is necessary to find a compromise between the accuracy and the simplicity. In this regard, it is possible to notice some specific patterns in the charging process that allows to linearize the patterns within a certain working boundaries or to neglect some effects.

3.1.1 Battery's usage limits

The SoC-Voltage Equation (2.2) curve of a typical has a constant approximately between the 20% and 80% SoC. On the other sides the polarisation effect bends the curve. Between 0-20% SoC there is a prevalence of the Voltage Polarisation where there is a retardation of the electrochemical reactions. On the other side there is the Resistance Polarisation which is a phenomenon that happens when the battery is almost fully charged 80-100% SoC, in that

range the internal resistance increases, therefore will be an additional voltage component due to the interaction between the current and the Polarisation Resistance, which will be a function of : SoC, current and battery's parameters Equation (3.1) that could be derived with the method presented in [27].

$$V_{batt} = E_0 + R_{int} \cdot I + R_{pol}(I, SoC) \cdot I \tag{3.1}$$

In order to verify which is the actual effect on a battery with Table 2.7 table's characteristic, the Tremblay's method to extrapolate the parameters that are necessary in order to build Equation (2.3) equation. Normally it would be necessary to study graphically the SoC-Voltage manufacturer's curve to extract the points of interest, however *SIMULINK*^{TM} allows a fast extrapolation of the parameters by introducing the nominal parameters of the battery (capacity and voltage). By using the automatical tracking, it is possible to obtain: E_0, R, K, A and B Figure 3.1.

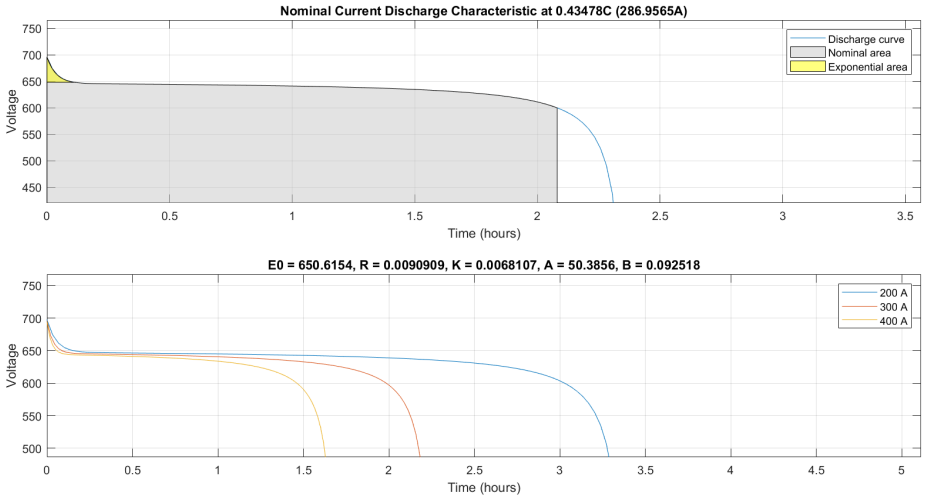

Figure 3.1: SoC-Voltage and Extracted parameters.

Subsequently the equation Equation (2.3) has been built and the E_0 term was extracted in order to verify what is the magnitude of the polarisation effect on the voltage when the battery is overcharged with a current of 600A. Since the polarisation effect is proportional to the current Equation (3.2), it was chosen the worst case in order to verify the discrepancy between the rated and distorted voltage.

$$V_{V.Pol} = K\frac{Q}{Q - it} \cdot it, V_{R.Pol} = K\frac{Q}{it - 0.1 \cdot Q} \cdot i \tag{3.2}$$

The final result that is possible to appreciate in Figure 3.2 shows that with a rated voltage E_0 of 650V the divergence of this value during the charging pattern is not significant since it is less than 5V (0.77%) in the signed range. Therefore it is possible to use the rated voltage curve as reference. In addition there is the possibility to considerate the voltage constant during the charging process because the produced error could be neglected.

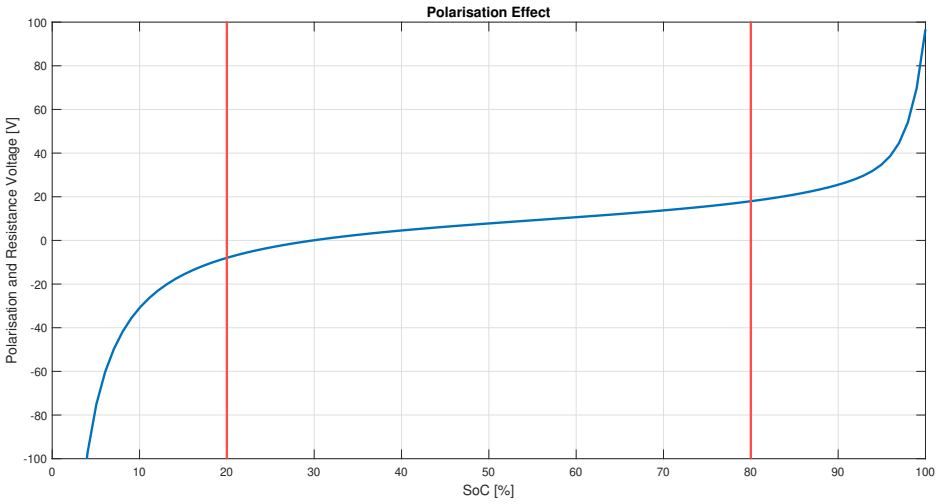

Figure 3.2: Limited Polarisation effect between 20% and 80% SoC.

The test was mainly done to justify analytically the 20-80% SoC range, which is coherent with the literature because the fast charging processes cannot be used in the 80-100% SoC range due to the already mentioned Resistance Polarisation, because the high magnitude of the current would increase the voltage at the terminals and react with the increased R_{int} by producing heat with the Joule Effect. On the other side for the safety reasons of the battery and the connected devices, the battery is not used between the 0-20% range (the 20% is considered as virtual zero).

The algorithm uses as input voltage a spline-polyfit of the Figure 2.1 manufacturer's curve in order to have more accuracy during the energy calculation Equation (3.3). The $MATLAB^{TM}$'s "Spline" function has produced the curve by using 54 different cubic polynomials. The quantity of pieces is justified by the necessity to use a large amount points on the middle part of the curve due to the natural shape of a cubic polynomials which tends to produce high parabolas between the enlivened points.

$$E[Wh] = \int_0^t i(\tau)v(SoC(\tau))d\tau \tag{3.3}$$

3.1.2 Current controlled DC/DC Buck behaviour

In order to have linear relationships it is necessary to modify the behaviour of the inputs so the energy stored Equation (3.3) will behave with a linear or constant shape. Since the batteries are used usually in CC mode in fast charging range, the analytical Equation (2.1) expression could be rewritten without the voltage terms and if the current is considered constant with discrete time steps, it is possible to simplify the SoC expression an linearize it Equation (3.4). Subsequently, since this SoC formulation is related to the [Ah] unit of measurement, it is necessary to modify it in terms of energy in [Wh] in order to easily compare with the data form the DAEM. To

do so it is used the Equation (2.2) relation, more specifically the spline-plolifitted function. Therefore, the energy in Equation (3.3) becomes Equation (3.5).

$$SoC_{\Delta t} = \frac{I \cdot \Delta t}{C_{rated}[Ah]} \cdot 100 \tag{3.4}$$

$$E[Wh] = \frac{SoC \cdot C_{rated}[Ah]}{100} \cdot V(SoC(I)) \tag{3.5}$$

With a view to the power of the process linearity, it is more useful to exploit the analytical expression that allow to forecast the actual energy on the following discrete time step. With the equation Equation (3.6) it is possible to find the new SoC level and the linearity of the formulation is clear. The computation of the new charge level is more comfortable in SoC form, then it is finally converted in Equation (3.7).

$$\begin{aligned} SoC_{t+1} = \left(\frac{100 \cdot V(SoC_t) \cdot \Delta t}{C_{rated}[Ah] \cdot V_{rated}} \cdot \right) I + SoC_t \\ y = m \cdot x + q \end{aligned} \tag{3.6}$$

$$E_{t+1}[Wh] = E_t + \frac{SoC_{t+1} \cdot V_{rated} \cdot C_{rated}[Ah]}{100} \tag{3.7}$$

The Equation (3.6) has to be verified by simulating the charging process by including the Buck's switching effect, with different constant currents in order to confirm the linearity with the model built in $SIMULINK^TM$ Figure 3.3

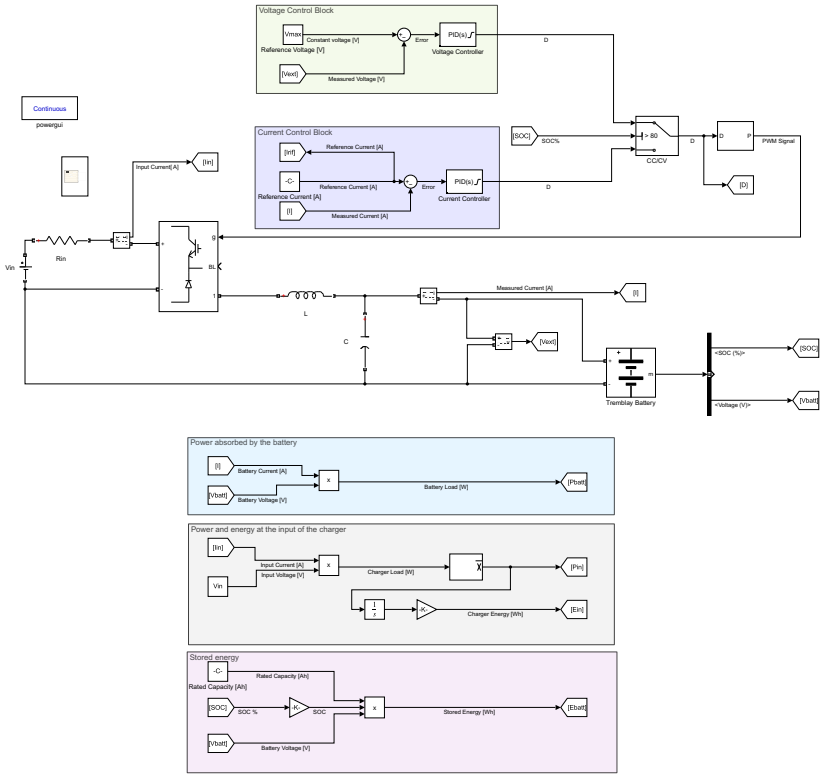

Figure 3.3: Charger $Simulink^{TM}$ Model.

In order to control the DC/DC Buck in constant current mode it is necessary to build up a transfer function of the average behaviour of the converter Figure 2.11. The first step is to explicate the state variables so the inductor's current i_L and the capacitor's voltage v_C in Equation (3.8).

$$\begin{cases} \frac{di_L}{dt} = \frac{1}{L}\left((V_{in} - v_c)D + (-v_c)(1-D)\right) \\ \frac{dv_c}{dt} = \frac{1}{C}\left((i_L - I_o)D + (i_L - I_o)(1-D)\right) \end{cases} \rightarrow \begin{cases} \frac{di_L}{dt} = \frac{V_{in}}{L}D - \frac{v_c}{L} \\ \frac{dv_c}{dt} = \frac{1}{C}i_L - \frac{I_o}{C} \\ i_L = i_C + I_o \end{cases} \tag{3.8}$$

Then it is necessary to label the state variables, the output and input so it is possible to find at the end a single relationship with just the input (current), the output (duty cycle) and the parameters Equation (3.9).

$$\begin{cases} D = u \\ i_l = x_1 \\ v_c = x_2 \\ I_0 = x_3 = y \end{cases} \rightarrow \begin{cases} \frac{dx_1}{dt} = -\frac{1}{L}x_2 + \frac{V_{in}}{L}u \\ \frac{dx_2}{dt} = \frac{1}{C}x_1 - \frac{1}{C}x_3 \\ x_3 = C \cdot \frac{dx_2}{dt} + x_1 \end{cases} \tag{3.9}$$

Then it is necessary to apply the Laplace Transform to Equation (3.9), obtain Equation (3.10) and explicate the final transfer function Equation (3.11). By testing the stability with the $MATLAB^{TM}$ "isstable" function, was

founded that the transfer function is unstable with an open-loop control. However by controlling the current with a closed-loop system the final transfer function Equation (3.12) turns out to be stable.

$$\begin{cases} sX_1 = -\frac{1}{L}X_2 + \frac{V_{in}}{L}U \\ sX_2 = \frac{1}{C}X_1 - \frac{1}{C}X_3 \\ X_3 = C \cdot s \cdot X_2 + X_1 \end{cases} \tag{3.10}$$

$$\frac{Y(s)}{U(s)} = \frac{s^2(2LCV_{in}) + 2V_{in}}{sL\left[s^2(LC) + sL + 2\right]} \tag{3.11}$$

$$\frac{Y(s)}{Y_{ref}(s)} = \frac{s^2(2LCV_{in}) + 2V_{in}}{s^3(L^2C) + s^2(2LCV_{in} + L^2) + s(2L) + 2V} \tag{3.12}$$

In order to test the step response of Equation (3.12) transfer function, it is necessary to size the parameters. Since the equation is related to a Buck converter, it is possible to use Equation (3.13) in order to size: the max duty cycle D_{max}, the inductor L and the capacitor C. By introducing a test battery's inputs in Equation (3.13) it is possible to obtain the parameters Table 3.1.

$$D_{max} = \frac{V_{out}}{V_{in}}, \quad L \geq \frac{(V_{in} - v_{out}) \cdot D_{max}}{\Delta i_L \cdot f_s}, \quad C = \frac{1 - D_{max}}{8Lf_s^2 \Delta v / V_{out}} \tag{3.13}$$

Table 3.1: Buck's input and output parameters.

Input		Output	
$V_{in}[V]$	5	D_{max}	0,86
$V_{out}[V]$	4,3	$C[\mu F]$	73
$f_s[Hz]$	10000	$L[\mu H]$	602
$\Delta i_L[A]$	0,1		
$R[\Omega]$	0,001		
$\Delta v / V_{out}$	0,004		

The step response of Equation (3.12) Laplace equation with the parameters of table Equation (3.1) is then adjusted with the auto-tuned PID controller of *SIMULINK*^{TM}. The PID parameters are therefore tuned as showed in table Table 3.2, in order to do not have a large over current before the settling. The settling time is not a priority since it is acceptable even without the controller because the algorithm does not use a real time control, but a step wise control every 15 minutes. This is because the load curve is taken from the DAEM which updates its data every 15 minutes, therefore it is not necessary to have an higher accuracy. The step response of the current is then represented in Figure 3.4 graph.

Table 3.2: PID parameters.

P	0,040161268
I	9,835618635
D	3,56E-05
N	5736,98636

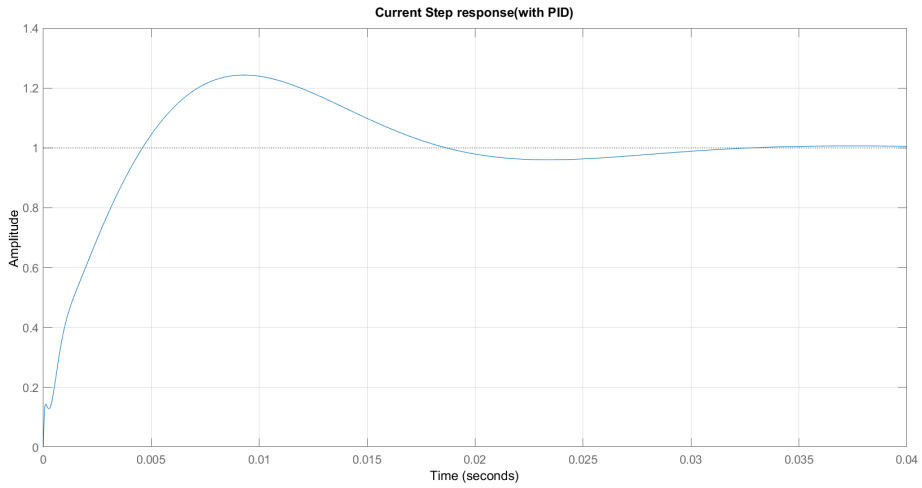

Figure 3.4: Current step-response with PID.

By controlling the current with different values as in Figure 2.15, the power Figure 3.5 and the energy Figure 3.6 at the DC/DC Buck terminals follow relatively a linear and a constant pattern proportional to the current's magnitude even with the additional effects caused by the Buck's switching effect. In conclusion, since it is possible to use all linear relations, it is proved that by using a more complex model that includes the polarisation effects, it is still possible to have linear energy/power if the battery is used in the 20-80% SoC range with a step-wise current's pattern. Consequently, it is possible to associate the current and power quantities to $MATLAB^{TM}$'s vectors and compute easily the current needed. This is done because in the algorithm's case it is required to test several times the energy of the vehicles in the time step $t + 1$ until the entire energy of the charging station matches with the objective. This would require a not indifferent computational effort by using the Equation (2.3) equation for each EB and the convergence would not be guaranteed.

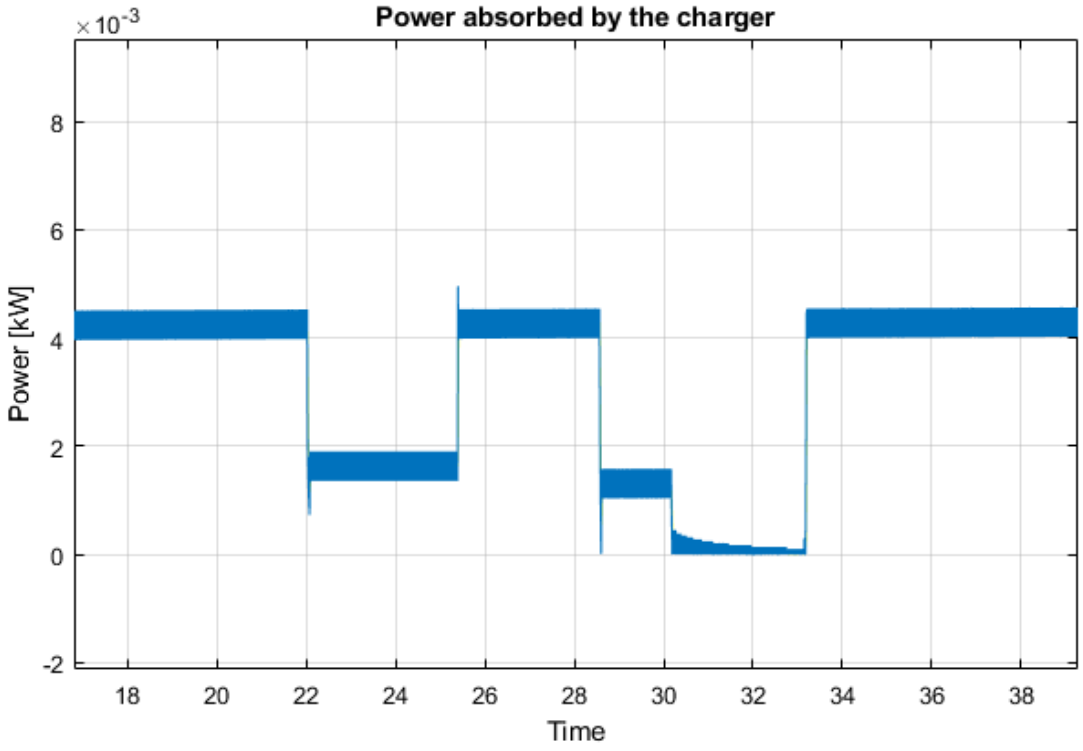

Figure 3.5: Buck's Power

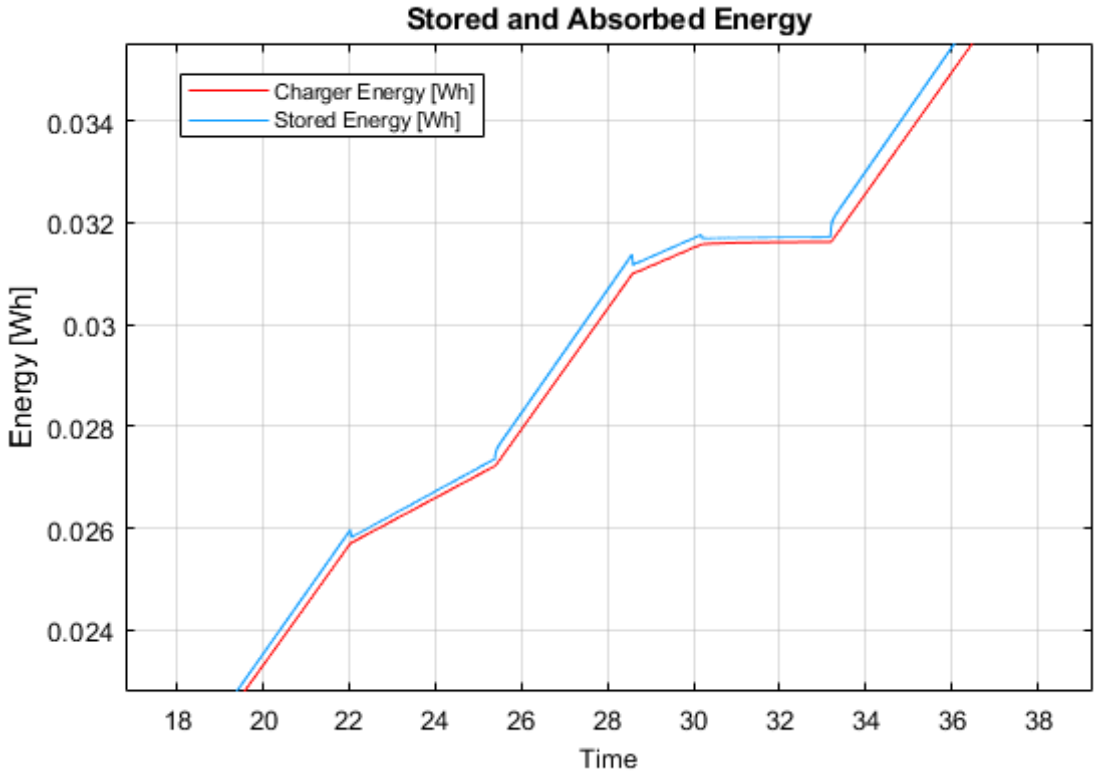

Figure 3.6: Buck's Energy

3.2 Algorithm

Some methods for managing electric buses or charging stations can be found in the literature. Zhuang P. and Liang H. proposed a stochastic method [53], Han B. et al. a method that uses timetables and routing as constraints [54], and Hasan M.M. et al. a method that improves electric motor efficiency [55]. Gkiotsalitisin K. emphasized the necessity of regular charging periods for EBs in lowering passenger travel time [56]. Zhang C. proposed a strategy for overall optimization of EB scheduling [57].

The algorithm presented in this study intends to propose a solution that may be employed in a smart grid transition by leveraging readily available data (DAEM, data-sheets, etc.) to construct a CS load profile and the EB scheduling, to achieve a given demand shape in a restricted DN. Furthermore, exact currents and EB schedules are prepared every 15 min for general CS management purposes.

The algorithm, written in $MATLAB^{TM}$, requires the load curve from the DAEM Figure 3.7 and the manufacturer's SoC-Voltage curve Figure 2.1. More specifically, the load curve was taken from the Italian TSO forecast [58].

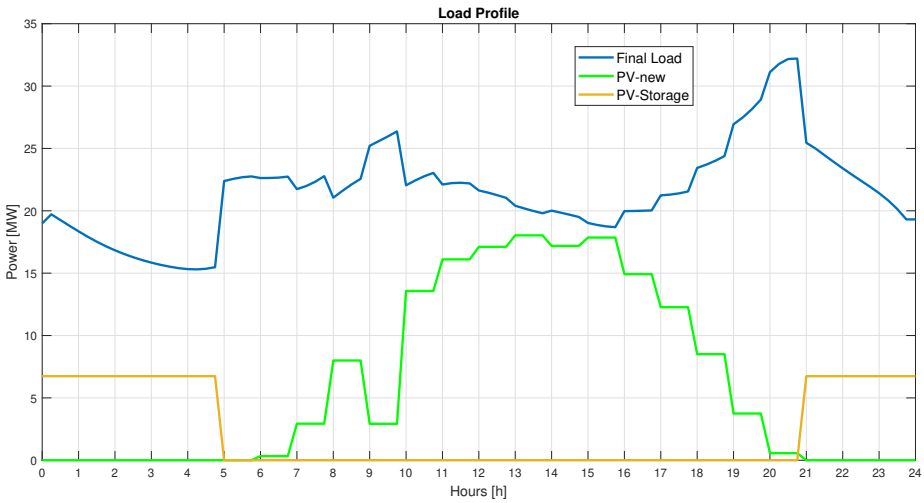

Figure 3.7: DAEM Load curve.

The load was scaled down in order to obtain values consistent with a DN and it was included the Photovoltaic (PV) power and the self consumption. In order to be able to simulate different scenarios, it is possible to modify the quota of the PV installed in the DN and the self consumption as percentage of its rated installed power. Since the PV's power that is stored for the self consumption is not part of the normal load, it reduces the PV's curve, so the Duck Shape is mitigated, while the load is further reduced during the dark hours, where the demand is already low. In addition to this, there is the possibility to regulate the produced power from 0-100% of the rated PV's power to simulate different weather conditions.

The initial demand curve is then polifitted in order to obtain Equation (3.14). The algorithm requires what is the desired level for the relative day, it could be a partial peak-shaving or a total load-levelling, so it is produced

a vector that contains the objective demand per each time step $\mathbf{P}_{objective}$. Since the $\mathbf{P}_{objective}$ is in a discrete form, in order to compare the actual demand with the objective the Equation (3.14) is discretized by computing the average power in a $\Delta t = 0.25[h]$ time span (the one used in the DAEM), and it turns into its vectorial form $\mathbf{P}_{load}$.

Subsequently, is computed the difference of energy between the actual demand and the objective, for every time step i long Δt so it is produced the $\mathbf{E}_{load}$ Equation (3.15) which with $n = 20h/\Delta t = 96$ elements. The power absorbed by thee charging station will be already incorporated in the $\mathbf{P}_{load}$ by considering every EB absorbing constantly the rated current I_r. On the other hand, during the $\mathbf{P}_{objective}$ the vehicles will absorb a "smart current" I_s depending on their $SoC_{\%}$ condition.

$$P_{load} = f(t) \tag{3.14}$$

$$\mathbf{E}_{load} = (\mathbf{P}_{load} - \mathbf{P}_{objective}) \cdot \Delta t, i \in [1, n] \tag{3.15}$$

Per each time step, the algorithm imposes the I_r current to every vehicle j by computing the new SoC with Equation (3.6), and then converting it in [kWh] by using Equation (3.7) it is possible to obtain the energy $E_{j(r)}$. In order to set the smart charging process it is imposed as starting current $I_s = 0$ to produce $E_{j(s)}$. Then in order to compute the difference of the energy between the normal operation and the smart process, it is explained the entire CS's energy transition with all m vehicles Equation (3.16). During the smart charging process the EBs will be charged with the same I_s except for the vehicles that if they were charged with I_s, they would exceed the $SoC = 80\%$. Therefore, for these vehicles the smart current will be charged with a current I_e computed with Equation (3.17).

$$\Delta E_{CS} = f(I_s) = \sum_{j=1}^{m} (E_{j(r)} - E_{j(s)}) \tag{3.16}$$

$$I_e = (80 - SoC_{\%}) \cdot \frac{C_r \cdot V_r}{100 \cdot V \cdot \Delta t} \tag{3.17}$$

The algorithm will perform firstly the energy for each EB in order to obtain Equation (3.16) for the i time step, then it is tested the objective function Equation (3.18). More explicitly, it is tested if the chosen current I_s produces the right reduction/increase of energy of the CS at time step i. If the condition is not satisfied, the process is repeated by increasing I_s by 0.1A until it is fulfilled. Then, for the following time steps $i + 1$ the SoC_{i+1} obtained by Equation (3.6) is assigned to SoC_i and the procedure is repeated until the last time step $i = n$ for each element of $\mathbf{E}_{load}[i]$. It is possible to notice graphically in Figure 3.8 that is not the energy already stored in the vehicles that matters for the final load shape, but the rise/reduction between each time step of the energy that has an effect. In the specific case there is $I_s > I_r$ with $\mathbf{P}_{load}[i] \ll \mathbf{P}_{objective}[i]$. Internally, the algorithm discretizes the power and computes the power from the energy of the CS, if the CS is able to levelize the power the lines matchese, otherwise the CS' power saturates at the maximum level, and shows in which timesteps the load-levelling will not be accurate as in Figure 3.9.

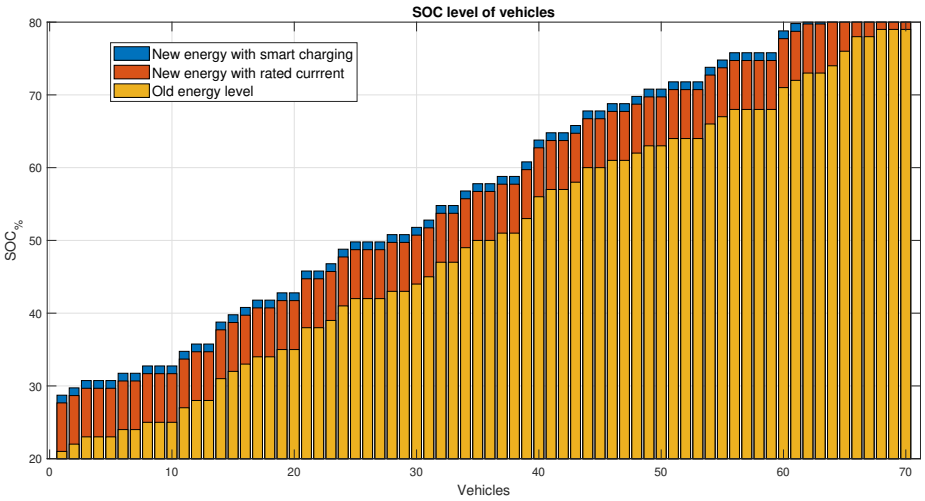

Figure 3.8: EBs SoC at time step t and t+1.

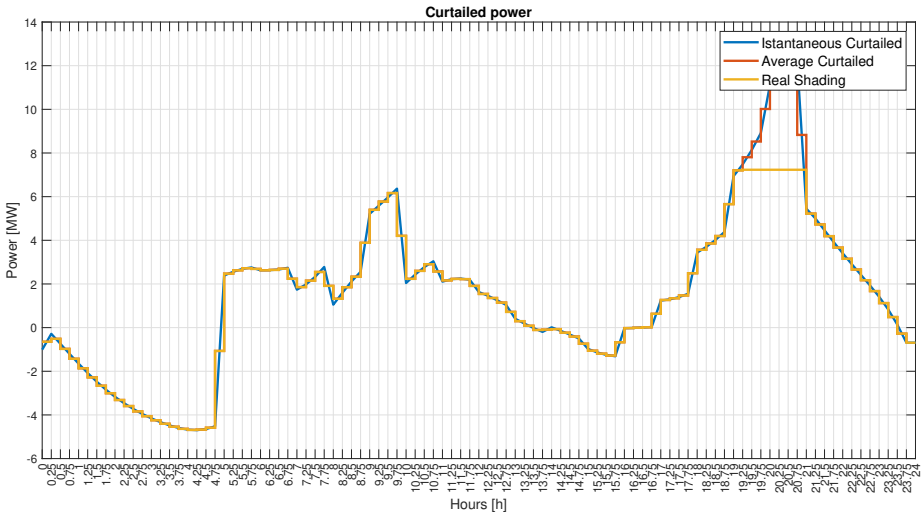

Figure 3.9: Internal power matching and discretization.

The smart current I_s will have four cases Equation (3.19). For any case it is not possible to have convergence problems, while the most critical case is when the difference between the demand and the objective power is more than the one that the CS could flatten ($\mathbf{P}_{load}[i] \gg \mathbf{P}_{objective}[i]$), in such chase the algorithm imposes $I_s = 0$ so it turns off the entire CS and reduces the load as far as the CS could do. The $\mathbf{P}_{load}[i] \ll \mathbf{P}_{objective}[i]$ case could require a long computational time since the current increases just with 0.1A every iteration until it reaches the right value or the maximum eligible current. An adaptive current increment could be used to improve this aspect. The last

unmarked case with $I_s < 0$ could be done just with a DC/DC Half-Bridge, therefore is not taken into account.

$$\Delta E_{CS}(I_s) - \mathbf{E}_{load}[i] \leq 0 \tag{3.18}$$

$$\begin{cases} \mathbf{P}_{load}[i] \gg \mathbf{P}_{objective}[i] \Rightarrow I_s = 0 \\ \mathbf{P}_{load}[i] < \mathbf{P}_{objective}[i] \Rightarrow I_s > I_r \\ \mathbf{P}_{load}[i] > \mathbf{P}_{objective}[i] \Rightarrow I_s < I_r \\ \mathbf{P}_{load}[i] = \mathbf{P}_{objective}[i] \Rightarrow I_s = I_r \end{cases} , i \in [1, n] \tag{3.19}$$

Consequently, the currents (I_s, I_e) and the $SoC\%$ are saved in Equation (3.20) every time step i for every EB j at each iteration. The vehicles that reach $SoC = 80\%$ at the time step i are then connected at $i + 1$ with a vehicles with $SoC = 20\%$ when it is considered the ideal case.

$$\mathbf{SoC}_{\%}[j, i], \mathbf{I}_s[i, j], i \in [1, n] j \in [1, m] \tag{3.20}$$

The tracking of the vehicles that reach $SoC = 80\%$ is saved in a vector **Cnn** Equation (3.21) that will contain $z_i < m$ EBs that have reached the limit. Then, the whole fleet is computed as Equation (3.22) in order to do an ideal load levelling. The **Cnn** vector is used to build the time slots where it is necessary to connect the vehicles. During the time steps where the number of ideal connected vehicles is higher, there is the necessity to have more EBs ready to be connected. Generally the Equation (3.22) will produce values that has no physical and economical meaning (e.g. 70 vehicles in the CS with a fleet of 1000 EBs), therefore the value is normalised by introducing the real size of the fleet that is available. At this stage, the algorithm assigns the real amount of EBs uniformly in the **Cnn** slots, and produces the $\mathbf{Cnn}_{real}$ Equation (3.23) vector that will have as elements $z'_i \leq z_i$ vehicles, the remaining will be set automatically in idle mode ($I_s = 0$) by Equation (3.17). Virtually, there will be some vehicles with $I_s = 0$ that stay in the CS because there are not enough EB ready to be connected, in reality the vehicles in idle mode (with $SoC = 80\%$) could start their mission. In other words, there is not the necessity to have m vehicles in the CS every instant. This vector could be used to built the timetables of the CS and graphically it is possible to know which are the most important time steps to actuate the connection, in order to coordinate the mission with the electrical demand requirements Figure 3.10.

$$\mathbf{Cnn}[1, n] = [z_1, z_2, ..., z_n] \tag{3.21}$$

$$F_{ideal} = m + \sum_{i}^{n} \mathbf{Cnn}[i] \tag{3.22}$$

$$\mathbf{Cnn}_{real}[1, n] = [z'_1, z'_2, ..., z'_n] \tag{3.23}$$

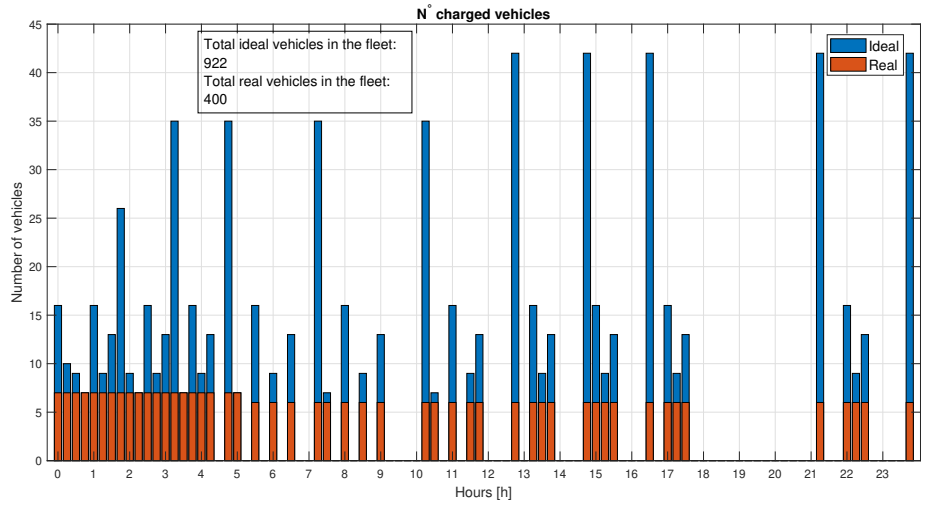

Figure 3.10: Ideal and real connection patterns.

In addition, it is necessary to set correctly the initial $SoC_{\%}$ value in order to do not have unfeasible connection patterns. If all the EBs are set at $t = 0$ with a $SoC = 20\%$, the connection patter would be like Figure 3.11, on the other hand, a uniform distribution of the initial SoC will produce a reasonable connection pattern Figure 3.12

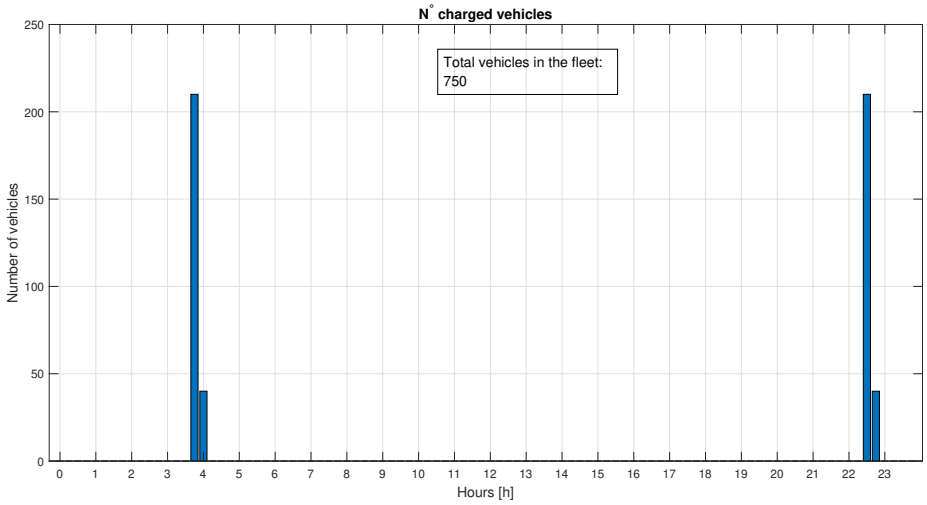

Figure 3.11: Connection with initial $SoC = 20\%$ for all EBs

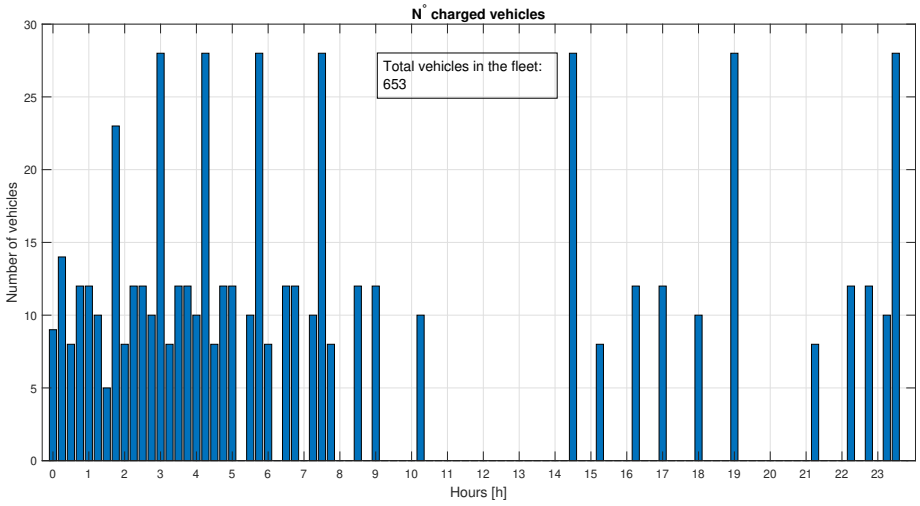

Figure 3.12: Connection with uniformly distributed SoC

The final mutual effects are computed in terms of power in order to be compared with the initial power demand. The power $\mathbf{P}_{r(cs)}$ of the CS when the EBs absorb I_r is computed with Equation (3.24), and the total power absorbed by the CS with I_s is $\mathbf{P}_{s(cs)}$ computed with Equation (3.25). The final load is then computed with Equation (3.26) and then plotted in order to verify the accuracy of the load levelling/peak shaving Figure 3.13.

$$\mathbf{P}_{r(CS)}[i] = \frac{1}{\Delta t}\sum_{j=1}^{m}(E_{i,j(r)}), i \in [1,n] \tag{3.24}$$

$$\mathbf{P}_{s(CS)}[i] = \frac{1}{\Delta t}\sum_{j=1}^{m}(E_{i,j(s)}), i \in [1,n] \tag{3.25}$$

$$\mathbf{P}_{newload} = \mathbf{P}_{load} - (\mathbf{P}_{s(CS)} - \mathbf{P}_{s(CS)}) \tag{3.26}$$

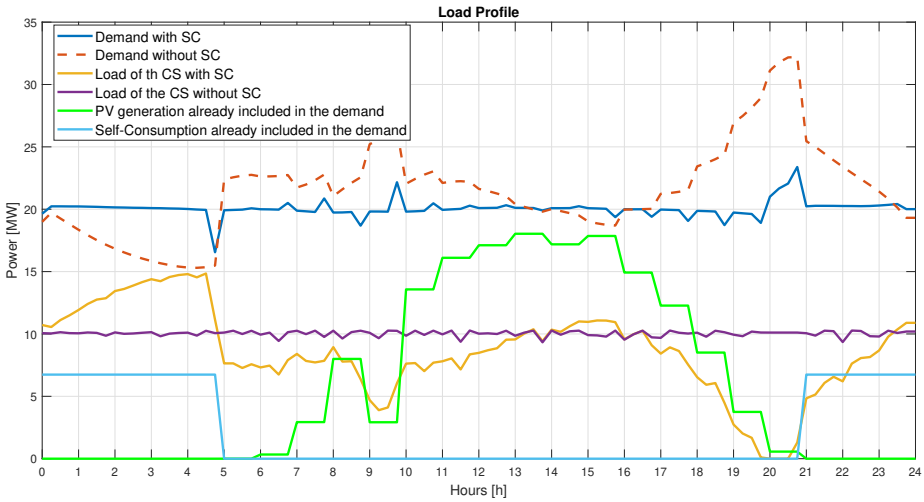

Figure 3.13: Final demand with load levelling.

The graph Figure 3.13 describes:

- The red line the demand without smart charging
- The blue line the demand when the CS enables the smart charging
- The green line the PV production
- The light blue line the self consumption
- The purple line the CS's absorbed power without smart charging
- The yellow line the CS's absorbed power with smart charging

In conclusion, in figure Figure 3.14 is shown a review of the whole algorithm.

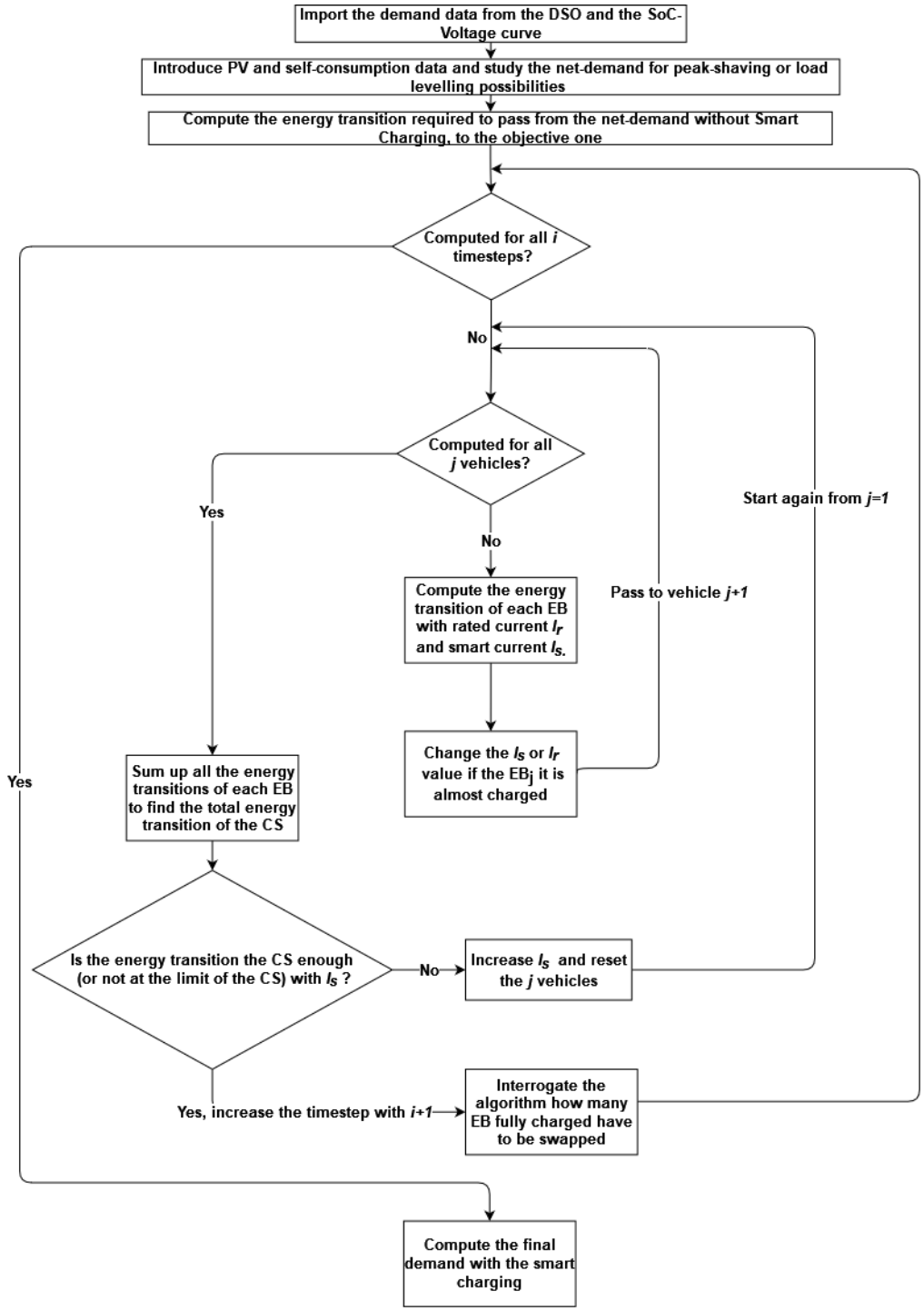

Figure 3.14: Algorithm flowchart.

3.3 Colour Maps

Another type of output that the algorithm produces are the colour maps by using the data stored in Equation (3.20). The maps are produced directly from two matrices sized $[i, j]$ which could be transposed into $Excel^{TM}$'s tables in order to have a schedule for the charging pattern for each EB, every time step. The graphical representation is needed in order to have a global view of what is happening in the CS. In addition, it is possible to observe that the magnitude of the absorbed current, reflects the networks behaviour. The $\mathbf{I}_s$ matrix, in the ideal case and the $\mathbf{SoC}_{\%}$ have respectively this form Figure 3.16 and Figure 3.15. In the current's map Figure 3.16 the x axis is the numbers of the EBs' charging slots, on the y axis it is shown the time in hours for a 24h day. Each vehicle's current is represented by a small coloured square * with the gradient that indicates the magnitude of the charging current. There are some squares that are not harmonised with the others Figure 3.16, those are the representation of the Equation (3.17) when the vehicles are almost fully charged. Therefore the squares right after the not-harmonised ones represents another vehicle. This aspect is better represented in Figure 3.15 when the gradient changes abruptly from red to blue. Apart from the almost charged vehicles, the others have the same charging current, that is why the colour looks uniform during a time step i. It is possible to notice that during 24h the colour does not change monotonously, this is because it reflects the networks requirements: red (high I_s) when $\mathbf{P}_{load}[i] < \mathbf{P}_{objective}[i]$ and gradually becomes blue (low/zero I_s) when $\mathbf{P}_{load}[i] > \mathbf{P}_{objective}[i]$.

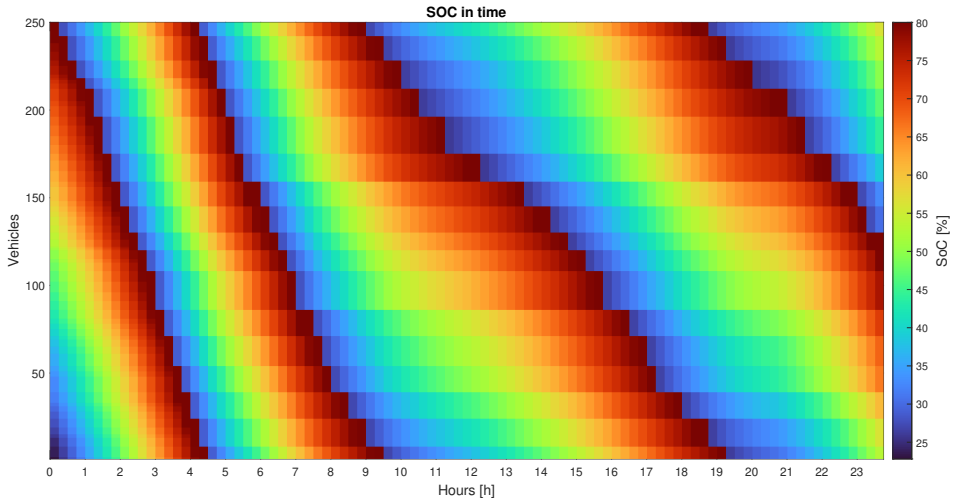

Figure 3.15: Colour map $\mathbf{SoC}_{\%}$.

*Normally the squares should be divided by black lines that enhances the contrast between each value. It is not possible to use them when there are many vehicles because the size of the line becomes comparable to the square's one.

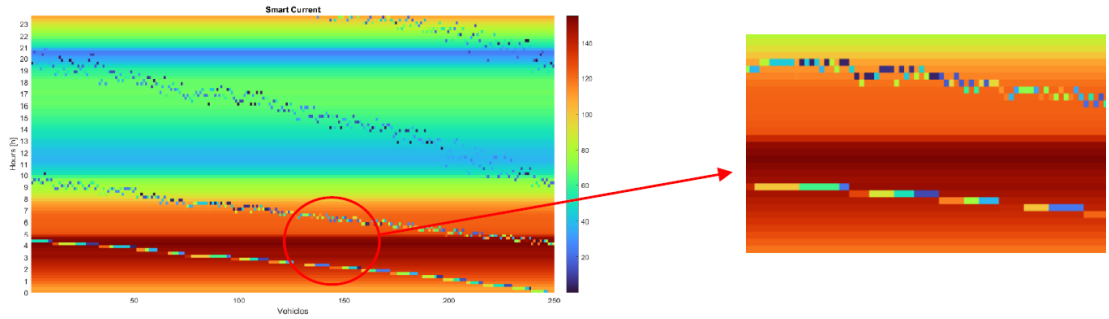

Figure 3.16: I_e representation.

Since the current is represented as % of the I_r there are some specific cases:

- Dark Blue when $I_s = 0$
- Light blue when $I_s < I_r$
- Green/Orange when $I_s \simeq I_r$
- Red when $I_s > I_r$

On the other hand the *SoC* map Figure 3.15 it is useful to represent the connection points and the velocity of the charging process. When the gradient takes more time to arrive from blue to red, it means that the CS is absorbing less current and vice versa. The map is useful in order to verify graphically the amount of time that the vehicles would require in order to e fully charged just by looking at the Δt between the top blue square, to the last red one.

4 Scenarios

4.1 Ideal Scenarios

The algorithm allows to simulate how the actual demand from DAEM would change if the smart charging would be enabled. In addition to this, it is possible to use it also to simulate different CS and network's conditions. It is possible to change the primary transformer rated power in order to simulate a DN that absorbs more power, or to change the charger's parameters (voltage, rated current, EB's slots, etc.) in order to verify what is the best configuration. It is also possible to create some scenarios with different levels of DRG and storage.

Is is interesting to analyse firstly how the CS and the network respond to different DRG scenarios in order to find which is the best charging condition in the ideal case and to verify if the algorithm produces meaningful values in different working conditions. The ideal case assumes that it is possible to connect as many vehicles as needed, therefore every time a vehicle reaches $SoC = 80\%$, the next time step is changed with a $Soc = 20\%$. This will produce a fleet's size that will have no physical meaning. When the real fleet size is imposed, it always worsen the behaviour, therefore for an overview of the best scenario it is sufficient to study the ideal condition and then analyse more deeply the real behaviour of that one. The algorithm requires the ideal result anyway, therefore the study of the scenarios with the ideal hypothesis requires half of the computational effort, since the real result is obtained by processing a second time the algorithm.

Will be considered three scenarios: the one without PV and storage, the one with PV and lastly the one with PV and storage for the self consumption. For the test will be used CS and EB's parameters that are not the one used in reality by Volvo Table 2.7, but a CS with worse performances (with an Opp-Charger). The parameters for the test are Table 4.1 where the voltage is lower than the one used in Table 2.7 in order to verify how much the EBs would be stressed on the current side. The P_{PV} is the PV's installed power which is then modulated in order to simulate a cloudy day during the no-PV scenario. The $P_{Self\%}$ is considered as quota of the installed PV, which has a mutual effect on the power produced by the PVs. The energy used to charge the storage for the self consumption

is a quota taken from the PV's production that will not satisfy the demand, therefore if the self consumption is included, the power available from the PV is lower. The self consumption is hypnotised to be activated during the "dark hours" therefore when the PV's production is zero. The final objective of each scenario is to actuate a load levelling with 25MW constant for 24h.

Table 4.1: Scenarios' parameters.

$P_{transt.}$	$P_{objective}$	m	V_{rated}	I_r	C_{rated}	P_{PV}	$P_{Self\%}$
30 MW	25 MW	250	400 V	100 A	400 kWh	10MW	20%

4.1.1 Scenario without PV and storage

In the first scenario simulates the absence of the PV's power. The load demand before the smart charging process assumes a shape that could be the one of a DN during a winter day Figure 4.1. The new demand with the smart charging process is represented in Figure 4.2.

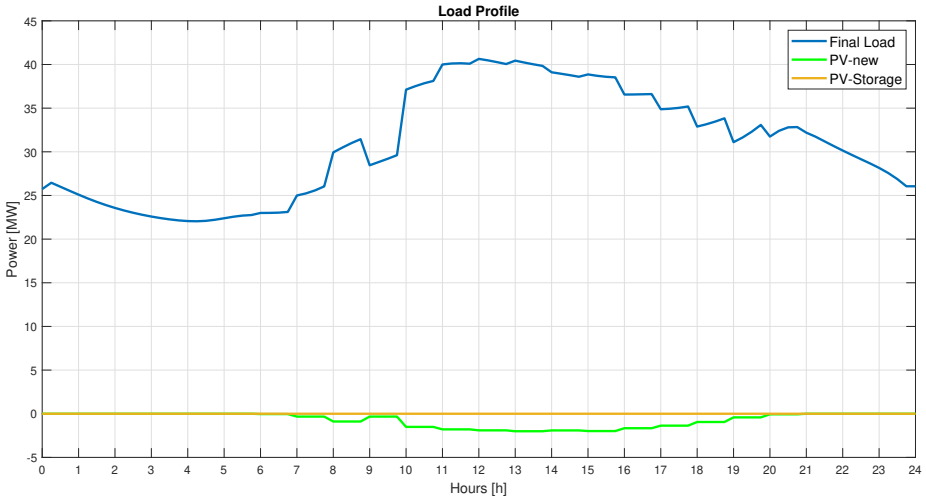

Figure 4.1: Demand with no PV

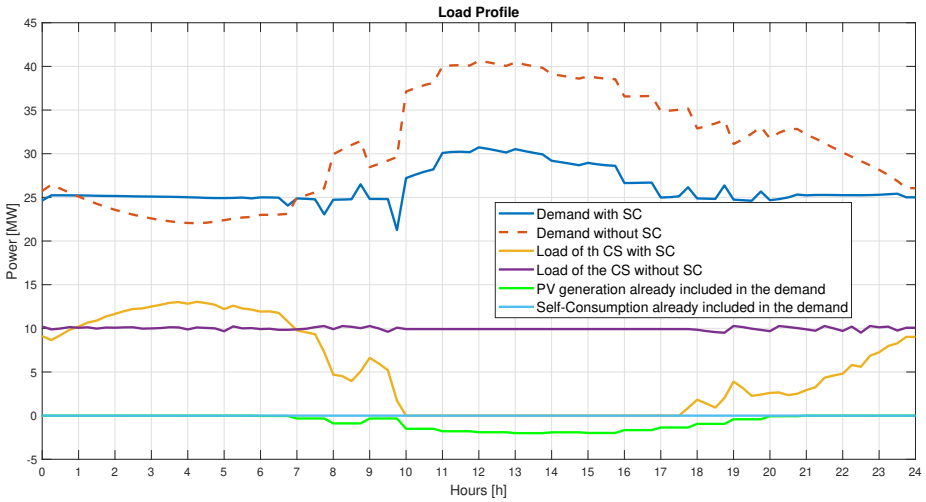

Figure 4.2: New Demand with no PV

The transformer is over-loaded during the peak demand at noon and there is a large difference between the highest and lowest peak. This has a heavy impact on the achievement of the load levelling. Since it is assumed that

during the working condition without smart charging the CS assigns 100A to each EB, the maximum power that the CS could shut down is 10MW. The difference between the peak and the objective power in Figure 4.1 is more than 10MW, therefore the CS is not able to achieve perfectly the load levelling. The purple line in Figure 4.2 shows the ideality of the connection process because in every time step there are enough vehicles ready to be changed. In real conditions the CS's would absorb a variable power even with the I_r imposed to each EB because the number of vehicles in the CS would not be always m. It is expected that with a real fleet size the result would be worsen because the difference between $P_{r(CS)}$ (purple) and $P_{s(CS)}$ (yellow) should be lower, so there should be less power available for the ancillary service. The only case that might allow to achieve the objective is to do not limit the $P_{s(CS)}$ lower boundary (0MW), in that case the power will be negative so the vehicles will deliver power to the network. However this is not possible with the unidirectional smart charging, but easily adaptable in the algorithm. It just depends on the technology on which it is tailor made, in this case it is related to a current controlled DC/DC Buck. The current I_s and the $SoC_{\%}$ represented relatively in Figure 4.3 and Figure 4.4. The current follows anti-symmetrically the load's behaviour as expected, with a complete shut down of the CS during the noon's peaks and an over-load of 120% of the I_r during the morning demand valley. The ideality of the connection in this case is made evident by the fact that horizontally every time step i the colour is uniform. Similarly, in the Figure 4.4 it is possible to appreciate the difference of the charging time between the vehicles connected in the morning (fast gradient) and the ones charging at noon (slow gradient). Without comparing the results with other scenarios, it is possible to appreciate that the results show the expected behaviour, thus it confirms the veracity of the algorithm's effectiveness.

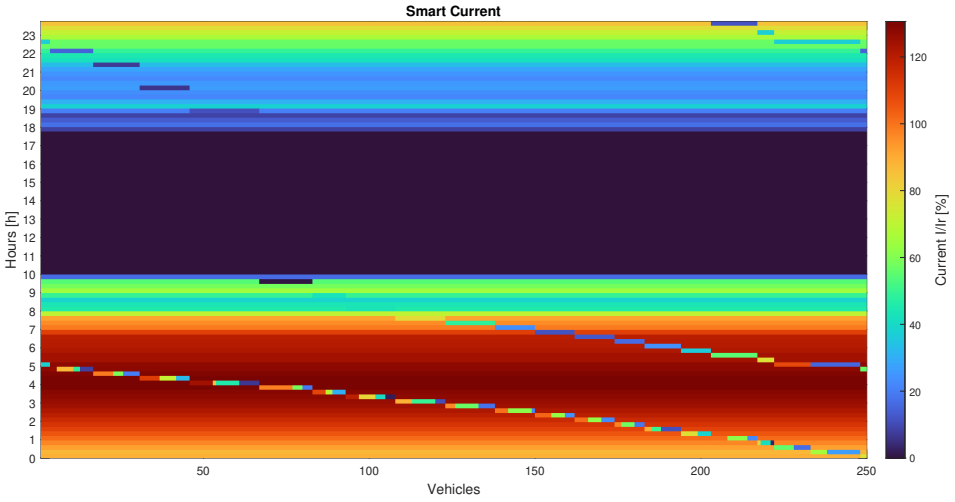

Figure 4.3: Current with no PV

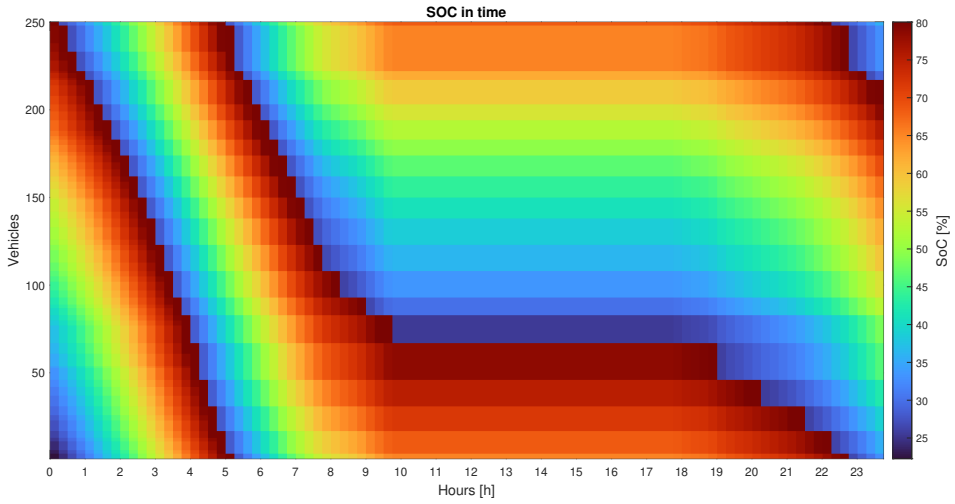

Figure 4.4: $SoC_{\%}$ with no PV

The schedule of the vehicles that have to be connected is shown in Figure 4.5. With a CS that hosts 250 EBs in a total fleet of 807 vehicles, it is possible to appreciate that is the intention id to actuate a load levelling with high difference between the valleys and peaks, the number of vehicles that will pass though the CS will not be uniform in 24h. During the over current the vehicles charge faster, therefore it is necessary to replace them (in the ideal case) often, on the other side during the noon's hours there are not conenctions because the vehicles are not charging.

In conclusion, in a no-PV scenario would be preferable to assign to the CS two separate peak-shaving less challenging to cut the highest peak and to fill the valley, but at the same moment to do not have the CS shut down for long periods or in over-load mode.

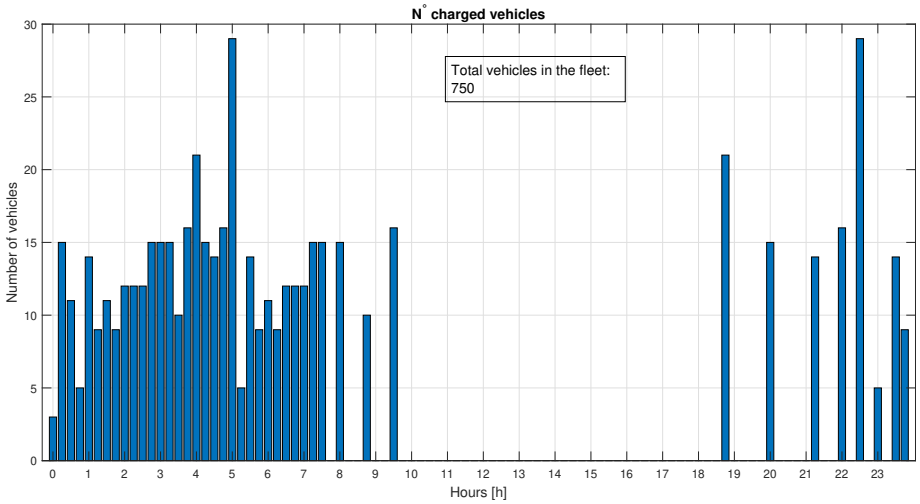

Figure 4.5: Connection with no PV.

4.1.2 Scenario with PV

In the scenario that includes the PV generation it is assumed that the PVs are working at 100% of their rated power (a sunny day). The load before the smart charging is Figure 4.6 and the new load is Figure 4.7.

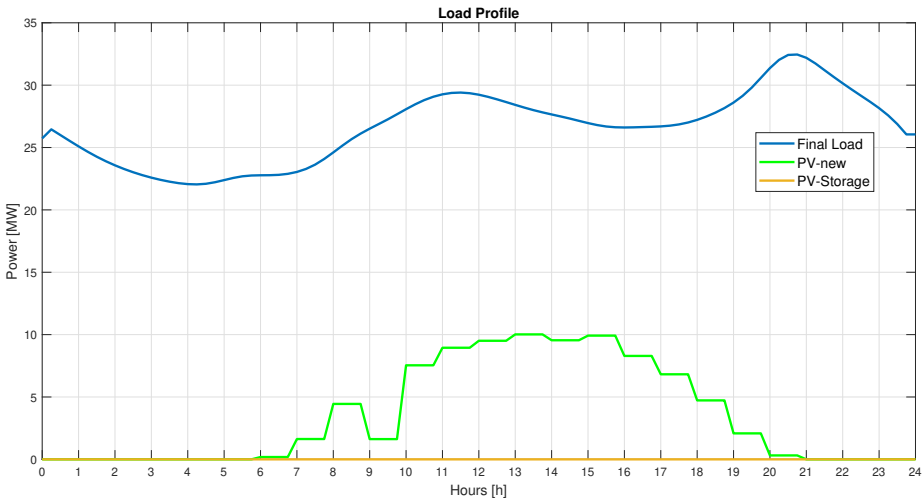

Figure 4.6: Demand with PV

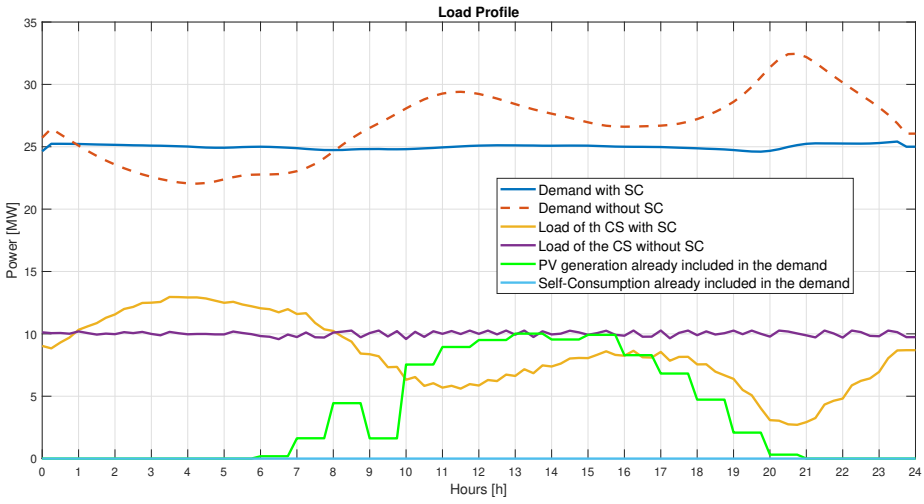

Figure 4.7: New Demand with PV

Differently from Figure 4.2 in Figure 4.7 the load levelling could be considered completely achieved. This is because the PV's production creates thee typical duck curve, therefore the previous highest noon's peak is greatly

attenuated. The power difference between the peaks is reduced, therefore the CS is able to do not shut down during the peaks. Therefore in such a scenario it is possible to assign to the CS the load levelling task without compromise the charging process. On the current and $SoC_{\%}$'s side Figure 4.8 and Figure 4.9 it is possible to appreciate how internally the CS's is working and the effects of the PV's introduction. Thee main difference between the Figure 4.3 and Figure 4.8 is that the current is no longer zero at noon, but oppositely. With the PV scenario the CS has two peaks of overload during the 24h, with the second one proportional to the PV's power installed in the DN. The number of the gradient's repetitions in Figure 4.9 show that vehicles are charged faster during this scenario. The overload during the night time is unchanged.

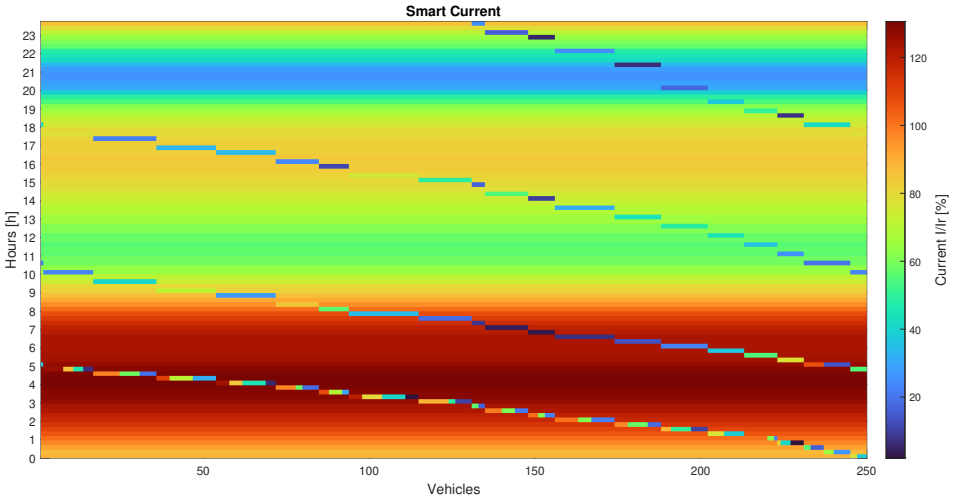

Figure 4.8: Current with PV

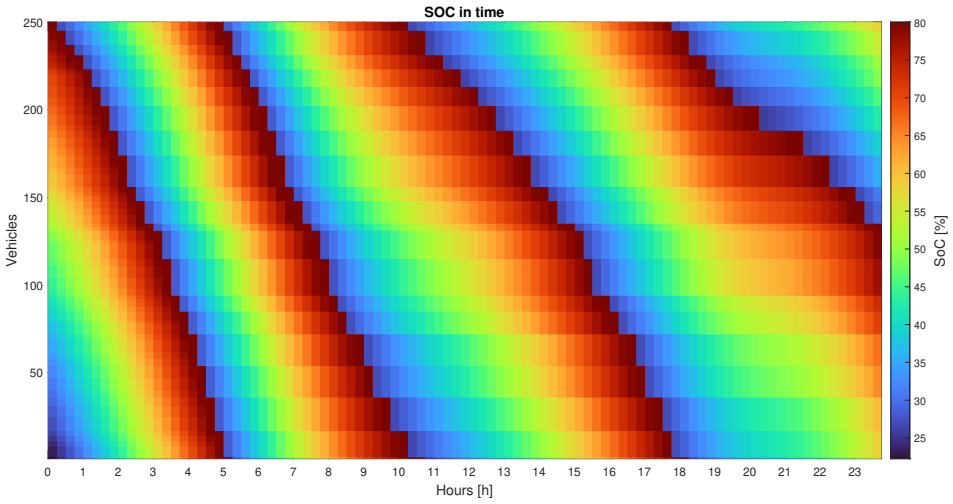

Figure 4.9: $SoC_{\%}$ with PV

The connected vehicles represented in Figure 4.10. The graph shows a relatively homogeneous distribution of EBs if it is compared with Figure 4.5.

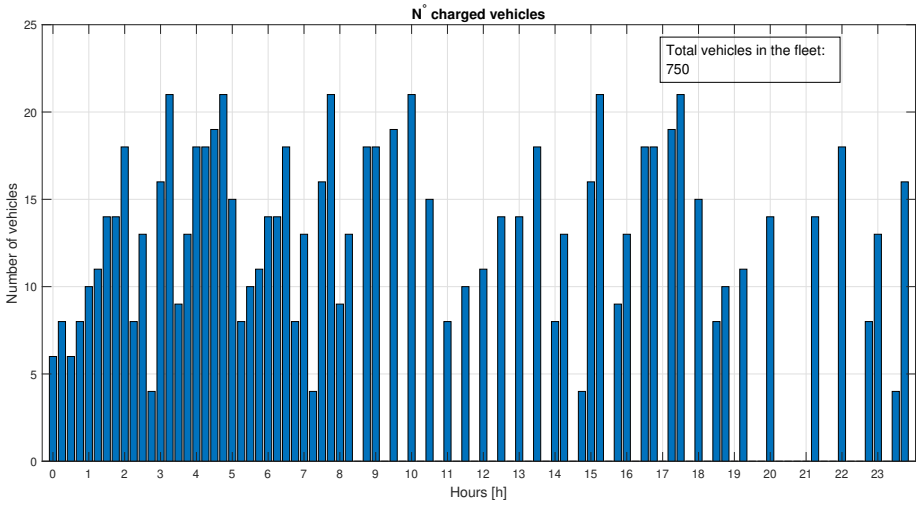

Figure 4.10: Connection with PV.

It is possible to distinguish the highest peaks of connection during the over loads. However the fleet necessary to actuate the load levelling with PV requires 1112 vehicles in the ideal case. This information is useful when it is compared with the real available size of the fleet, if the values largely diverges, it is necessary to assign carefully the available vehicles into the Figure 4.5 blue slots. More the value between the ideal blue one and the real one are different, higher is the risk to do not have an accurate load levelling/peak shaving.

4.1.3 Scenario with PV and Storage

In the last scenario it is assumed to activate the PV (100% of their rated power, so a sunny day) and to store 20% of P_{PV} in order destine it to the self-consumption. The relative load behaviours are represented in Figure 4.11 and Figure 4.12.

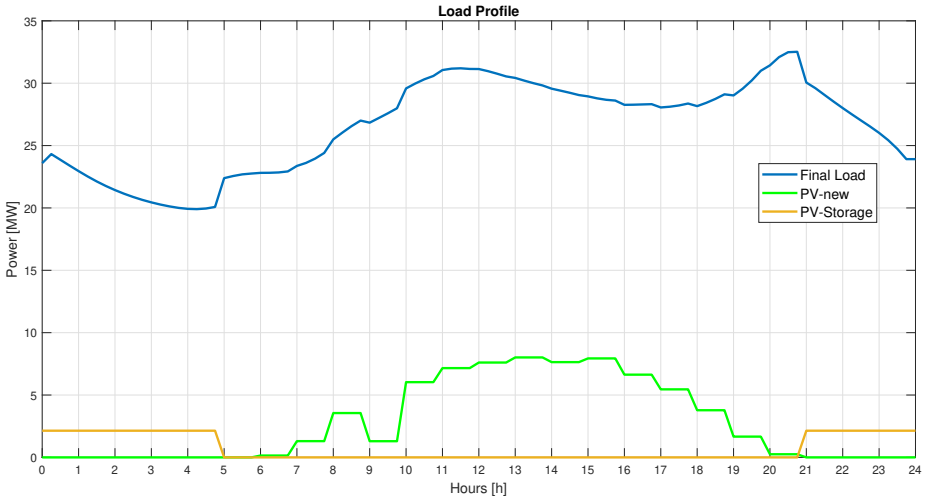

Figure 4.11: Demand with PV+Storage

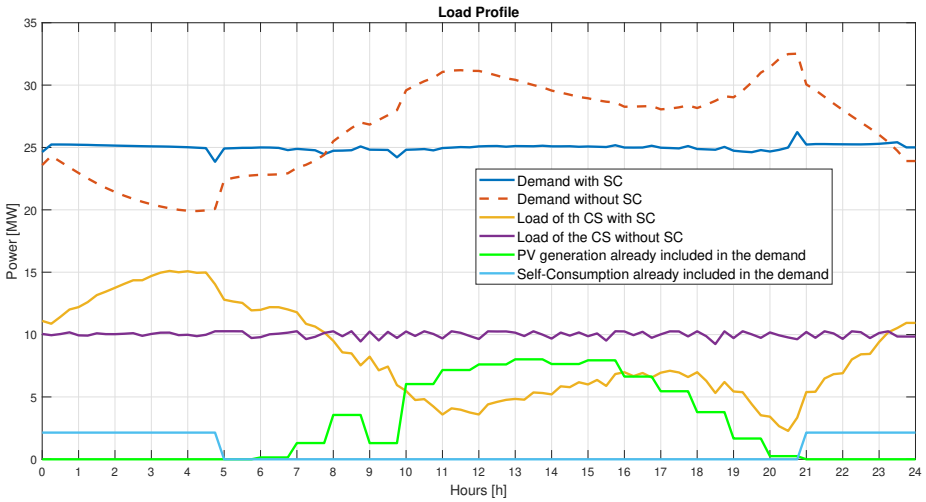

Figure 4.12: New Demand with PV+Storage

Differently from Figure 4.6, in Figure 4.11 the addition of the night self consumption, decreases the PV's power that is able to reduce the demand. This has some effects to the initial demand, firstly the duck curve is mitigated

during the noon and the night load's valley is enhanced. With this DN's configuration it is possible to achieve a full load levelling, therefore both scenarios are suitable for such service.

The current and the $SoC_{\%}$ are represented in Figure 4.13 and Figure 4.14.

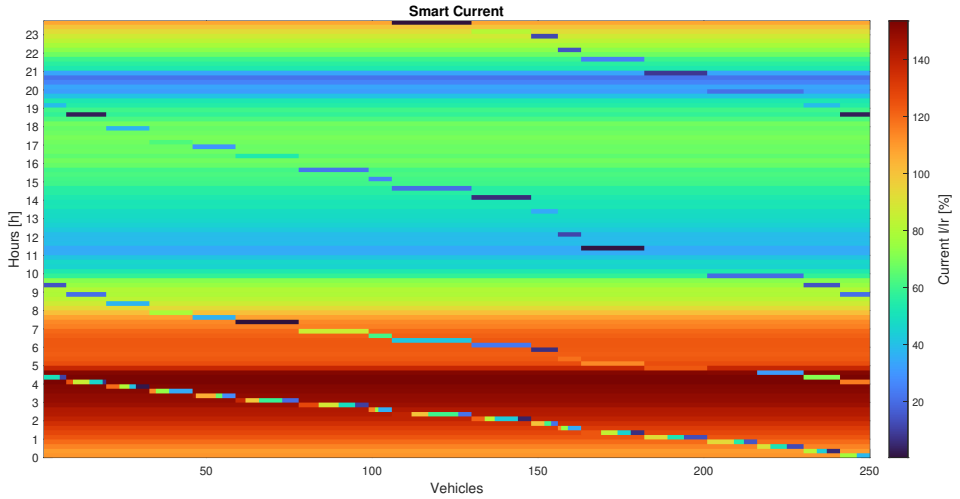

Figure 4.13: Current with PV+Storage

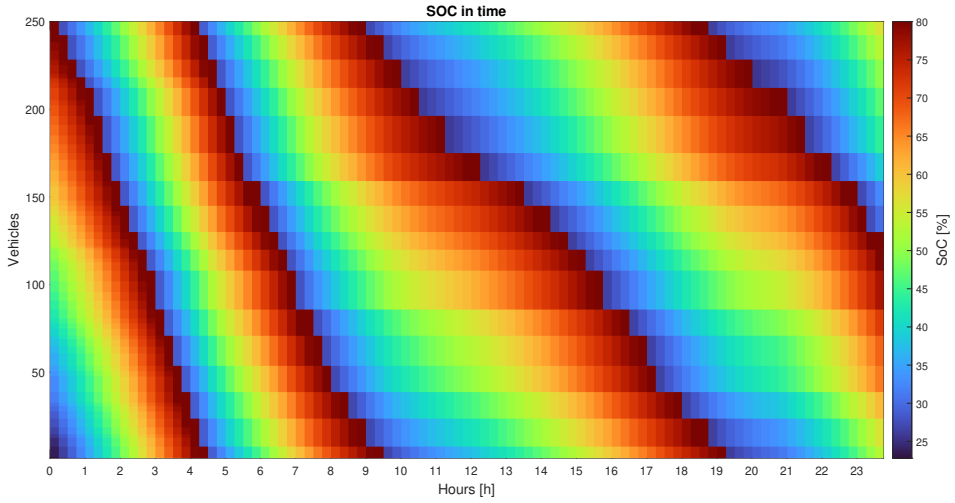

Figure 4.14: $SoC_{\%}$ with PV+Storage

The current absorbed by the EB's are better balanced during the noon's hours because PV's power is reduced. On the other hand it is possible to notice that in Figure 4.13 the current during the night hours are increased by 150% rather than the previous 120%. This is because the initial demand moves away from from the normal

demand due to the night self consumption. The charging Figure 4.14 is not uniform, during the night time the vehicles are charged faster rather than the day's charge. The connection distribution represented in Figure 4.15 shows that is is required a total fleet of 1106 vehicles that are close to Figure 4.10. Even if the charging current is restrained during the noon, during the night hours the number of EBs that are not charged during the day, are charged and connected faster during the night.

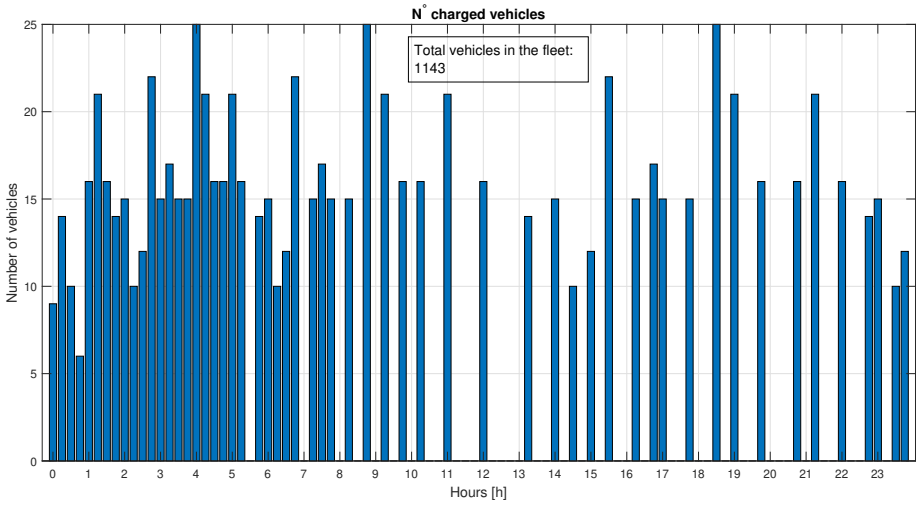

Figure 4.15: Connection with PV+Storage.

In order to verify how the different scenarios DN's scenarios interact with the CS it is chosen to judge graphically if the load levelling is satisfied and to use the F_{ideal} in Table 4.2. It could be added the current's peak as parameter, but since the over-loads last's for a limited amount of time, and the Opp-Charger could sustain currents up to 600A, it was chosen to do not consider it as index.

Table 4.2: Scenarios results.

	Load levelling	F_{ideal}
Base Load	Not Perfect	807
Base Load + PV	Perfect	1112
Base Load+ PV+Storage	Perfect	1106

4.2 Optimisation of the charging station

In conclusion it is possible to use the algorithm to verify how the vehicles have to be charged and connected during different DN and CS's conditions. The most interesting case that worth to be analysed is the last scenario. It allows

to design the CS and the EBs' patterns by taking into account that the DN is evolving in that direction (storage and RES). The objective is to test different voltage, rated current and number of charging slots m in order to verify which is the best configuration when it is considered the F_{ideal}, the difference between $\mathbf{P}_{newload}$ and $\mathbf{P}_{objective}$. Since the graphical interpretation is not rigorous, the load levelling achievement is valued by computing Equation (4.1) which assigns a value to the graphical interpretation Table 4.3.

$$Error = RMS(\mathbf{P}_{newload} - \mathbf{P}_{objective}) \tag{4.1}$$

Table 4.3: Numerical allocation of the load levelling graphical error.

	Load levelling
$Error \geq 1$	Not Perfect
$0.3 < Error < 1$	Not Perfect during the peaks
$Error \leq 0.3$	Perfect

The problem in this case uses three variables it is challenging to produce a graph with the two outputs in order to evaluate which is the combination that minimises the F_{ideal} and the error. Optimisation $MATLAB^{TM}$'s functions as "fmincon" is not able to minimise two values contemporary. There are also convergence problems due to the fact that optimisers usually uses a single value as objective, in this case if a predefined small fleet size is imposed, the algorithm would impose non possible inputs (which are bounded by the optimiser's setting). Therefore it was used a Propensity Score Matching method where random inputs are imposed to the process and the results are grouped in subsets in order to monitor which is the relation among the inputs that produces almost the same result.

In addition to the CS and the fleet parameters optimisation, it is useful to to verify where it is positioned in terms of performance the Volvo's table Table 2.7. By assuming the fact that Volvo's parameters are designed in order to be the optimal ones, it could be used as test in order to verify the algorithm's accuracy. If the chosen inputs produce more performant results by getting close to the Volvo's one, it could be used as proof of the algorithm's effectiveness.

In the table Table 4.4 are represented several attempts on the PV with self consumption scenario. It is possible to extrapolate some information from the table on how the DN responds to the variations of the CS's parameters. It is possible to notice that CS with less m charging slots produces a restrained number of EBs required in the fleet. Therefore it is possible to assume that it is not necessary to have a huge CS (in terms of charging slots) to have the best performances. An high charging voltage allows to keep lower the charging current and sustain and high absorbed power (in order to be effective for the load levelling) from the CS. In this case an higher voltage is best-endured by the Opp-Charger, thus it is preferable to have low currents magnitude which might cause polarisation effects as seen in Equation (3.1). In conclusion, the error and F_{ideal} are sensible to the I_r and it is possible to notice that with 100A the F_{ideal} is very acceptable at the expense of the Error. In the other hand, if the I_r is increased just by 50A, on the DN's side the error is greatly reduced by doubling the required fleet. Thus, it is necessary to choose correctly the current.

Table 4.4: CS input parameters test.

$C_{rated}[kWh]$	m	$V_{rated}[V]$	$I_r[A]$	F_{ideal}	Error
400	250	400	50	614	0.6
400	250	300	50	529	1.1
400	250	300	100	864	0.3
400	50	400	100	228	2.1
400	50	500	200	404	0.6
400	50	600	300	754	0.3
400	50	600	200	488	0.4
400	50	700	200	582	0.3
400	50	700	100	306	1.2
400	50	700	150	427	0.6
400	70	700	150	635	0.3
400	70	700	100	432	0.6
400	60	700	150	532	0.3
400	55	700	125	404	0.7

Since it is expected to have an error increase proportional to the difference between the ideal and real fleet's size, it was chosen to have more error margin. Therefore best case is considered the one with: $V_{rated} = 700V$, $I_r = 150A$, and $m = 70$. The parameters extracted are suitable with the Volvo's one in Table 2.7 therefore it validates the algorithm's operation.

4.3 Real-world fleet consideration

The vehicles that are shown in Figure 4.15 are undoubtedly not feasible from a real word point of view. It is not possible to change the fleet's size according to the DN's daily requirements. Moreover when the required ones overcome become meaningless from an economical and physical point of view. Therefore it is taken the best scenario (by using the error as reference) from table Table 4.4 and it is applied on it the F_{real} constrain. By recalling the algorithm with an uniform distribution of the EB in the predetermined connection slots Figure 4.16, it is possible to observe how the error slightly increases in table's Table 4.5 second line. It was chosen a $F_{real} = 350$ by using as example the Dublin's total fleet of busses [59]. The total fleet size in this case is more than 1000 vehicles with garages that can host from 70 to more than 200 vehicles spread around the Dublin's area, it is possible to assume that a charging station with 70 charging slots with a small fleet of 350 EB's are values in line with the real world data. The under-size of the assigned values allows to consider a more precautionary case.

Table 4.5: Results with real world fleet.

$C_{rated}[kWh]$	m	$V_{rated}[V]$	$I_r[A]$	F_{ideal}	Error
400	70	700	150	635	0.3
400	70	700	150	350	0.6

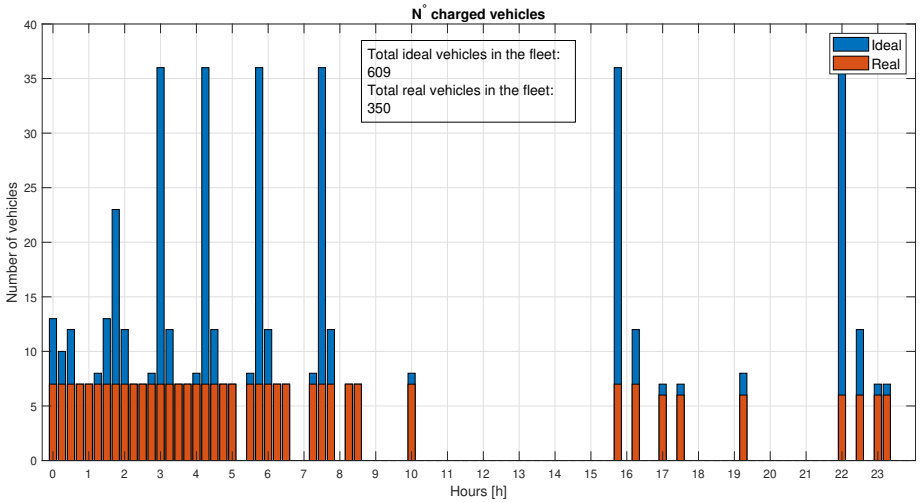

Figure 4.16: Real connection with PV+Storage.

In addition, it is possible to notice that in Figure 4.16 the $F_{ideal} = 606$ which is different from thee 635 of the first run of the algorithm. This is caused by the random allocation of EB's $SoC_{\%}$ at time step $t = 0$, therefore when the algorithm does the second run by imposing the real fleet size, the ideal value varies slightly. This has not

an incisive effect on the final result, since element that is crucial during the EB's allocation are the non zero slots of $\mathbf{Cnn}_{ideal}$ vector, rather than the actual values.

Thus, it is possible to visualise how the application of the real fleet size has modified the curve from Figure 4.12 to Figure 4.17.

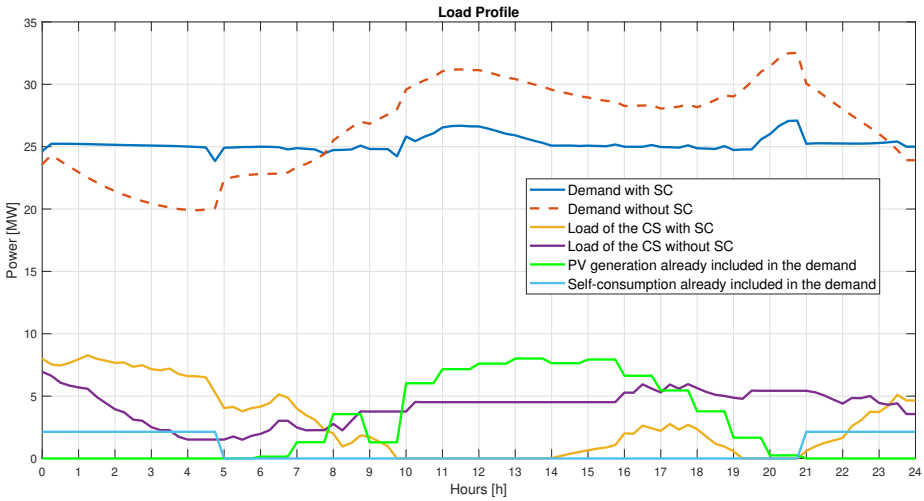

Figure 4.17: New real Demand with PV+Storage.

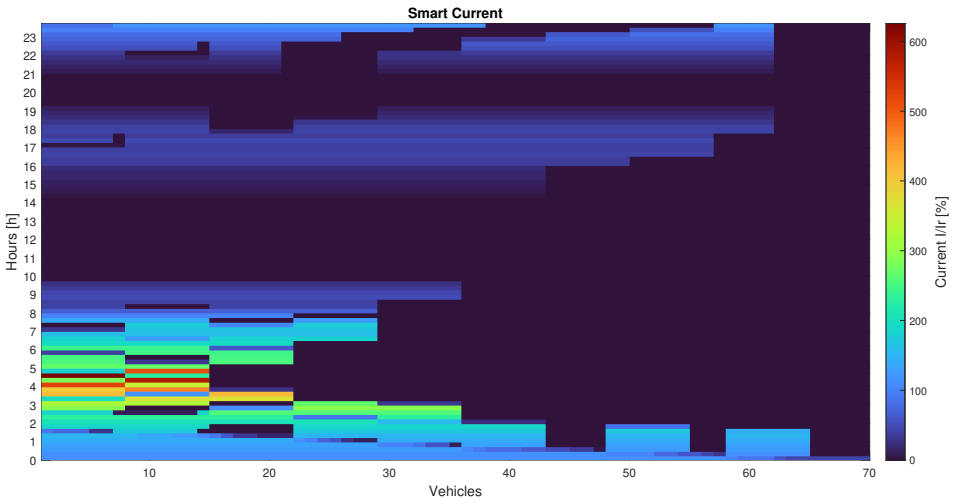

Figure 4.18: Real Current with PV+Storage

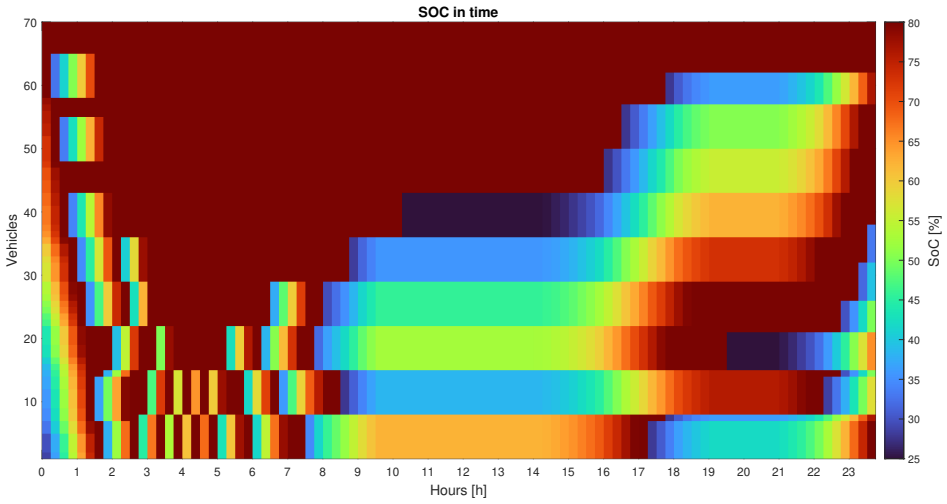

Figure 4.19: Real $SoC_{\%}$ with PV+Storage

The new demand compared to the ideal case is not fully levelled during the most impactful peaks and valleys. However the error moved from 0.3 to 0.6, therefore if it had been taken into consideration to choose a value with a lower F_{ideal} and $Error = 0.6$ from table Table 4.4, the error (so the final demand's shape) would be worse when the real fleet is applied.

It is possible to notice that the CS's load without smart charging (purple) from figure Figure 4.17 is not anymore constant because the number of the vehicles in the CS could be instantaneously less than m. Even so, since it is the difference between the purple and the yellow (CS's load with smart charging) that has an effect on the demand rather than their actual magnitude, thus it is possible to achieve the service.

It is possible to notice a significant difference between the Figure 4.18 and Figure 4.13. In the real configuration there are many dark blue rectangles that represents vehicles with $I_s = 0$. The algorithm considers them as vehicles connected but because they are fully charged but not possible to connect. However, it would be possible to disconnect them in order to start their mission. In the ideal case, every time an EB goes out from the CS, another discharged one is connected. In the real configuration the incoming and outgoing EBs are decoupled. This allows to consider that the algorithm does not require m vehicles connected, which is less prohibitive and simulates a more realistic scenario.

In addition to the introduction of the "realistic" size of the EBs fleet F_{real}, the data used initially are anticipated by the DN in the DAEM, so they may not be completely reliable. As a result, to appreciate the final demand at the main transformer, it was important to analyze how the DN responds when the CS absorbs the computed power, but with the true demand of the after-effect. This situation is examined in Figure 4.20, where the dashed lines represent the predicted scenario and the continuous ones represent the actual shape. The error computed with Equation ((4.1)) shows that, even if the process was investigated in the most favourable case (PV+Storage), the information on which the whole algorithm is based comes from an aleatory source, and hence the quality of the load levelling is related to the demand accuracy in the DAEM. The error produced in this case is 1.3744.

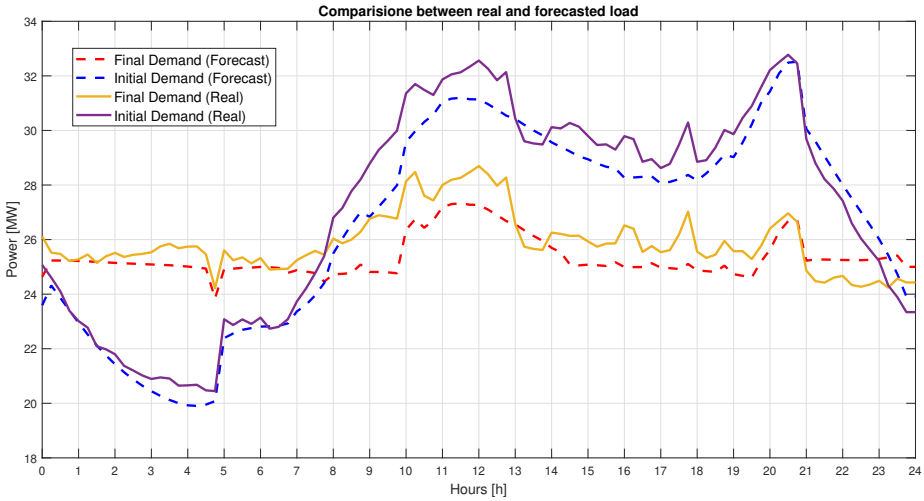

Figure 4.20: Comparison between forecasted and real demand

5

Effects on the Distribution Network

5.1 Power Flow

As the study provided herein is predicated on the consideration of the demand at the primary transformer, the effects on the nodes and lines cannot be determined using the algorithm's results alone. In other words, a study of the impacts created by the CS demand is required to gain an appreciation of the situation and determine whether it is viable to connect this load to the DN without introducing significant compromises in terms of over/under-voltage and system losses. As a result, a NEPLAN^{TM} study on an 11-Node feeder inspired and adapted from a CIGRE benchmark of a typical European radial DN [60], as in Figure 5.1 with different sorts of loads in Table 5.1, such as commercial and residential were developed in order to have variation in active and reactive absorbed power. The lines characteristics in Table 5.2 and the transformers in Table 5.3. The non labeled arrows represent the commercial and residential loads, the labeled ones represents the PV generation and the black arrow is the CS.

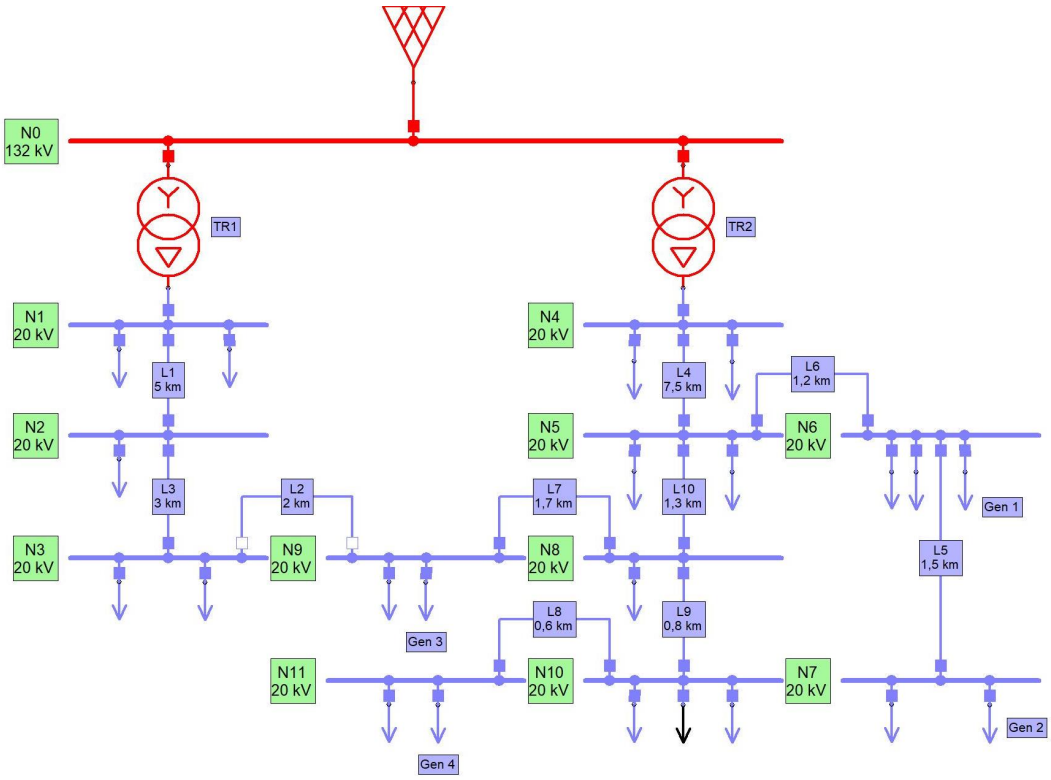

Figure 5.1: Eleven-Node Feeder.

Table 5.1: PV and loads data.

Node	S_n **Res.**	$\cos\phi_R$	S_n **Comm.**	$\cos\phi_C$	S_n **PV**	$\cos\phi_{PV}$
	$[MVA]$		$[MVA]$		$[MVA]$	
1	9	0.98	3	0.98		
2			1.5	0.85		
3	4	0.97	1	0.85		
4	8	0.98	2	0.98		
5	0.98	0.97	1.225	0.85		
6	1.552	0.97	1.150	0.85	4	1
7	2.067	0.97			4	1
8	2.067	0.97				
9			0.5	0.85	4	1
10	1.687	0.97	1.460	0.85		
11	1.172	0.97			4	1

Table 5.2: Data lines.

Line	L	r	x	C	I_n
	[km]	[Ω/km]	[Ω/km]	[μF/km]	[A]
1–2	5	0.55	0.37	0.015	210
3–9	2	0.35	0.28	0.15	250
2–3	3	0.55	0.37	0.015	210
4–5	7.5	0.35	0.28	0.15	250
6–7	1.5	0.35	0.28	0.15	250
5–6	1.2	0.35	0.28	0.15	250
8–9	1.7	0.35	0.28	0.15	250
10–11	0.6	0.35	0.28	0.15	250
8–10	0.8	0.35	0.28	0.15	250
5–8	1.3	0.35	0.28	0.15	250

Table 5.3: Data transformers.

Nodes	Primary	Secondary	v_{cc}	p_{cc}	S_n	m
	[kV]	[kV]	[kV]	[%]	[MW]	
0–1	132	20	12	0.1	25	1
0–4	132	20	12	0.1	25	1

The active power of each load and PV is adjusted, with the coefficients explained in Table 5.4, in accordance with Figure 5.2 to achieve the same demand as shown in Figure 4.11 and 4.12.

Table 5.4: Load coefficients legend.

K_c	Blue	Commercial
K_r	Orange	Residential
K_{pv}	Yellow	PV
k_{cs}	Purple	CS

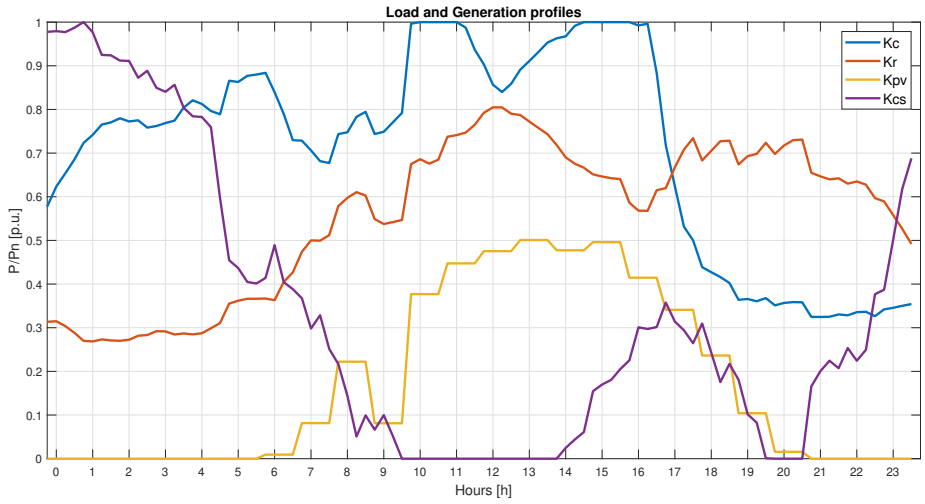

Figure 5.2: Load coefficients.

In this case study, the CS was connected to each node of the Feeder in Figure 5.1 to determine which node is the most reasonable in this circumstance. Sensitivity was assessed using the worst voltage drop or over voltage, as well as the peak of the line reactive and active losses. As seen in Table 5.5, where each connection is summarized with the relative effects on the worst node and losses, the best nodes are those at the secondary of the two primary transformers. In this example, the PV production is not as incisive (the self-consumption is modelled as a reduction in commercial/residential loads), and a compete line change is not a practical degree of freedom; but, if the PV output is enhanced, the CS's connection can be moved to further nodes. The key factor influencing the predicted active power is line losses. The reactive power absorbed by the loads and lines, on the other hand, is not adjustable with the suggested method, implying that the form and magnitude are uncontrollable. The scenario in this case is the one with PV and storage, with the CS and EBs characterized 70 m charging slots with a Fleet F_{real} of 350 EBs, thus close to the Volvo data and the fleet size of a typical Dublin EB. The automated voltage of the primary feeder and the tap-changers on the primary transformers were activated in the power-flow simulation.

Table 5.5: Summary of the performances by changing CS's node.

CS Position	N1	N2	N3	N4	N5	N6	N7	N8	N9	N10	N11
Worst Node	N1	N3	/	N1	N1	N1	N1	N1	N1	N1	N1
Voltage %	103%	94,46%	/	103%	107%	107%	107.50%	109%	109%	109%	109.50%
Max Qloss [Mvar]	1.7	1.9	/	1.7	2.4	2.5	2.6	2.5	2.5	2.5	2.5
Max Ploss [MW]	0.6	0.8	/	0.6	1.4	1.5	1.7	1.5	1.7	1.6	1.7

Each DN's node has a minimum drop voltage of 95% and a maximum over voltage of 105% of the rated voltage (Figure 5.3, where are depicted the voltage of the most sensible nodes).

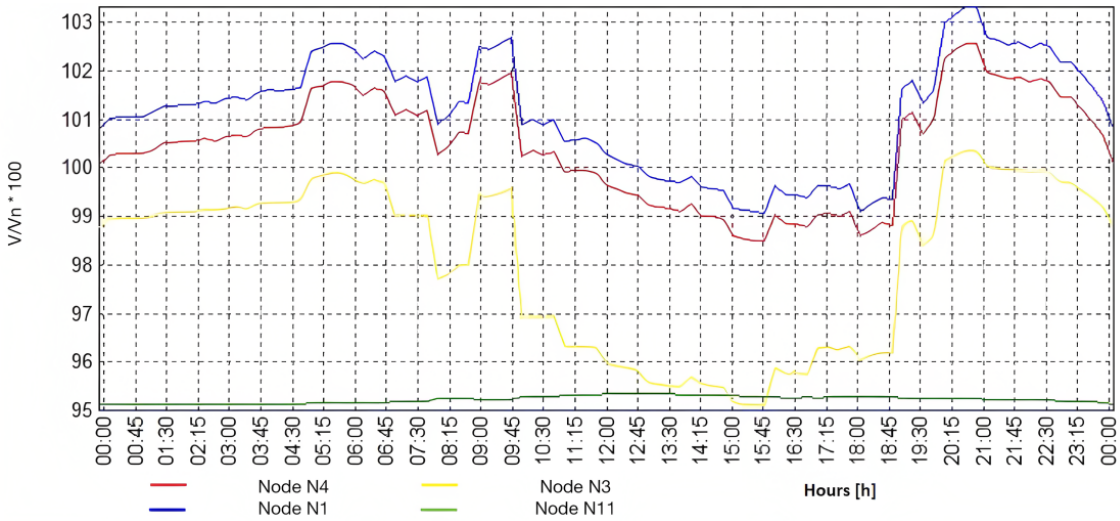

Figure 5.3: Voltage profile at sensible nodes.

Power losses on the line are uncontrollable and amount to about 6% of total absorbed power (Figure 5.4).

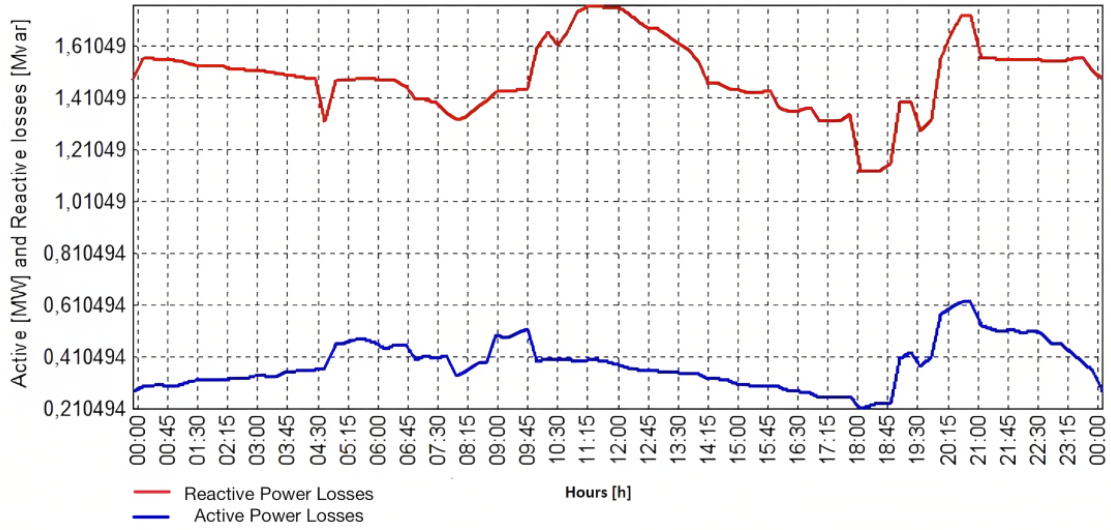

Figure 5.4: Power line losses.

Since the commercial loads in Table 5.1 have a low $\cos\phi$, the reactive power absorbed by the loads is not trivial, especially given that CS employs DAEM as a reference, which does not account for reactive power (Figure 5.5).

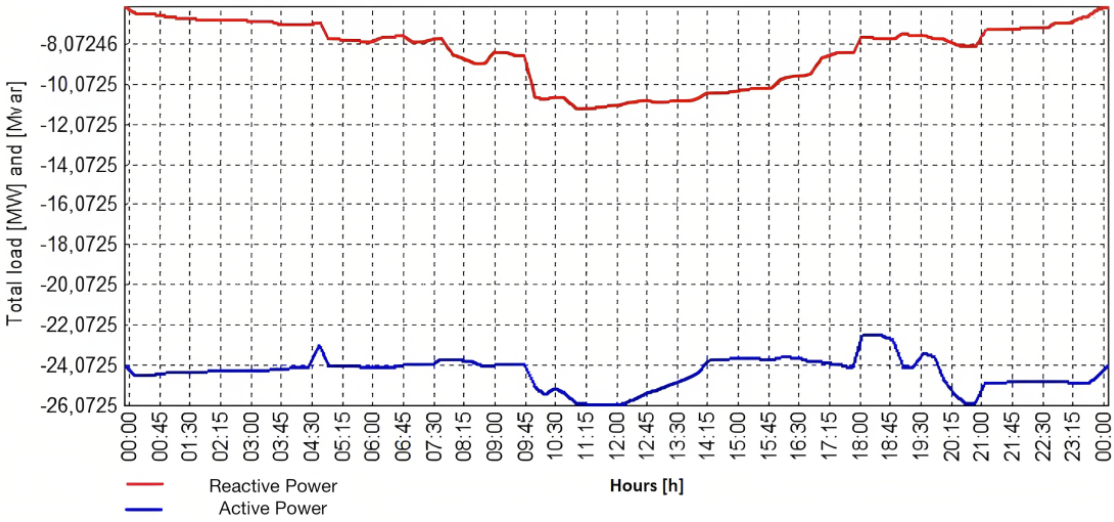

Figure 5.5: Active and reactive power at feeder node.

In general, the effect of load levelling on active power is satisfactory. However, it deviates from the algorithm's prediction by the amount of active line losses. The largest severe impact is from unmanaged reactive power (losses and loads), although the DSO actually imposes a limit on the $\cos\phi = 0.95$ (which will increase in future). Furthermore, in the context of RDG, the inverters must be set to $\cos\phi = 1$ until the distributed reactive power controls are available.

5.2 Discussion

The first aspect that has a considerable impact on the charging pattern of the EBs is the demand shape. Table 4.1 considers a case study with approximately 1/3 of the production supplied by renewable RDG (PVs) during daylight hours, as well as self-consumption. When only PV production is considered, the net demand has the shape of a standard "duck curve". The self-consumption eventually reduces demand during low-demand periods. Even if self-consumption storage reduces the peak of PV production marginally, the end result is a net-demand that is noticeably non-uniform. This non-uniformity causes power cost imbalances, DN instability, and high start-up costs for turning on/off heat generators, and it may also damage the electrical system at the Transmission Network (TN) level [46]. As demand refers to the primary transformer that connects the DN to the TN, an increase in DN demand has mutually beneficial impacts at both levels. If it is expected to provide a full load levelling function, as shown in Table 4.1, the correlations mentioned in Equation (3.19) become more significant. When the disparity between net-demand and desired demand grows, the CS response must become more acute. The smart current I_s will increase during lower peak-hours and decrease during higher peak-hours.

During peak hours, it is vital to avoid using more power than the CS can handle because the reduction in absorbed energy by the CS may not be sufficient to meet the requirements (Equation (3.15)). As indicated by Equation (3.26),the load levelling process will not obtain the target power $\mathbf{P}_{objective}[i]$ in those time frames. The CS will no longer absorb current, therefore its power $P_{s(cs)}[i]$ in those time spans will be zero (Equation (3.26));

the result will be not charging the EBs during this time, which may be considered unsatisfactory if this occurs on a regular basis.

The goal of making the new demand equal to the expected load (Equation 5.2) may be readily fulfilled in a reverse power-flow scenario, but such a facility will allow the EBs to discharge, which is outside the scope of the presented work. If the goal is to completely achieve load levelling, a CS with more charging locations m is required. Alternatively, focus on the demand side by increasing PV production (if the peak is during the day) or self-consumption (if the peak is during the night).

$$\begin{cases} \mathbf{P}_{s(cs)}[i] = 0 \\ \mathbf{P}_{newload}[i] = \mathbf{P}_{load}[i] - (\mathbf{P}_{r(cs)}[i] - \mathbf{P}_{s(cs)}[i]) \end{cases} \tag{5.1}$$

$$\mathbf{P}_{newload}[i] = \mathbf{P}_{objective}[i]. \tag{5.2}$$

When there are significantly lower peak-hours, the CS will begin to absorb more smart current I_s in order to meet the $\mathbf{P}_{objective}[i]$. In the suggested approach, Equation (5.2) is always attained, although there may be some constraints that must be considered. When the $\mathbf{P}_{newload}[i] \ll \mathbf{P}_{objective}[i]$ is reached, the algorithm will iterate by adding 0.1 A to I_s until it reaches the condition specified in Equation (3.18). If the difference in Equation (3.18) is too large, the method will take a long time to converge. If the convergence time is met, the final magnitude of I_s may be insurmountable for the converters or securely supported by the batteries. A feasible approach would be to set a maximum (I_s). As in Equation (5.1), this will result in a limit on the CS to satisfy the load levelling service. If the goal is as specified in Equation (5.2), and no constraints are imposed on I_s, it should be essential to increase the F_{real}. This will distribute the requested power among more vehicles by lowering the magnitude of I_s to an acceptable level.

When the ultimate outcome, as shown in Figure 4.17, is examined, it is clear that the difference between the power absorbed by the CS (by imposing the rated current I_r to each EB) and the charging power facilitated by smart current I_s has an impact. As a result, it is not the magnitude of the power with EBs charged with the rated current $\mathbf{P}_{r(cs)}$ and the power with smart current $\mathbf{P}_{s(cs)}$ that influences final demand, but their difference Equation (5.1).

The OppCharger [41] could enable a fast and automatic exchange that is initiated when the EB is parked, allowing an electrical connection to be made in a reasonably short period if the mission is properly timed and there are no downsides. The connection timetable generated from Equation (3.23) only tells the time when the new EB must begin charging, not their mechanical connecting time. As a result, the EBs"in-coming' planning might be defined as anticipating the mechanical connection time to have some margin before an electrical connection. When vehicles reach the $SoC = 80\%$ Equation (3.20) and are still not connected out, the algorithm allows them to be viewed as being connected with an $I_s = 0$ state. As a result, they could be considered "virtually" connected, but they could also predict the disconnection and begin their mission.

Finally, the algorithm simultaneously accomplishes load levelling and smart charging of the EB without significant sacrifices. When contrasted with the $\mathbf{P}_{load}$ plot, the power absorbed from the CS will naturally take on a mirrored shape. This indicates that the CS will absorb less power during higher peaks when the electricity price is higher, and vice versa. This will not ensure that EB charging is prioritized economically. However, when considering the behavior of $\mathbf{P}_{r(cs)}$, which only charges the EBs with rated current, the proposed smart charging will

produce more economical outcomes. Because public services, such as EB transportation, are characterized by incentives and rewards [61], there is potential for a reward system based on the daily quality of the load levelling/peak shaving sought.

The method might be employed in two ways: the first is for the construction of a CS to meet DN's requirements; in this case, the parameters of the CS and EB must be set by trial and error to discover the condition that best approached the aim. The second modality takes the EB and CS parameters as input to test the effects of an existing system on various DN scenarios. In the study, both methodologies are illustrated in Sections 4.1.1, 4.1.2 and 4.1.3 the test of different scenarios and, in Section 4.2, the test of different CS and EBs parameters to verify which offers the best performances. In particular, it was discovered that the requirements for the CS and EB converge to market-available and regulated ones. This confirms the main goal of the paper, which is to determine the feasibility of present technology.

Finally, by mounting the CS on different DN nodes and computing the power-flow, it was feasible to see that the ideal position is determined by the lines' capabilities and the PV's penetration. In particular, if RDG is sparse, the most practical connection point is the one closest to the secondary of the main transformer as seen in Table 5.5. However, with greater PV, the node could be moved further. Even if the grid-side inverter does not inject reactive power since it operates at $\cos\phi = 1$, the reactive power from the loads and lines is uncontrollable unless there is real-time control measurement, which is beyond the scope of this study. However, because the CS currently performs two functions (load leveling of the active power and managing the EBs connection schedule), it may be possible to implement additional dedicated systems such as a synchronous condenser, condenser, static Var compensator, BESS, or batteries disposed solely for fine-tuning active and reactive power [62, 63, 64]. Assuming that the inverter on the grid side is capable of decoupling active and reactive power regulation, reactive power management could be conducted separately by employing alternative control techniques in accordance with Grid Codes or Aggregator requirements. This form of control has some limitations in terms of the inverter's power capabilities [65]—the collapse of the DC voltage side when an excessive capacitive-reactive power is absorbed, [66] or stability [67]. Therefore, the study assumes a working state of $PF = 1$ in order to simplify management.

The final data outputs Equations (3.20) and (3.23) are matrices and a vector that reflect the current values that must be imposed on each EB j as well as the number of vehicles that must be connected at time step i. They might be used directly to arrange and interpret the EBs schedule if they were represented as timetables. Meanwhile, the data from Equations (3.24) and (3.25) return the quality of the load leveling/peak shaving services as well as the amount of power that the CS will absorb.

The proposed algorithm employs the demand forecast as the primary source of data; thus, if the forecast is inaccurate, the inaccuracy caused propagates to the algorithm's outputs, as shown in Figure 4.20. One of the primary causes of uncertainty is the influence of the DRG [68] which may differ from the predicted condition. In such a case, the algorithm will be unable to fully achieve load-levelling because it operates in a "open-loop" form, with no ability to enable ex post modifications. In addition to RDG, there could be other uncertainty factors, such as the inability or delay of the EBs connection owing to charger failures, vehicle congestion, human errors, etc [69]. However, even a holistic strategy, such as the one suggested in this paper, can produce discrete results because it provides an easy and implementable CS control method.

The transitional context imposes a trade-off between the pursuit of ideal methods that rely on unavailable technology and the use of less performant means to execute services (such as EBs charging) that must be managed in some way so as not to disrupt the DN service. The proposed algorithm also allows for an adaptable structure

by merely acting on the software side, allowing for the future introduction of alternative working modalities such as bidirectional smart charging and active/reactive power control in real time

From the perspective of DN management, there is also the chance that additional parties will participate in the ancillary service, managed directly by the DSO or an aggregator figure [70]. In a transitory context, it is not possible to coordinate all of the players connected to the same DNs at the same time (lack of smart metering, fast communication infrastructure, etc). However, in a situation where the structures cannot communicate and coordinate in real-time, this multi-player arrangement is even more critical and requires enhanced focus and action. As the suggested method takes a target power as input, the load-levelling share of the CS can be assigned in advance. A possible segmented strategy would involve only the allocation of the power quota (e.g., 10 MW to compensate at 4 a.m.) by the DSO or an Aggregator. The power that must be levelled, as determined by the management figure, might be partitioned (for example, 6 MW to CS1 and 4 MW to CS2) and thus provided to the relative participants. As a result, the proposed technique could be used in a DN with multiple participants by using a coordinator that manages the power-quota of different players. The coarse regulation using EBs might also be intended as the structure of the new load, where devices with lower capacity and higher uncertainty could gradually be introduced as fine regulation (EVs, private PV production, etc.) to achieve better load levelling.

In summary, the proposed algorithm does not necessitate a complicated communication infrastructure because it depends on DAEM data and technologies that are readily available in a municipality. However, it is not intended to be a stand-alone solution, but rather a transitional technology that may be incrementally improved until the system is ready to host the complete V2G service. Furthermore, depending on the DC/DC converter used, the CS may be reused for reverse power flow. Furthermore, it may be feasible to change the assignment of the real fleet, not only in a non-uniform distribution, but also in accordance with actual practical capability. Regarding the overall results, the suggested algorithm manages CS and EBs in an appropriate manner for a coarse regulation of the active power for a suitable management of the EB's schedule.

Future advances could include designing the algorithm, CS, and EB mutual effects so that they can be easily upgraded to real-time control systems that can account for many charging stations in the same DN and reactive power regulation. Or, at the very least, to ensure a smooth transition to more sophisticated systems, when Smart Grids will be able to properly handle the communication/control of the DN's components without changing the entire infrastructure, but only the control approach.

5.3 Conclusion

In conclusion, the algorithm simultaneously accomplishes load levelling and smart charging of the EB without significant sacrifices. It might be used to design the charging station as a function of the DN's total demand shape, or to test the effects of several DN scenarios on a given charging station. The output findings might be used immediately to build and read the EB's timetable, producing instruction ready for use by the CS's operators. Because the connecting node for the CS cannot be changed due to network restrictions, the position that created the less acute effects (line losses and node voltage drop) can be relocated away from the primary node in proportion to the installed power of the PV. However, even though real-time sophisticated communication and control systems are not used, the compatibility of a high-capacity CS is consistent with the eventual penetration of RDG in the DN. The limits originate from the unreliability of DAEM data and the inability to manage reactive power, which

might be delegated to other specified systems. In summary, the proposed algorithm does not necessitate a complex communication infrastructure, and it is not intended to be a stand-alone solution, but rather a transitional technology that can be incrementally modified until the system is ready to host the V2G service entirely. Future work may concentrate on the algorithm's scalability for future technological settings or on enhancing the design to appropriately house them, as well as to control additional CS or electrical users connected to the same DN in order to correctly assign the load-leveling effort, based on the available EBs.

References

[1] N. Darii, R. Turri, and K. Sunderland, "Electric Bus Demand Management through Unidirectional Smart Charging," pp. 1–6, 11 2022.

[2] N. Darii, R. Turri, K. Sunderland, and F. Bignucolo, "A novel unidirectional smart charging management algorithm for electric buses," *Electronics*, vol. 12, p. 852, 2 2023. [Online]. Available: https://www.mdpi.com/2079-9292/12/4/852

[3] R. Uhlig, N. Neusel-Lange, and M. Zdrallek, *Smart Distribution Grids for Germany's Energiewende*, 2014.

[4] D.-C. Urcan and D. Bică, *Integrating and modeling the Vehicle to Grid concept in Micro-Grids; Integrating and modeling the Vehicle to Grid concept in Micro-Grids*, 2019.

[5] A. Thingvad, S. Member, L. Calearo, P. Bach Andersen, M. Marinelli, and S. Member, "Empirical Capacity Measurements of Electric Vehicles Subject to Battery Degradation From V2G Services," *IEEE TRANSACTIONS ON VEHICULAR TECHNOLOGY*, vol. 70, no. 8, p. 7547, 2021. [Online]. Available: https://www.ieee.org/publications/rights/index.html

[6] S. Aphale, K. K. Wagh, S. Lulla, A. Kelani, S. Mutha, and V. Nandurdikar, "Li-ion Batteries for Electric Vehicles: Requirements, State of Art, Challenges and Future Perspectives; Li-ion Batteries for Electric Vehicles: Requirements, State of Art, Challenges and Future Perspectives," 2020.

[7] S. Grolleau, A. Delaille, and H. Gualous, "Predicting lithium-ion battery degradation for efficient design and management," 2013.

[8] K. Liu, Y. Shang, Q. Ouyang, and W. D. Widanage, "A Data-Driven Approach With Uncertainty Quantification for Predicting Future Capacities and Remaining Useful Life of Lithium-ion Battery Index Terms-Electric vehicles (EVs), data-driven approach, lithium-ion (Li-ion) batteries, remaining useful life (RUL), uncertainty management," *IEEE TRANSACTIONS ON INDUSTRIAL ELECTRONICS*, vol. 68, no. 4, 2021. [Online]. Available: http://ieeexplore.ieee.org.

[9] A. Hoke, A. Brissette, D. Maksimović, A. Pratt, and K. Smith, *Electric Vehicle Charge Optimization Including Effects of Lithium-Ion Battery Degradation*, 2011.

[10] A. Verma and B. Singh, *Control and Implementation of Renewable Energy Based Smart Charging Station Beneficial for EVs, Home and Grid; Control and Implementation of Renewable Energy Based Smart Charging Station Beneficial for EVs, Home and Grid*, 2019.

[11] C. Gong, L. Ma, Z. Chi, B. Zhang, R. Shi, R. Jiao, S. Zeng, and J. Chen, *Study on the impacts and analysis of EV and PV integration into power systems; Study on the impacts and analysis of EV and PV integration into power systems*, 2015.

[12] Q. Ali, H. Zahid, B. Syed, and A. A. Kazmi, *Integration of Electric Vehicles as Smart Loads for Demand Side Management in Medium Voltage Distribution Network; Integration of Electric Vehicles as Smart Loads for Demand Side Management in Medium Voltage Distribution Network*, 2018.

[13] H. Klaina, P. Guembe, P. Lopez-Iturri, J. J. Astrain, L. Azpilicueta, O. Aghzout, A. Vazquez Alejos, and F. Falcone, "Aggregator to Electric Vehicle LoRaWAN Based Communication Analysis in Vehicle-to-Grid Systems in Smart Cities."

[14] M. Niasse, Q. Zheng, A. Xin, and F. A. F. Quan, "Implementation of Vehicle-to-Grid Scheme in Hydro-Dominant Grid Subjected to Ultra-Low Frequency Oscillations; Implementation of Vehicle-to-Grid Scheme in Hydro-Dominant Grid Subjected to Ultra-Low Frequency Oscillations," 2021.

[15] S. Deb, R. L. Chetri, A. K. Goswami, and R. Roy, "Congestion Management Considering Plug-in Electric Vehicle Charging Coordination in Distribution System; Congestion Management Considering Plug-in Electric Vehicle Charging Coordination in Distribution System," 2021.

[16] S. Pazouki, A. Mohsenzadeh, and M.-R. Haghifam, "The Effect of Aggregated Plug-In Electric Vehicles Penetrations in Charging Stations on Electric Distribution Netwroks Reliability," Tech. Rep., 2014.

[17] U. C. Chukwu, "The Impact of V2G Location on Energy Loss Reduction; The Impact of V2G Location on Energy Loss Reduction," Tech. Rep., 2020.

[18] O. A. Nworgu, U. C. Chukwu, C. G. Okezie, and N. B. Chukwu, *Economic prospects and market operations of V2G in electric distribution network; Economic prospects and market operations of V2G in electric distribution network*, 2016.

[19] R. Rahmani, S. Aghaee, S. H. Hosseinian, and S. H. H. Sadeghi, *Determining Maximum Penetration Level of Distributed Generation Sources in Distribution Network Considering Harmonic Limits and Maintain Protection Coordination Scheme*, 2017.

[20] H. B. Sassi, F. Errahlmi, and N. Es-Sbai, *V2G and Wireless V2G concepts: State of the Art and Current Challenges; V2G and Wireless V2G concepts: State of the Art and Current Challenges*, 2019.

[21] Jingchao, Zhang, Jinhua, Linchang, Mei, N. Song, Xiaolei, and Li, "The implementation of the Internet of Things technology in Henan smart distribution network demonstration project; The implementation of the Internet of Things technology in Henan smart distribution network demonstration project," Tech. Rep., 2016.

[22] K. Pavan Inala, S. K. Bose, and P. Kumar, *Impact of Communication Network on V2G System in a Smart Grid Scenario*.

[23] K. Thirugnanam, T. P. Ezhil, R. Joy, M. Singh, and P. Kumar, "Modeling and Control of Contactless Based Smart Charging Station in V2G Scenario," *IEEE TRANSACTIONS ON SMART GRID*, vol. 5, no. 1, 2014.

[24] C. Iclodean, B. Varga, N. Burnete, D. Cimerdean, and B. Jurchiş, "Comparison of Different Battery Types for Electric Vehicles," in *IOP Conference Series: Materials Science and Engineering*, vol. 252, no. 1. Institute of Physics Publishing, 10 2017.

[25] J. Van Roy, S. De Breucker, and J. Driesen, "Analysis of the Optimal Battery Sizing for Plug-in Hybrid and Battery Electric Vehicles on the Power Consumption and V2G Availability," Tech. Rep., 2011.

[26] J. V. Barreras, E. Schaltz, S. J. Andreasen, and T. Minko, "Datasheet-based modeling of Li-Ion batteries," in *2012 IEEE Vehicle Power and Propulsion Conference, VPPC 2012*, 2012, pp. 830–835.

[27] O. Tremblay and L.-A. Dessaint, "Experimental Validation of a Battery Dynamic Model for EV Applications," Tech. Rep.

[28] T. Amietszajew, E. McTurk, J. Fleming, and R. Bhagat, "Understanding the limits of rapid charging using instrumented commercial 18650 high-energy Li-ion cells," *Electrochimica Acta*, vol. 263, pp. 346–352, 2 2018.

[29] A. Gaehring, R. Kripalani, O. Rondeau, and N. Schlag, "Modeling Li-ion Battery Behavior to Identify Safety Limits; Modeling Li-ion Battery Behavior to Identify Safety Limits," 2021.

[30] P. Yannick, P. Marc, and K. Willett, "A Public Policy Strategies for Electric Vehicles and for Vehicle to Grid Power," Tech. Rep., 2013.

[31] C.-H. Lin, C.-L. Chen, Y.-H. Lee, S.-J. Wang, C.-Y. Hsieh, H.-W. Huang, and K.-H. Chen, *Fast Charging Technique for Li-Ion Battery Charger*.

[32] S. Ullah Khan, K. Khalid Mehmood, Z. Maqsood Haider, S. Basit Ali Bukhari, S.-J. Lee, M. Kashif Rafique, and C.-H. Kim, "Energy Management Scheme for an EV Smart Charger V2G/G2V Application with an EV Power Allocation Technique and Voltage Regulation." [Online]. Available: www.mdpi.com/journal/applsci

[33] N. Mohan, T. M. Undeland, W. P. Robbins, and L. Legoprint, "Elettronica di potenza : convertitori e applicazioni," 2005. [Online]. Available: https://www.hoepli.it/libro/elettronica-di-potenza/9788820334284.html

[34] M. Farzam Far, M. Paakkinen, and P. Cremers, "A Framework for Charging Standardisation of Electric Buses in Europe; A Framework for Charging Standardisation of Electric Buses in Europe," 2020.

[35] "Trucks and Buses – Analysis - IEA." [Online]. Available: https://www.iea.org/reports/trucks-and-buses

[36] L. Noel and R. Mccormack, "A Cost Benefit Analysis of a V2G-Capable Electric School Bus Compared to a Traditional Diesel School Bus," Tech. Rep.

[37] "ASSURED project concludes and launches Clean Bus Report – News – ASSURED project." [Online]. Available: https://assured-project.eu/news-and-events/news/assured-project-concludes-and-launches-clean-bus-report

[38] "Home – ZeEUS – Zero Emission Urban Bus System." [Online]. Available: https://zeeus.eu/

[39] "J1772_201710: SAE Electric Vehicle and Plug in Hybrid Electric Vehicle Conductive Charge Coupler - SAE International." [Online]. Available: https://www.sae.org/standards/content/j1772_201710/

[40] B. Wang, S. Member, P. Dehghanian, S. Wang, M. Mitolo, and S. Member, "Electrical Safety Considerations in Large-Scale Electric Vehicle Charging Stations; Electrical Safety Considerations in Large-Scale Electric Vehicle Charging Stations," *IEEE TRANSACTIONS ON INDUSTRY APPLICATIONS*, vol. 55, no. 6, p. 6603, 2019. [Online]. Available: http://www.ieee.org/publications_standards/publications/rights/index.html

[41] "OppCharge - Fast charging of electric vehicles." [Online]. Available: https://www.oppcharge.org/

[42] "Volvo Buses | Sustainable public transport systems." [Online]. Available: https://www.volvobuses.com/it/

[43] M. Ahmed, "Modeling Lithium-ion Battery Chargers in PLECS ®," Tech. Rep.

[44] Coppo Massimiliano, Lorenzoni Artuto, and Bano Laura, *Principles of electricity markets economics*. Esculapio, 2020.

[45] R. Tonkoski and L. A. Lopes, "Impact of active power curtailment on overvoltage prevention and energy production of PV inverters connected to low voltage residential feeders," *Renewable Energy*, vol. 36, no. 12, pp. 3566–3574, 12 2011.

[46] L. A. Wong and V. K. Ramachandaramurthy, "A Case Study on Optimal Sizing of Battery Energy Storage to Solve 'Duck Curve' Issues in Malaysia," *2020 8th International Conference on Smart Grid and Clean Energy Technologies, ICSGCE 2020*, pp. 1–4, 10 2020.

[47] M. Uddin, M. F. Romlie, M. F. Abdullah, S. Abd Halim, A. H. Abu Bakar, and T. Chia Kwang, "A review on peak load shaving strategies," *Renewable and Sustainable Energy Reviews*, vol. 82, pp. 3323–3332, 2 2018.

[48] K. A. Joshi and N. M. Pindoriya, *Day-ahead dispatch of Battery Energy Storage System for peak load shaving and load leveling in low voltage unbalance distribution networks; Day-ahead dispatch of Battery Energy Storage System for peak load shaving and load leveling in low voltage unbalance distribution networks*, 2015.

[49] X. Zhao, R. Xu, Y. Zhou, D. Feng, Z. Liu, C. Fang, S. Shi, and H. Wang, "Aggregator-Based Demand Response Mechanism for Electric Vehicles Participating in Peak Regulation in Valley Time of Receiving-End Power Grid," *2020 IEEE/IAS Industrial and Commercial Power System Asia, I and CPS Asia 2020*, pp. 187–193, 7 2020.

[50] "Electric car sales share in the Net Zero Scenario, 2000-2030 – Charts – Data & Statistics - IEA." [Online]. Available: https://www.iea.org/data-and-statistics/charts/electric-car-sales-share-in-the-net-zero-scenario-2000-2030

[51] "Global electric car stock, 2010-2021 – Charts – Data & Statistics - IEA." [Online]. Available: https://www.iea.org/data-and-statistics/charts/global-electric-car-stock-2010-2021

[52] M. J. Nieuwenhuijsen and H. Khreis, "Car free cities: Pathway to healthy urban living," *Environment International*, vol. 94, pp. 251–262, 9 2016.

[53] P. Zhuang and H. Liang, "Stochastic Energy Management of Electric Bus Charging Stations With Renewable Energy Integration and B2G Capabilities; Stochastic Energy Management of Electric Bus Charging Stations With Renewable Energy Integration and B2G Capabilities," *IEEE TRANSACTIONS ON SUSTAINABLE ENERGY*, vol. 12, no. 2, 2021. [Online]. Available: https://www.ieee.org/publications/rights/index.html

[54] B. Han, H. Liu, C. Zhang, F. Xue, and S. Lu, "Electric Bus Energy Management and Routing Scheduling Considering Timetable Constraints," pp. 1058–1063, 11 2022.

[55] M. M. Hasan, M. El Baghdadi, and O. Hegazy, "Energy Management Strategy in Electric Buses for Public Transport using ECO-driving," *2020 15th International Conference on Ecological Vehicles and Renewable Energies, EVER 2020*, 9 2020.

[56] K. Gkiotsalitis, "Bus rescheduling in rolling horizons for regularity-based services," *Journal of Intelligent Transportation Systems: Technology, Planning, and Operations*, vol. 25, no. 4, pp. 356–375, 2021.

[57] C. Zhang, "Charging schedule optimization of electric bus charging station considering departure timetable," *IET Conference Publications*, vol. 2019, no. CP764, 2019.

[58] "Total Load - Terna spa." [Online]. Available: https://www.terna.it/en/electric-system/transparency-report/total-load

[59] "Dublin Bus Fleet - Dublin Bus." [Online]. Available: http://www.dublinbus.ie/About-Us/Dublin-Bus-Fleet/

[60] Conseil international des grands reseaux electriques. Comite detudes C6. and Impr. Conformes), *Benchmark systems for network integration of renewable and distributed energy resources*. CIGRE, 2014.

[61] S. Krawiec, B. Łazarz, S. Markusik, G. Karoń, G. Sierpiński, K. Krawiec, and R. Janecki, "Urban public transport with the use of electric buses - Development tendencies," *Transport Problems*, vol. 11, no. 4, pp. 127–137, 2016.

[62] A. R. Jordehi, M. S. Javadi, and J. P. Catalão, "Energy management in microgrids with battery swap stations and var compensators," *Journal of Cleaner Production*, vol. 272, p. 122943, 11 2020.

[63] H. Fedayi, M. Ahmadi, A. B. Faiq, N. Urasaki, and T. Senjyu, "BESS based voltage stability improvement enhancing the optimal control of real and reactive power compensation," *AIMS Energy*, vol. 10, no. 3, pp. 535–552, 2022.

[64] X. Zhou, K. Wei, Y. Ma, and Z. Gao, "A review of reactive power compensation devices," *Proceedings of 2018 IEEE International Conference on Mechatronics and Automation, ICMA 2018*, pp. 2020–2024, 10 2018.

[65] "(PDF) NERC | Report Title | Report Date I Reliability Guideline Power Plant Model Verification for Inverter-Based Resources." [Online]. Available: https://www.researchgate.net/publication/327704143_NERC_Report_Title_Report_Date_I_Reliability_Guideline_Power_Plant_Model_Verification_for_Inverter-Based_Resources

[66] D. Lu, X. Wang, and F. Blaabjerg, "Influence of Reactive Power Flow on the DC-Link Voltage Control in Voltage-Source Converters," *2018 IEEE Energy Conversion Congress and Exposition, ECCE 2018*, pp. 2236–2241, 12 2018.

[67] H. Li, Y. Xu, S. Adhikari, D. Tom Rizy, F. Li, and P. Irminger, *Real and reactive power control of a three-phase single-stage PV system and PV voltage stability*, 2012.

[68] V. S. Simankov, P. Y. Buchatskiy, A. V. Shopin, S. V. Teploukhov, and V. V. Buchatskaya, "Control of an Autonomous Energy Complex with Renewable Energy Sources, taking into account the Type of Input Information Uncertainty," 2021.

[69] N. Z. Xu and C. Y. Chung, "Uncertainties of EV Charging and Effects on Well-Being Analysis of Generating Systems," *IEEE Transactions on Power Systems*, vol. 30, no. 5, pp. 2547–2557, 9 2015.

[70] H. Wu, M. Shahidehpour, A. Alabdulwahab, and A. Abusorrah, "A game theoretic approach to risk-based optimal bidding strategies for electric vehicle aggregators in electricity markets with variable wind energy resources," *IEEE Transactions on Sustainable Energy*, vol. 7, no. 1, pp. 374–385, 1 2016.